# DOCTORAATSPROEFSCHRIFT

2012 | Faculteit Wetenschappen

## Discovery of an Anionic Polymerization Mechanism for High Molecular Weight PPV Derivatives via the Sulfinyl Precursor Route

Proefschrift voorgelegd tot het behalen van de graad van
Doctor in de Wetenschappen, Chemie, te verdedigen door:

Jimmy WOUTERS

Promotor: prof. dr. Dirk Vanderzande
Copromotoren: prof. dr. Thomas Cleij
prof. dr. Peter Adriaensens

D/2012/2451/3

universiteit hasselt

# Table of Contents

# Chapter 1:
# General introduction

*ABSTRACT: IN THIS CHAPTER, A CONCISE INTRODUCTION IS GIVEN ABOUT CONJUGATED POLYMERS IN GENERAL. FURTHERMORE, THE DIFFERENT PRECURSOR ROUTES ARE BRIEFLY INTRODUCED SINCE THREE DIFFERENT PRECURSOR ROUTES WILL BE INVESTIGATED AND COMPARED IN THE LAST CHAPTER. THE POLYMERIZATION MECHANISM AND IMPORTANT STUDIES OF THESE ROUTES WILL BE COVERED. FINALLY AT THE END OF THIS CHAPTER, A SHORT DESCRIPTION OF THE USE OF CONJUGATED POLYMERS IN THE FIELD OF BIOSENSORS IS GIVEN.*

Polymers, or plastics as they are generally called, are long chain molecules made of carbon atoms. We use many polymers, for example polystyrene and polyethylene, in our everyday lives. In general polymers are insulators, *i.e.* they do not conduct electricity or heat. In fact one of the most common uses of a plastic is as an insulation material for electric wires. However scientists have discovered that a certain class of polymers called conjugated polymers, which have a backbone consisting of alternating single and double bonds (see Figure 1-1), are actually semi-conductors with unusual electrical properties.

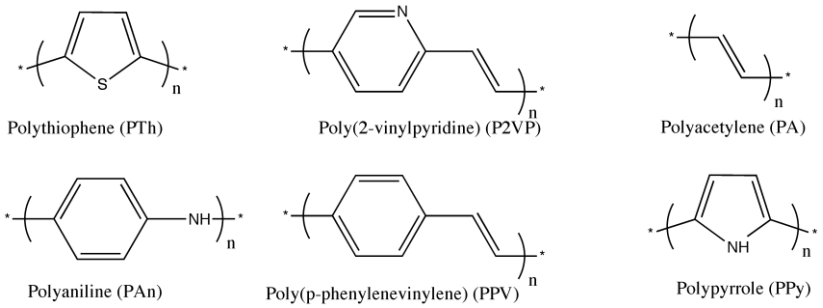


**Figure 1-1: Some examples of conjugated polymers**

Nowadays, conjugated polymers attract much interest for use as active components in electronic, optical and optoelectronic applications, such as light-emitting diodes (Figure 1-2)[1,2], light-emitting electrochemical cells[3,4], photodiodes[5,6], photovoltaic cells (Figure 1-3)[7,8], field-effect transistors[9,10], optocouplers[11] and optically pumped lasers in solution[12,13] and solid state[14-16]. They combine the properties of classical macromolecules, such as low density, good mechanical behavior and straightforward processing with semiconductor properties, arising from their typical electronic structure. The overlap of $\pi$ bonding and $\pi^*$ antibonding molecular orbitals results in a continuous system of electron density along the backbone. The extent of this overlap determines the HOMO-LUMO bandgap. Conjugated polymers have bandgaps in the range of 1 to 4 eV, allowing stable optical excitations and mobile charge carriers.

**Figure 1-2: Organic LED**

**Figure 1-3: Organic solar cell**

From a synthetic point of view, two different approaches for obtaining PPV derivatives are known. A first approach is the direct synthesis of PPV where the double bond is generated *in situ* (Figure 1-4). Known examples of such routes are the Wittig[17] and Knoevenagel polycondensation reactions[18,19]. In addition, palladium catalyzed reactions have been applied in the PPV synthesis, *e.g.* in the Heck[20] coupling reaction between ethylene and aromatic dibromides. However, these routes to PPV have the disadvantage of giving insoluble and unmeltable material, which is very difficult to process. As an alternative, the solubility of PPV can be enhanced by attaching long and flexible chains (usually alkyl, alkoxy, or phenyl) onto the polymer backbone.2[,21,22] In this way a soluble conjugated material can be obtained, although these side groups can modify the optical and electronic properties of the polymer. Notwithstanding, the above mentioned reactions yield polymers with only a low or moderate molecular weight, which can jeopardize their film forming properties.

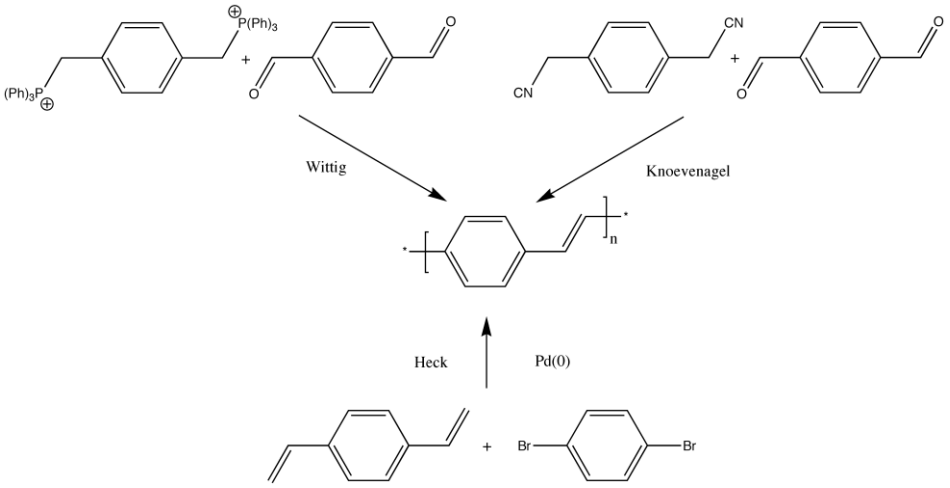


**Figure 1-4: An overview of some direct routes towards PPV**

Another possible strategy is the use of a soluble precursor polymer that can be appropriately processed into thin films and fibers prior to being thermally converted into insoluble PPV under expulsion of a small molecule per monomer unit. Furthermore, in case of the presence of solubilizing side chains, direct conversion of the precursor in solution can be realized.

Over the last 40 years different precursor routes have been developed to synthesize PPV derivatives, all using the polymerization behavior of the *p*-quinodimethane system. Examples are the Gilch[23], Wessling[24], sulfinyl[25], xanthate[26] and dithiocarbamate routes[27]. The general principle of such a precursor route is depicted in Figure 1-5. All these methods have in common that they proceed *via* the *in situ* formation of a *p*-quinodimethane system **2**, which is formed *via* a base induced elimination on the premonomer **1**. Subsequently, the *p*-quinodimethane system **2** polymerizes to form the precursor polymer **3**. Thermal treatment of this precursor polymer affords the fully conjugated material **4**. The routes differ in the substituents on the *p*-xylene derivative and will be discussed separately in the following sections.

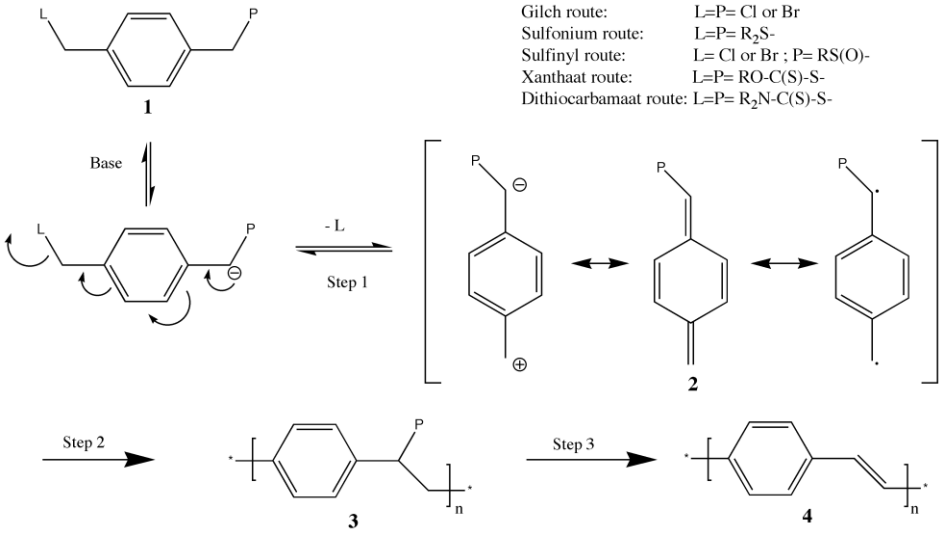


**Figure 1-5: General reaction scheme of the five precursor routes towards PPV**

# *1.1 The precursor routes*

In this work, several precursor routes were utilized. Although mostly the sulfinyl route was used, also the Gilch route and the dithiocarbamate route will be studied.

## 1.1.1 Gilch precursor route

At present the Gilch route, which is also known as the dehalogenation route, is the most widely used route for the synthesis of soluble conjugated PPV derivatives such as poly[2-methoxy-5-(2'-ethyl-hexyloxy)-1,4-phenylene vinylene] (MEH-PPV) and poly[2-methoxy-5-(3',7'-dimethyloctyloxy)-1,4-phenylenevinylene (MDMO-PPV) (Figure 1-6). It was first reported by Gilch and Wheelwright[23]. It involves basic treatment of a $\alpha,\alpha'$-dihalogen (mainly chlorine) *p*-xylene derivative **5** with an excess of base (potassium t-butoxide) in organic solvents to afford insoluble "unsubstituted PPV" **8**. In order to obtain a more soluble precursor polymer **7** through this route, one equivalent of base has to be used instead of a tenfold excess.[28] However, the thus obtained precursor polymer is insoluble in most common organic solvents, such as acetone, chloroform and tetrahydrofuran (THF). Adding

substituents as phenyl, alkoxy and alkylgroups on the premonomer **5** can improve the solubility.[29-31] Unfortunately, the chlorine precursor polymer **7** is not very stable in time. The precursor polymer can be converted into the conjugated structure **8** by thermal treatment (300 °C, 1 hour) in a thin film or by a base induced elimination in case of a completely soluble PPV derivative.

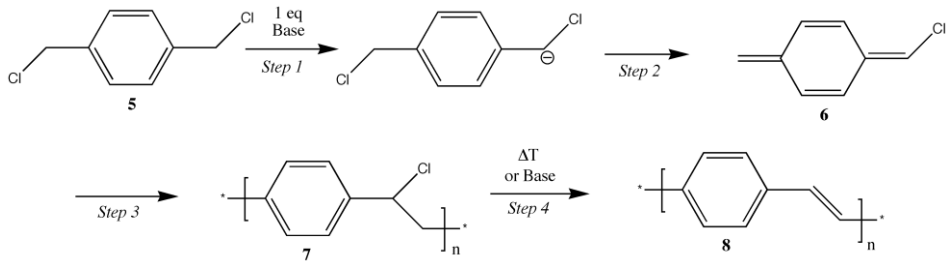


**Figure 1-6: General scheme for the Gilch precursor route**

Note that in this route hydrogen chloride or bromide (*step 4*) is set free during elimination, which has to be removed in order to avoid poor device performance.

### 1.1.2 Sulfonium precursor route

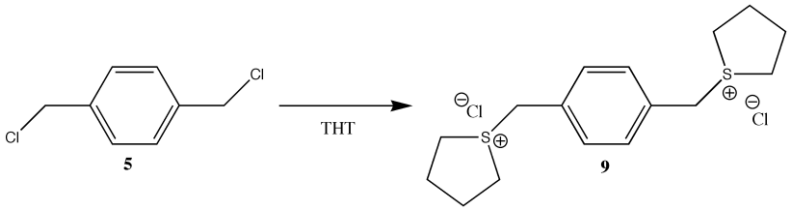


**Figure 1-7: Sulfonium premonomer synthesis**

In 1968 Wessling and Zimmerman discovered the bissulfonium precursor route towards PPV.[24,32] In literature this route is often referred to as the Wessling route. (Figure 1-8).

Premonomer synthesis is straightforward to perform and can be achieved by reacting α,α'-dichloro-*p*-xylene **5** with an excess of dialkyl sulfide (Figure 1-7). Both linear and cyclic thioethers can be used for this reaction, but the latter are preferred due to fewer unwanted side reactions.[33]

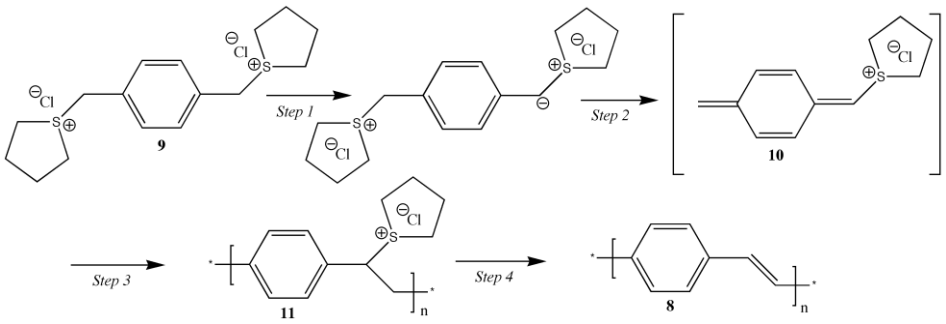


**Figure 1-8: General scheme for the Wessling precursor route**

Polymerization of the bissulfonium salt **9** is achieved by basic treatment of the salt in water or methanol. This gives a *p*-quinodimethane system **10,** which acts as the true monomer in the polymerization. The *p*-quinodimethane system readily polymerizes to give the precursor polymer **11**.

Low temperatures (T< 0 °C), dilute monomer concentrations (0.05 - 0.2 mM) and the use of equimolar or slightly less than one equivalent of base do afford high molecular weight polymers in an excellent yield (up to 90%). [34]

Since an ionic precursor polymer is obtained, GPC measurements are rather difficult and unreliable. Therefore substitution of the remaining sulfonium groups is performed with phenyl thiolate [35] or methoxide [36] anions to give a precursor polymer, which is both soluble in chloroform and THF.

The sulfonium group in the precursor polymer **11** is a good leaving group and as a result the precursor shows reduced stability and undergoes a variety of side reactions, such as substitution and preliminary elimination to create a partial conjugated structure eventually leading to an insoluble product. These possible defect structures are shown in Figure 1-9. [37-38]

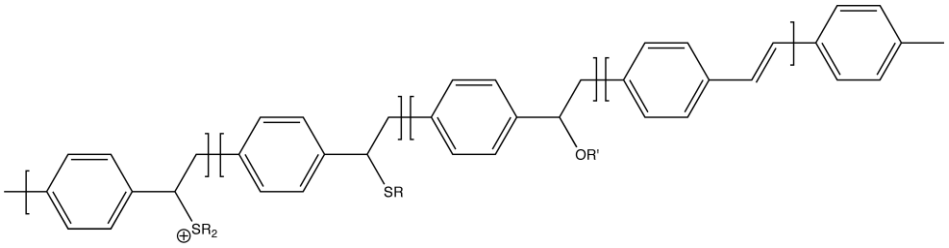


**Figure 1-9: Possible defect structures in a Wessling precursor polymer**

The precursor polymer **11** can be converted into the conjugated analogue **8** by thermal treatment in a temperature range of 160-300 °C during 2 to 20 hours. [39,40]

### 1.1.3 Sulfinyl precursor route

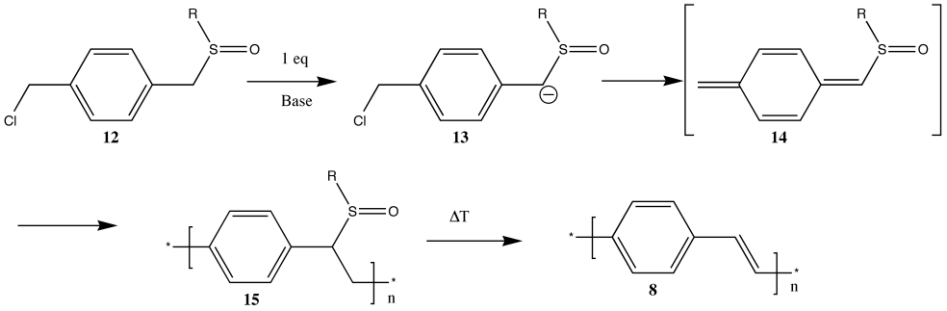


**Figure 1-10: General scheme for the sulfinyl precursor route**

The actual precursor route, which is mainly used in this work, is the sulfinyl precursor route[25]. The two routes described in the previous sections have in common that they use a symmetrically substituted *p*-xylene derivative as the premonomer, in which the same functional group not only acts as a leaving group to yield a *p*-quinodimethane system, but also acts as a polarizer, which is expelled during thermal treatment resulting in the conjugated structure. Due to this symmetry, the polarizer is also a good leaving group and this can cause unwanted side reactions such as substitution or preliminary elimination and hence will have a negative impact on device preparation and performance.

To overcome these problems a non-symmetrically substituted *p*-xylene derivative can be synthesized. This premonomer has a sulfinyl (S=O) group

acting as a polarizer and a halogen as the leaving group. The halogen has as an advantage that it is a good leaving group. In addition, it does not increase the acidity of the $\alpha$-hydrogen much. The polarizer has to fulfill four important functions. It allows for an easy proton abstraction at the benzylic position next to the sulfinyl group, guaranteeing a good *p*-quinodimethane formation. A second function is that it allows a good solubility for the eventual precursor polymer, which makes processability from solution possible. A third key feature of this group is that it is stable at lower temperatures, but that it is easily expelled at elevated temperatures to realize complete elimination to yield the fully conjugated structure. Last but not least, the fourth function is the polarization of the quinodimethane system to ensure regular head to tail coupling during the polymerization. Interestingly, during the elimination process of the sulfinyl group no harmful hydrogen halides are produced unlike the Wessling and Gilch precursor routes. Due to a combination of steric and electronic effects the sulfinyl *p*-quinodimethane systems also guarantee a good head-to-tail addition, resulting in fewer sp and $sp^3$ defect structures as compared to the previously mentioned routes. [41, 42]

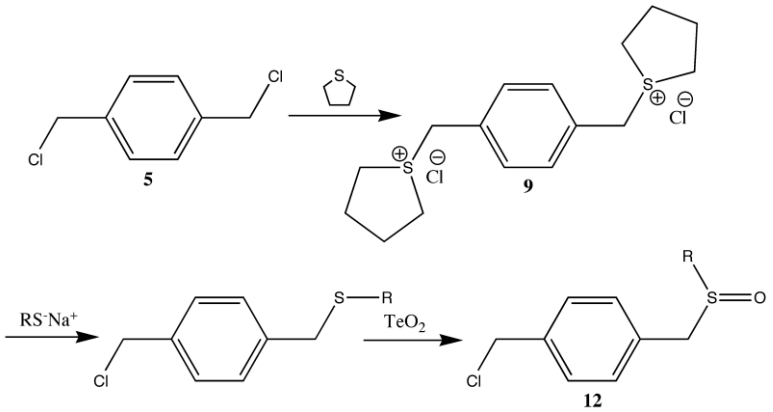


**Figure 1-11: General scheme for the synthesis of sulfinyl premonomer**

The sulfinyl premonomer can be synthesized starting from the Gilch premonomer in 3 easy steps. The first step consists of a nucleophilic substitution, which is straightforward to perform and the reaction has a very high yield. The second step creates the asymmetry to which the sulfinyl route owns its success. This step is not a substitution reaction as would

appear at first sight, but in actuality a quinodimethane system is formed as an intermediate product after deprotonation by the thiolate anion and elimination of a sulfonium group. Addition of the deprotonated alkylthiol and substitution of the sulfonium group by chlorine results in the formation of the sulfanyl premonomer. [43] The resulting premonomer is oxidized to form the sulfinyl premonomer in the last step. A general scheme for the sulfinyl precursor polymerization route is depicted in Figure 1-10. The sulfinyl compound **12** is treated with a base solution resulting in the formation of a benzylic anion **13,** which can undergo a 1,6-elimination to afford the *p*-quinodimethane system **14** being the true monomer in this type of polymerizations. The *p*-quinodimethane systems polymerizes spontaneously to a high molecular weight precursor polymer **15**.

The precursor polymer can be obtained and/or purified by precipitation in a non-solvent and collected through filtration. The precursor is stable at room temperature and conversion to the conjugated structure **8** is achieved by applying a thermal treatment at a temperature of about 100 °C. The sulfinyl route has proven to be a versatile route allowing the polymerization of different PPV derived premonomers, either with electron withdrawing or donating substituents to yield high molecular weight polymers. This is in contrast to the Wessling route where polymerization of electron poor premonomers has failed. [44,45]

The probable mechanism for elimination is a concerted syn-elimination (Figure 1-12), in which the transition state has a planar structure. There are two possibilities for the elimination, one giving a cis-double bond, and the other creating a trans double bond. Sterical hindrance ensures that only trans double bonds are obtained.

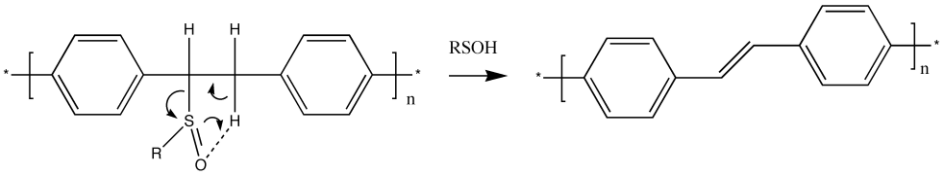


**Figure 1-12: Elimination to form the conjugated system**

### 1.1.4 Xanthate precursor route

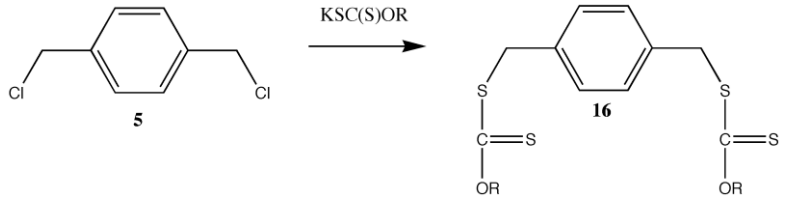


**Figure 1-13: General synthesis of xanthate premonomer**

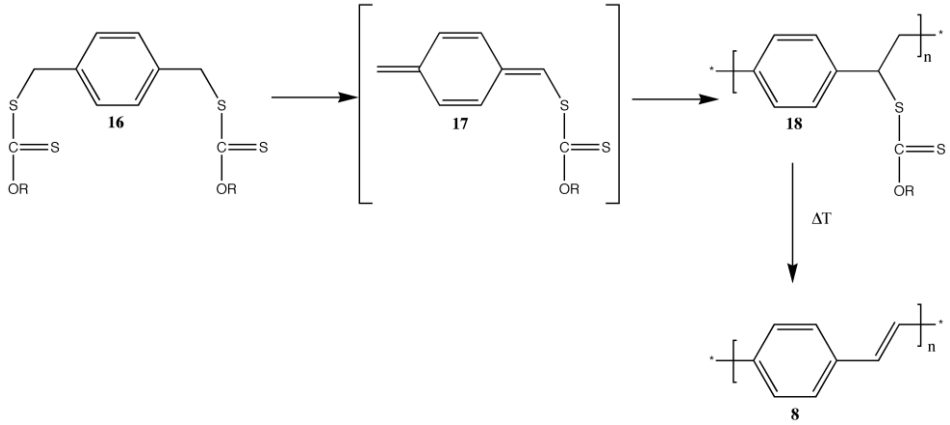


**Figure 1-14: The xanthate precursor route**

In 1995, the xanthate precursor route was developed by Son and co-workers. [26] The premonomer in this route is readily obtained by reacting a $\alpha,\alpha'$-dihalogen *p*-xylene with the commercially available potassium xanthic acid (Figure 1-13). Basic treatment with potassium *t*-butoxide in THF at 0 °C yields a precursor polymer that is soluble in common organic solvents (Figure 1-14). Moderate yields of a high molecular weight polymer can be obtained when the polymerization temperature is sufficiently low.

Elimination of a xanthate group from the precursor polymer is best performed between 160 and 250 °C. Compared to the Wessling route, the xanthate precursor route offers certain advantages, such as the enhanced stability of the precursor.

### 1.1.5 Dithiocarbamate precursor route

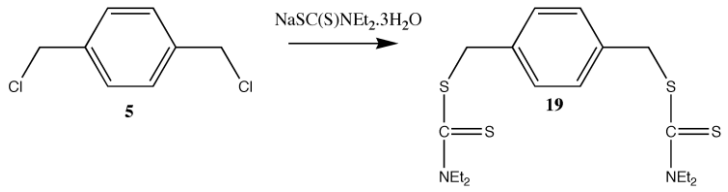


**Figure 1-15: General synthesis of the dithiocarbamate premonomer**

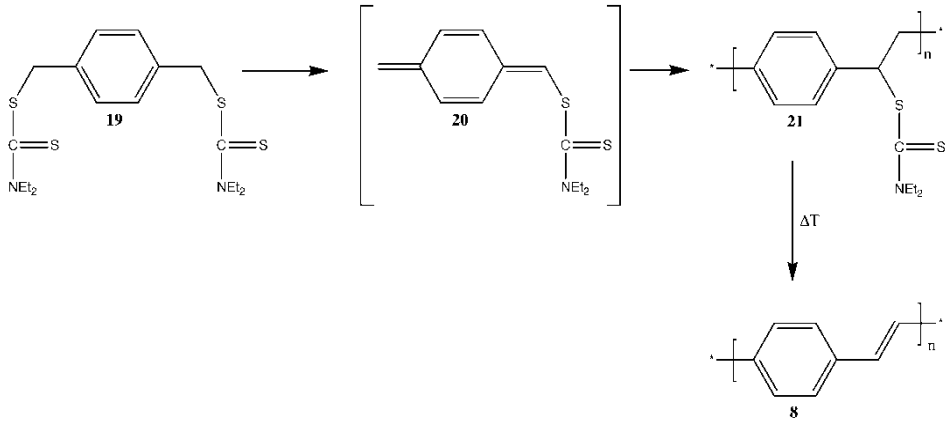


**Figure 1-16: The dithiocarbamate precursor route**

In 2003 Henckens and coworkers reported on a new precursor route, the dithiocarbamate precursor route (Figure 1-16).[27] The synthesis of Poly(thienylene vinylene) PTV and its derivatives[46] and PPV and its derivatives[47] was performed using this route before. However, in both cases the polymerization procedure still needs to be optimized. The premonomer **19** synthesis is more straightforward than the synthesis of the premonomers for the sulfinyl route (Figure 1-15). As will be demonstrated in chapter 5, this polymerization route also yields polymers with a low defect level, which is similar to the sulfinyl route. Therefore we can say that the dithiocarbamate precursor route combines the easy premonomer synthesis of the Gilch route with the superior polymer quality of the more complex sulfinyl route.

# *1.2 Polymerization mechanism*

As discussed in the previous sections, all precursor routes can be represented by a general polymerization scheme consisting of three steps as represented before in Figure 1-5, page 4. The first step is a base induced elimination that leads to the true monomer, namely the quinodimethane system. It is generally accepted that this proceeds through an $E_{1cb}$ reversible elimination mechanism, in which the rate-determining step is the expulsion of the leaving group. This has been verified experimentally for the sulfonium route by Cho and coworkers[48-50] and for the sulfinyl precursor route[51] by our group at Hasselt University.

The next step, *i.e.* the polymerization of the quinodimethane monomer, has been the subject of much debate. It is generally accepted that the polymerization is a chain polymerization, which starts immediately when the initiating particles are formed. For the actual polymerization both radical and anionic mechanisms have been proposed (Figure 1-17).

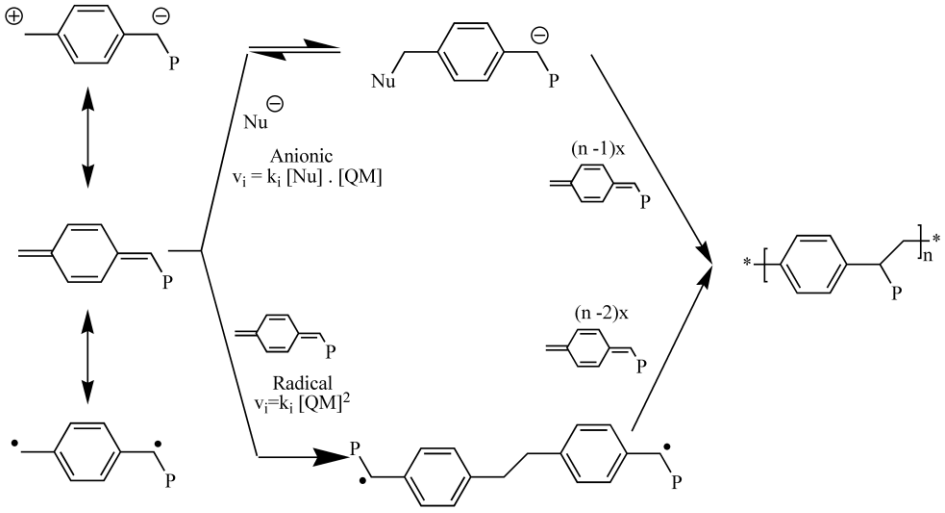


**Figure 1-17: Radical and anionic polymerization mechanism**

In classical polymerizations to synthesize non-conjugated polymers, an anionic polymerization usually takes place with monomers possessing electron-withdrawing groups such as nitrile, carboxyl, phenyl, and vinyl. These polymerizations are initiated by a nucleophilic addition to the double

bond of the monomer. This nucleophile can be an ion such as hydroxide, alkoxide, cyanide or a carbanion. In the absence of impurities, usually no termination will occur. The typical coupling and disproportionation type of termination processes that occur for free radical polymerizations are not possible with anionic polymerizations due to the coulombic repulsion of two negatively charged species. Termination involves a proton transfer from another species such as a solvent, monomer, polymer or water. Non-terminated polymeric species are referred to as "living" polymers. In this case the chain end is still active. If more monomer is added to the system, the polymer will continue to propagate.

In ionic polymerizations a counter-ion is always present. Anionic polymerizations in solution may have association with the counter-ion in the following ways:

| | |
|---|---|
| $P\text{-}M^- X^+$ | *intimate ion pair* (A) |
| $P\text{-}M^- /S/X^+$ | *solvent separated ion pair* (B) |
| $P\text{-}M^- + X^+$ | *pair of free ions* (C) |
| $P\text{-}M^- + S/X^+$ | *solvated ion* (D) |

The more free the anionic end is, the more reactive it will be towards the monomer. Thus, solvent effects can be very important.

In case of living anionic polymerization, the molecular weight can be readily predicted from the amount of starting materials used. When one considers that each initiating molecule can only initiate one chain, that all initiations occur essentially simultaneously and that the anions produced compete equally for the entire amount of monomer present, the number average degree of polymerization, DP, is given by

$$DP = \frac{[M]_0}{[I]_0} \rho$$

where $[M]_0$ and $[I]_0$ are the initial molar concentrations of the monomer and initiator, respectively and $\rho$ is the conversion percentage.

For high polymerization degrees, in which the mass of the initiator and terminator is no longer significant compared to the total mass of the polymer, the molecular weight can be easily calculated by multiplying the degree of polymerization with the molecular weight of the repetition unit.

$$M_n = DP \times M_{uni}$$

In order to prove whether a polymerization is anionic or not, an appropriate initiator is used in different concentration, and a reverse linear relationship should be found when plotting molecular weight *versus* initiator concentration. On the other hand it can be proven that a radical polymerization is likely when the results of the polymerization can be influenced by the use of radical traps (*e.g.* TEMPO) or if radicals can be detected by Electron Paramagnetic Resonance (EPR) spectroscopy.

For the Wessling route an anionic polymerization mechanism was suggested by Latti *et al*..[52] Wessling however suggested a self-initiating radical polymerization mechanism.[32] This view was supported by both Cho *et al.* and the "Amherst group".[44,48] The later proved quite convincingly that the high molecular weight material in the Wessling route was indeed formed through a radical mechanism, and not an anionic mechanism.

For the Xanthate route, no mechanistic investigation was performed as far as we know.

For the Gilch route there is an ongoing discussion in the literature concerning the exact mechanism of polymerization. Both an anionic and a radical mechanism have been proposed. Support for the anionic polymerization can be found in articles from Hsieh *et al.* [53,54] and Ferraris *et al.* [55,56]. The latter even claims the possible occurrence of a living polymerization, "most probably of an anionic nature although radical processes cannot be excluded".

The argument made by Hsieh is based on the use of an anionic initiator, namely 4-*tert*-butylbenzyl chloride as additive.

| *4-tert-butylbenzyl chloride (%)* | *Mw (kD)* | *PD* | *Yield (%)* |
|---|---|---|---|
| 0 | gel | | 71 |
| 5.3 | > 2000 | 3.20 | 66 |
| 34 | 1060 | 3.29 | 50 |
| 40 | 988 | 3.18 | 45 |
| 50 | 350 | 3.80 | 40 |

*** Polymerization conditions: 0 °C, 4.4 mmol *t*-BuOK (1 M), 0.3 mg premonomer, 15 mL THF.**

**Table 1-1: PPV Polymerization* results upon addition of t-BuOK. Results taken from reference 51**

Although the additive has a clear effect, one can notice that the molecular weight still remains high, even when large amounts of additive are used. The author reasons that the additive is possibly consumed in a side reaction, or that a radical polymerization is present. Remark also the decrease in yield when higher amounts of additive are used.

Ferraris observed a similar effect using the additive 4-methoxyphenol in the Gilch polymerization. The drastically lower polydispersity obtained is claimed to be caused by the introduction of a "reversed addition" procedure in which the premonomer **1** is added to the base solution instead of base to a premonomer solution. Reversed addition would also promote anionic polymerization according to the article. Table 1-2 shows a clear effect of the additive on the molecular weight. However, the polydisperisity increases and the yield decreases when adding more additive to the reaction mixture. The claim for anionic polymerization is also here doubtful, since a decrease in yield when adding more initiator is not expected.

| *4-methoxyphenol (%)* | *$M_n$ (kD)* | *PD* | *Yield (%)* |
|---|---|---|---|
| 0 | 125.7 | 1.06 | 72 |
| 0.5 | 118.2 | 1.04 | 68 |
| 1.0 | 86.2 | 1.14 | 67 |
| 1.5 | 57.7 | 1.43 | 56 |
| 2.0 | 51.3 | 1.52 | 50 |

**Table 1-2: Effect of 4-methoxyphenol on the Gilch polymerization. Results taken from reference 53**

Recent work of our group[57,58] and also Rehahn[59,60] *et al*, substantiate that radical processes occur and are responsible for the formation of high molecular weight polymer in the Gilch route. A recent article of Rehahn suggests that the previously obtained results of Hiesh *et al*. and Ferraris *et al*. can be explained by the plasticizing effects of the additives used in their studies. The article suggests that the additive speeds up the detangling of the physical gel that forms during a classical Gilch polymerization. This would explain the link that was found between the amount of additive (anionic initiator) used and the molecular weight, even though the polymerization is radical in nature.

Many years ago when our laboratory studied the sulfinyl precursor route in N-methylpyrrolidone (NMP) as the solvent, we stumbled upon a bimodal behavior of the polymerization reaction (Figure 1-18). [61] Later it was proven that the high molecular weight material originated from a radical polymerization and the low molecular weight material from an anionic polymerization.[62-64] The low molecular weight part (OM), with a molecular weight typically less than 6 000, disappeared by addition of a small amount of water. To our knowledge there is no example in which unambiguously an anionic polymerization was observed for *p*-quinodimethane systems except for this example.

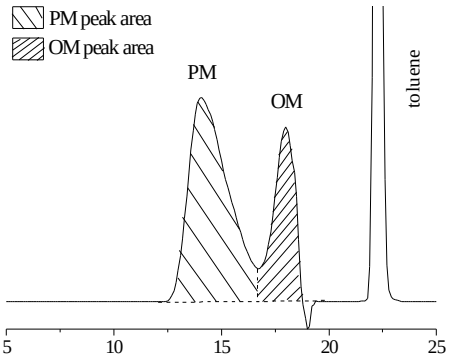


**Figure 1-18: Typical GPC-chromatogram for the polymerization of 12 in NMP. Results taken from reference 60**

The base (nucleophile) concentration appears explicitly in the expression of the initiation rate for the anionic polymerization and not for the radical

initiation. As a result a specific sensitivity for the initial base concentration *versus* initial premonomer concentration can be expected. An experiment that can demonstrate this hypothesis unambiguously is the effect of reversed addition (adding the premonomer solution to the solution of the base) on the polymerization result. All the other conditions were kept constant. (Table 1-3). To describe the extend of competition; the relative integrated surface in the GPC chromatogram of the polymer [PM] fraction *versus* the oligomer [OM] fraction is used, taking the sum of both surfaces as 100%.

| *Addition* | *Yield (%)* | *$M_w$ [PM] (kD)* | *PD [PM]* | *% [PM]* | *$M_w$ [OM] (kD)* |
|---|---|---|---|---|---|
| Normal | 61 | 170 | 2.5 | 87 | 3.5 |
| Reversed | 41 | 10.4 | 1.2 | 36 | 2.9 |

**Table 1-3: Results of polymerizations of premonomer – reversed compared to normal addition (Na*t*BuO, NMP), Results taken from reference 60**

Clearly reversed addition has a tremendous effect on the amount of polymer formed (% [PM]). These conditions, *i.e.* the high initial base concentration, apparently promote anionic initiation over radical dimerization. A second experiment, which can demonstrate the competition between anionic and radical initiation present under current reaction conditions, is a polymerization at lower temperature. As anionic initiation is typically a process with a low activation energy, it can be expected that lowering the polymerization temperature will increase the fraction of oligomers formed (Table 1-4). As expected, this is indeed observed. This effect can be solely related to the anionic polymerization, since the lowering of the temperature would actually increase the molecular weight for a radical polymerization.[65]

| *Temp.* | *Yield (%)* | *$M_w$ [PM] (kD)* | *PD [PM]* | *% [PM]* | *$M_w$ [OM] (kD)* |
|---|---|---|---|---|---|
| 25 °C | 68 | 182 | 2.6 | 90 | 3.0 |
| 0 °C | 43 | 54.0 | 2.1 | 52 | 3.3 |

**Table 1-4: Results of polymerizations of premonomer at 0 °C and 25 °C (Na*t*BuO, NMP). Results taken from reference 59**

These observations give a clear insight in the features of the anionic polymerization. It can be expected that the above drawn conclusions are quite general for the anionic polymerization of *p*-quinodimethane systems. This implies that typically for such polymerizations low molecular weight

materials are obtained. In this example termination could occur from deprotonation of the solvent (NMP: $pK_s$ 24). A second source of termination of the anionic species could come from the protonated base, which is formed during the reaction leading to the *p*-quinodimethane system (Figure 1-5, page 4). Since this process is a base induced reaction, one equivalent of *t*-butanol is formed, which can act as a proton donor for the anionic species. This process actually excludes a living anionic mechanism when tert-butoxide is used as the base. Furthermore, it implies that the use of a stronger base, *e.g.* lithiumdi(isopropyl)amide (LDA) in a strong aprotic solvent, *e.g.* tetrahydrofurane (THF) could create the condition towards controlled polymerization of *p*-quinodimethane systems.

## *1.3 Influence of polymerization parameters on the polymerization mechanism*

After this overview of the polymerization methods and mechanisms it is important to discuss the influence of the different polymerization parameters on the polymerization process. This will be done for the synthesis of sulfinyl precursor PPV, unless stated otherwise. The general aim of this discussion is to gather insight how the polymerization should behave when conditions are altered and to identify the actual conditions to obtain a full anionic polymerization. The advantage of anionic polymerization is the lack of significant termination or chain transfer reactions. Anionic polymerizations typically are carried out to close to 100% monomer conversion. If more monomer is added, and termination or chain transfer can be avoided, the living polymer reacts with the added monomer until it is also spent, still maintaining the reactive anion. Anionic polymerization of PPVs could enable the construction of polymers with specific end groups, block copolymers or more exotic architectures. These polymers in turn could be beneficial in a wide range of applications such as solar cells, FET or bio-sensors.

### 1.3.1 Influence of the temperature

As stated in the previous sections, the polymerization of sulfinyl premonomers in NMP yields a bimodal molecular weight distribution. Lowering of the temperature of this polymerization increases the amount of oligomers formed. Good evidence is available for the dimerization of a minor fraction of quinodimethane molecules into diradicals, which act as the initiating moiety in the radical polymerization mechanism. An anionic pathway can also be envisioned by the reaction of a nucleophile with one quinodimethane molecule. Since the anionic initiation typically is a process with a low activation energy compared to the radical initiation, it can be expected that a lowering of the temperature will indeed increase the relative amount of anionic polymerization, yielding a higher fraction of oligomers. The energy required for such a reaction is probably lower than what would be expected for the formation of the diradical radical initiator. The formation of a quinodimethane molecule is also much slower at lower temperatures. Therefore the temperature must have an effect on the competition between the anionic and radical mechanism in systems in which both mechanisms are active.

It is noteworthy that the molecular weight of the polymer fraction decreases upon lowering the temperature (Table 1-4, page 17). However, this is not an intrinsic quality of the radical polymerization, since when the polymerizations are performed in s-butanol, in which only a radical polymerization is possible, the molecular weight increases when lowering the temperature (Table 1-5). Therefore the reason for the lowering of molecular weight of the polymerization performed in NMP is most likely caused by a shortage of monomer.

Hence, it can be concluded that lowering the temperature increases the amount of anionic polymerization in case of competition. However, no relevant increase in the molecular weight of the oligomer fraction was observed.

| *Temperature (°C)* | *Yield (%)* | *$M_w$ (kD)* | *PD* |
|---|---|---|---|
| 75 | 90 | 150 | 1.80 |
| | 89 | 145 | 1.95 |
| 50 | 88 | 370 | 2.27 |
| | 83 | 450 | 2.85 |
| 30 | 78 | 535 | 2.98 |
| | 80 | 560 | 2.66 |
| 0 | 73 | 685 | 2.45 |
| | 65 | 680 | 2.96 |

**Premonomer dissolved in 14 mL sec-butanol, initial premonomer concentration [M]i = 143 mM; base (sodium tert.butoxide) dissolved in 6 mL sec-butanol; , initial base concentration [B]i = 434 mM; [B]i/[M]i = 3.03; base added to solution of premonomer**

**Table 1-5: Effect of temperature on the polymerization of sulfinyl premonomer in sec-butanol. Results taken from reference 63**

### 1.3.2 Influence of the premonomer concentration

Since a fully anionic polymerization procedure has never been observed for the sulfinyl premonomer, the effect of premonomer concentration could only be investigated for the radical polymerization.

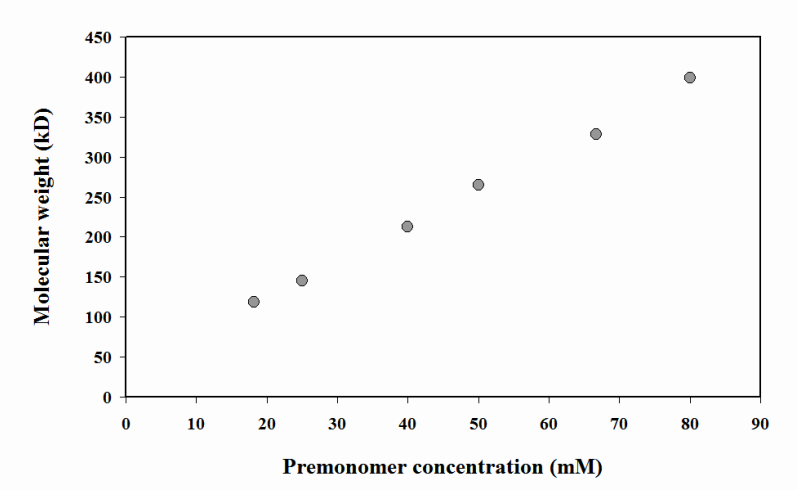


**Figure 1-19: Effect of premonomer concentration on the polymerization in s-butanol. Results taken from reference 63.**

For the radical polymerization of the sulfinyl premonomer in s-butanol, there is a very clear effect of the initial premonomer concentration (Figure 1-19). When the polymerization is attempted below a certain premonomer concentration, the polymerization will not succeed. Possibly, there has to be a minimum build-up of quinodimethane systems to create the initiating diradical. It is believed that the anionic polymerization does not have such a restriction.

### 1.3.3 Influence of the solvent and the counterion

The propagation rate constant and the polymerization rate for an anionic polymerization are usually dramatically affected by the nature of both the solvent and the counterion present. The pronounced effect of the solvent in the polymerization of styrene by sodium naphthalene is shown in Table 1-6. The apparent propagation rate constant is increased by 2 and 3 orders of magnitude in tetrahydrofuran and 1,2-dimethoxyethane, respectively, compared to the rate constants in benzene and dioxane. The polymerization is much faster in the more polar solvents. The increase in $K_p^{app}$ with increased solvating power of the reaction medium is mainly due to the increased fraction of free ions present, relative to ion pairs.

| *Solvent* | *Dielectric Constant ()* | *$K_p^{App}$ (L mol-1 s-1)* |
|---|---|---|
| Benzene | 2.2 | 2 |
| Dioxane | 2.2 | 5 |
| Tetrahydrofuran | 7.6 | 550 |
| 1,2-dimethoxyethane | 5.5 | 3800 |

**Table 1-6: Effect of solvent on anionic polymerization of styrene*. Results taken from reference 66**

The kinetics of the polymerization is also dependent on the counterion. In a polar solvent such as THF, the smaller $Li^+$ is most solvated, whereas the larger $Cs^+$ is the least solvated. This means that the relative amount of free anions is larger in case $Li^+$ is used as the counterion. Therefore, the polymerization is also faster as compared to the use of $Cs^+$ as the counterion.

In case a protic solvent is used, no anionic polymerization can exist, as the reactive anion at the chain end would be protonated by the solvent. In a protic solvent, the strength of the base is determined by the $pK_s$ value of the solvent. When an aprotic solvent is used, a competition is possible between the anionic and radical polymerization of the sulfinyl premonomer.

Analogous to the polymerization of styrene, we expect the anionic polymerization of PPV-type polymers to proceed faster in polar solvents, such as THF, as opposed to apolar solvents such as hexane and benzene.

### 1.3.4 Influence of the initial concentration of base and premonomer [67]

The various reactions in Table 1-7 differ from each other in initial concentrations, *i.e.* the division of the solvent (20 mL) over the premonomer and the base solutions prior to the polymerization reaction. The polymerization procedure has a global monomer concentration of 0.1 M (0.09 M for the second entry) after the base has been added. An increase of initial base concentration results in a decrease in the polymer molecular weight and an increase in the relative amount of oligomers present. This can be interpreted as an indication that the mechanisms of polymer and oligomer formation are in competition with each other. To describe the extend of competition; the relative integrated surface in the GPC chromatogram of the polymer (PM) fraction *versus* the oligomer (OM) fraction is used.

| *Ratio* mL(M)[a]/mL(B)[b] | *Total Yield (%)* | $[B]_i$ *(mM)* | $[M]_i$ *(mM)* | $\frac{[B]_i}{[M]_i}$ | $M_w$ *[PM] (kD)* | *PD [PM]* | *% PM* | $M_w$ *[OM] (kD)* |
|---|---|---|---|---|---|---|---|---|
| 14 / 6 | 38 | 0.37 | 0.14 | 2.6 | 77.0 | 1.9 | 68 | 3.2 |
| 14 / 8 | 40 | 0.28 | 0.14 | 2.0 | 123 | 2.4 | 80 | 2.9 |
| 10 / 10 | 69 | 0.22 | 0.20 | 1.1 | 182 | 2.6 | 90 | 3.0 |

**[a] amount of solvent in which the premonomer is dissolved; [b] amount of solvent in which the base is dissolved; $[B]_i$: initial base concentration; $[M]_i$: initial premonomer concentration**

**Table 1-7: Overview of results of polymerizations of the premonomer using various initial concentrations. Results taken from reference 59.**

We would like to recall here that in case only a radical polymerization occurs, changes of initial base or premonomer concentration do not give rise to strong variations in the outcome of the polymerization reaction. In other words, these results seem to point more to the conclusion that the more competitive the anionic mechanism is, the lower the molecular weight of the PM-fraction. In one way this should not be too surprising, as the more competitive the anionic mechanism is the less *p*-quinodimethane system is available for the radical polymerization, and the lower the obtained molecular weight will be for the PM-fraction.

### 1.3.5 Influence of the substituents

The substituents on the benzene ring of the monomer have a significant influence on the polymerization mechanism. Generally speaking, electron donating substituents promote the radical polymerization mechanism, and electron withdrawing the anionic mechanism. In addition, the yield is usually higher for monomers bearing electron donors.[64]

## *1.4 Application of PPV-type polymers in biosensors*

As stated before, the anionic polymerization of PPVs can yield polymers with unique architecture, but perhaps more importantly defined functional end groups. These functional end groups can be especially useful for the development of biosensors, as bio-molecules could be attached to these functional end groups.

Biosensors represent a rapidly expanding field, the major drive coming from the health-care industry but with some pressure from other areas, such as food quality assessment and environmental monitoring. Most of this current endeavor concerns potentiometric and amperometric biosensors and colorimetric paper enzyme strips.

A biosensor is an analytical device, which converts a biological response into an electrical signal. The biologically responsive material could be enzymes, antibodies, receptors, nucleic acids, whole cells, organelles or tissues.

Furthermore there is a transducer or detector element that transforms the signal resulting from the interaction of the analyte with the biological element into another signal that can be more easily measured and quantified.

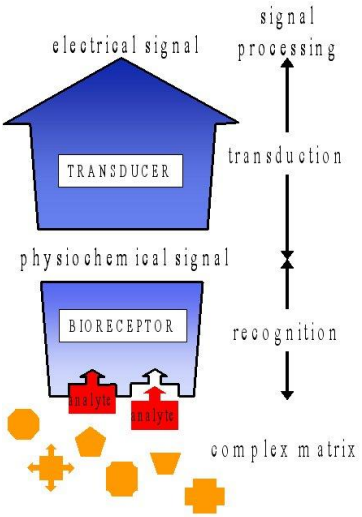


**Figure 1-20: Schematic diagram showing the main components of a biosensor**

The electrical signal from the transducer is often low and superimposed upon a relatively high and noisy baseline. The signal processing normally involves subtracting a 'reference' baseline signal, derived from a similar transducer without any biocatalytic membrane, from the sample signal, amplifying the resultant signal difference and electronically filtering (smoothing) out the unwanted signal noise. The relatively slow nature of the biosensor response considerably eases the problem of electrical noise filtration. The analog signal produced at this stage may be used as output directly but is usually converted to a digital signal and passed to a microprocessor stage at which the data are processed, converted to concentration units and outputted to a display or data storage device.

In recent years, an increased number of papers is published dealing with biosensors utilizing electrically conducting polymers in the transducer layer.[68,69] Conjugated polymers are promising transducer materials for biosensors, as they have an organic surface chemistry, which facilitates interactions with biological macromolecules. The read-out can occur *via* electronic and/or

fluorescence techniques. Fabrication of polymer based sensors is relatively low-cost, making them suitable for single use application and mass production.

Furthermore, conjugated polymers may also be quite effective in fluorescence-based biosensors as they contain a chromophore requiring low energy for excitation of an electron. Since it is highly delocalized, the excited electron can travel along the polymer until fluorescence or quenching occurs. Since the exiton can travel across the polymer backbone, it can 'sample' many receptor sites, causing it to be more sensitive. A fluorescence based biosensor has two modes of action. The fluorescense can be quenched in the presence of the analyte producing a 'turn-off' biosensor, or its fluorescence quenching is suppressed by the presence of the analyte producing a 'turn-on' biosensor.

During the past years, major progress was made in the Materials Physics research group (IMO) with impedimetric immunosensors based on thin films of MDMO-PPV.[70] Antibodies were immobilized on the spin coated polymer by physical adsorption from buffer solutions. The biofilm was tested in a prototype biosensor. From the first impedance measurements, it was concluded that antibodies could be successfully adsorbed onto a MDMO-PPV film while keeping their biological activity. The conjugated layer demonstrated a good sensitivity while converting the recognition event in a distinctive difference. Antigen concentrations as low as 10 pmol/mL were detected within minutes.

However, there were some drawbacks associated with immunosensors based on thin films of MDMO-PPV. First of all, non-specific interactions on the MDMO-PPV polymers film may result in fouling of the sensor surface. Moreover, the stability of the bio-functionalized MDMO-PPV films leaves room for improvement. Since the antibodies were immobilized on the spin coated polymer layer by physical adsorption, the bond between the polymer and the biomolecules is based on hydrophobic interactions instead of covalent bonds. These interactions have a tendency to denature antibodies and have a negative impact on the biosensor lifetime and stability. Due to the random immobilization of the antibodies, the sensitivity is lower.

If the antibodies, or other biomolecules, were bound to the polymer film by strong covalent bonds, one might expect higher stability of the biofilm and lower denaturization of the antibodies. More control would be gained over the orientation in which the antibodies are immobilized and therefore, higher sensitivity could be obtained.

In 2006, an immunosensor based on the thin film of a copolymer (MDMO-CPM)-PPV was tested.[71] The carboxylic acid-functionalized PPV was used to provide the covalent bonding to the antibodies. Since the density of carboxylic acid functionalities in pure CPM-PPV was found to be too high, a copolymer with MDMO-PPV was used. Contact angle measurements of distilled water with a film of the copolymer (MDMO-CPM)-PPV with different concentrations of immobilized antibody concentrations revealed that the antibodies also physically adsorb on the copolymer.

By using a controlled anionic polymerization, we hope to achieve similar results, with a different approach. Previously mentioned co-polymers were physically attached to the substrate by spin-coating. Even though that the layer of polymer is very thin, 100nm, it is still considerably thicker than needed. We would envision an ideal biosensor as a single layer of PPV-material, to which the antibodies are covalently attached. This could be achieved by self-assembly of a PPV-material, which has two different end functionalities on its chain. One functionality would attach firmly to a substrate; the other to the bio-molecule. Or by growing PPV polymer on a pre-treated surface using anionic polymerization. Both cases would result in having a biosensor with a thin transducer layer and chemically bounded links between carrier and PPV and PPV and antibody.

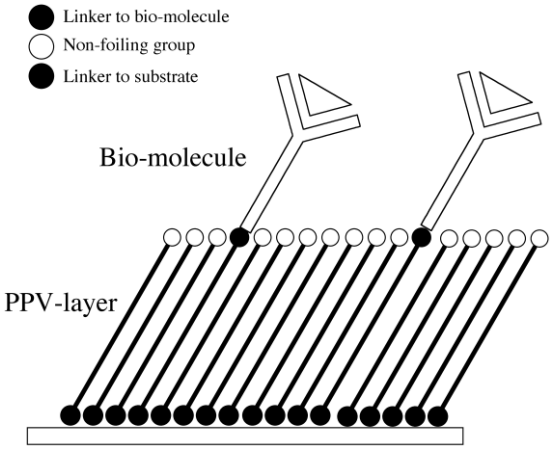


**Figure 1-21: Proposal for biosensor using self-assembled PPV layer**

Controlled anionic polymerization is the first step in the making of such biosensors. We would need to have good control over the initiation reaction, the termination and chain length. Although this could also be achieved through controlled radical polymerization, this work will only focus on the anionic polymerization. In addition, control over the end groups will be essential.

## *1.5 Aim and outline of the thesis*

The goal of this thesis is to study the presence of anionic and radical mechanism in the polymerization of poly(*p*-phenylene vinylene) and to optimize the anionic polymerization. In order to favor the anionic polymerization, an aprotic polar solvent has to be used. Protic solvents would quickly protonate the growing anionic chain and stop the polymerization, this in contrast to radical polymerizations, which can be performed in protic solvents such as s-butanol. Consequently the aprotic polar solvent, tetrahydrofuran (THF) was chosen as a suitable reaction medium. To deprotonate the premonomer, the base does not need to be very strong. However, the conjugated acid has to be weak enough to prevent protonation of the growing anionic polymer. This is why a relatively strong base has to be used, *e.g.* lithiumdi(isopropyl)amide (LDA). The used base has to be non-nucleophilic, since we do not wish the base to act as initiator and a nucleophile can act as an initiator for the anionic

polymerization. In the past, after the precipitation of a polymer synthesized with s-butoxide as the base, solvent substituted premonomer was often found in the filtrate.

To further promote the anionic polymerization, 'slow reversed addition' is used, *i.e.* the premonomer is slowly added to a solution of the base. It is called reversed because in the past all polymerizations were performed by adding the base in one shot to a solution of premonomer (fast normal addition). The presence of air can be detrimental to both the radical[72] as the anionic polymerization. Therefore it has to be excluded from the reaction medium as good as possible. Water must be excluded as well, since this will terminate any growing anionic chains. In order to exclude these impurities, dried and distilled THF was used and all polymerizations were performed under a nitrogen atmosphere. All glassware was flamed under vacuum and premonomer was also dried under vacuum.

In **chapter 2** a first attempt is made to achieve a fully anionic polymerization to synthesize MDMO-PPV. By changing the base from LDA to LHMDS, oligomers are obtained with a rather low molecular weight. It is shown that the reason for this low molecular weight originates from a less then optimal premonomer purity.

Based on the conclusions of chapter 2, another premonomer is chosen in **chapter 3**. When synthesizing unsubstituted PPV *via* the same method as in chapter 2, a higher molecular weight is obtained. We verified that LHMDS is a better base for the polymerization, and that the polymerization is indeed anionic in nature. We explored the effect of changing some of the polymerization parameters, in order to come to an optimized polymerization technique.

In **chapter 4** the use of initiators is explored as well as the concept of end capping. The initiator choice and the synthesis of relevant initiators is discussed. Using these initiators, the obtained molecular weight can be varied. A clear linear relationship is found between $M_n^{-1}$ and the amount of initiator used.

In the **final chapter**, $^{13}C$ labeling is used to identify defects in the different precursor routes. In previous studies the Gilch and sulfinyl precursor routes were already investigated for defects in the polymer chain. This study was extended to include the dithiocarbamate route. Also for the anionic polymerization of MDMO-PPV *via* the sulfinyl route such $^{13}C$ labeling study has been performed (see chapter 3).

The dissertation is completed with two summaries: one in Dutch, followed by one in English.

## 1.6 References

[1] J.H. Burroughes; D.D.C. Bradley; A.R. Brown; R.N. Marks; K. Mackay; R.H. Friend; P.L. Burn; A.B. Holmes, *Nature*, **347**, 539, (1990)
[2] D. Braun; A.J. Heeger, *Appl. Phys. Lett.*, **58**, 1982, (1991)
[3] Q. Pei; G. Yu; C. Zhang; Y. Yang; A.J. Heeger, *Science*, **269**, 1086, (1995)
[4] Q. Pei; Y. Yang, *Synthetic Metals*, **80**, 131, (1996)
[5] G. Yu; C. Zhang; A.J. Heeger, *Appl. Phys. Lett.*, **64**, 1540, (1994)
[6] G. Yu; K. Pakbaz; A.J. Heeger, *Appl. Phys. Lett.*, **64**, 3422, (1994)
[7] G. Yu; J. Gao; J.C. Hummelen; F. Wudl; A.J. Heeger, *Science*, **270**, 1789, (1995)
[8] J.J.M. Halls; C.A. Walsh; N.C. Greenham; E.A. Marseglia; R.H. Friend; S.C. Moratti; A.B. Holmes, *Nature*, **376**, 498, (1995)
[9] H. Koezuka; A. Tsumara; T. Ando, *Synthetic Metals*, **18**, 699, (1987)
[10] A. Assadi; C. Svensson; M. Wilander; O. Inganäs, *Appl. Phys. Lett.*, **53**, 195, (1988)
[11] G. Yu; K. Pakbaz; C. Zhang; A.J. Heeger, *J. Electron. Mater.*, **23**, 925, (1994)
[12] D. Moses, *Appl. Phys. Lett.*, **60**, 3215, (1992)
[13] H.J. Brouwer; V.V. Krasnikov; A. Hilberer; J. Wildeman; G. Hadziioannou, *Appl. Phys. Lett.*, **66**, 3404, (1995)
[14] N. Tessler; G.J. Denton; R.H. Friend, *Nature*, **382**, 695, (1996)
[15] F. Hide; M.A. Díaz-García; B.J. Schwartz; M.R. Andersson; Q. Pei; A.J. Heeger, *Science*, **273**, 1833, (1996)
[16] H.J. Brouwer; V.V. Krasnikov; A. Hilberer; G. Hadziioannou, *Adv. Mater.*, **8**, 935, (1996)
[17] H. Hörhold; H. Opfermann, J. *Makromol. Chem*., **131**, 105, (1970)
[18] R. W. Lenz; C. E. Handlovits, *J. Org. Chem*., **25**, 813, (1960)
[19] N. C. Greenham; S. C. Moratti; D. D. C. Bradley; R. H. Friend; A. B. Holmes, *Nature*, **365**, 628, (1993)
[20] R. F. Heck, *Accounts Chem. Res*., **12**, 146, (1979)
[21] F. Wudl; G. Sardanov, *US Patent* 5, **189**, 136, (1993)
[22] H. Becker; H. Spreitzer; W. Kreuder; E. Kluge; H. Schenk; I. Parker; Y. Cao, *Adv. Mater.*, **12**(1), 42, (2000)

[23] H. G. Gilch; W. L. Wheelwright, *J. Polym. Sci. Part A: Polym. Chem.*, **4**, 1337, (1966)
[24] a) R. A. Wessling, R. G. Zimmerman, *US Patent 3,401,152,* (1968); b) R.A. Wessling; R. G. Zimmerman, *US Patent 3,706,677,* (1972)
[25] F. Louwet; D. Vanderzande; J. Gelan; J. Mullens, *Macromolecules*, **28**, 1330, (1995)
[26] S. Son; A. Dodabalapur; A. J. Lovinger; M. E. Galvin, *Science*, **269**, 376, (1995)
[27] A. Henckens; L. Lutsen; D. Vanderzande; M. Knipper; J. Manca; T. Aernouts; J. Poortmans, *Proc. SPIE Int. Soc. Opt. Eng.*, **52***,* 5464, (2004)
[28] W. J. Swatos; B. Gordon, *Polym. Prepr.,* **31**(1), 505, (1990)
[29] D. Braun; E.G.J. Staring; R.C.J.E. Demandt; G.L.J. Rikken; Y.A.R.R. Kessener; A.H.J. Venhuizen, *Synthetic Metals,* **66**, 75, (1994)
[30] B.R. Hsieh; W.A. Field, *Polym. Prepr.,* **34**, 410, (1993)
[31] G.J. Sarnecki; P.L. Burn; A. Kraft; R.H. Friend; A.B. Holmes, *Synthetic Metals*, **55-57**, 914, (1993)
[32] R. A. Wessling, *J. Polym. Sci., Polym. Symp*., **72**, 55, (1985)
[33] R. W. Lenz; C.-C. Han; J. Stenger-Smith; F. E. Karasz, *J. Polym. Sci. Polym. Chem*., **26**, 3241, (1988)
[34] R. Garay; R. W. Lenz, *Makromol. Chem. Suppl*., **15**, 1, (1989)
[35] J. M. Machado; F. R. Denton; J. B. Schlenoff; F. C. Karasz; P. M. Lathi, *J. Polym. Sci. Part B: Polym. Phys.*, **27**, 199, (1989)
[36] M. J. Cherry; S. C. Moratti; A. B. Holmes; P. L. Taylor; J. Grüner; R. H. Friend, *Synthetic Metals*, **69**, 493, (1995)
[37] J. Gmeiner; S. Karg; M. Meier; W. Riess; P. Strhriegl; M. Schwoerer, *Acta Polym*., **44**, 201, (1993)
[38] B. R. Hsieh; H. Antoniadis; M. A. Abkowitz; H. Stolka, *Polym. Prepr.*, **33**, 414, (1992)
[39] R. O. Garay; U. Baier; C. Bubeck; K. Mullen, *Adv. Mater.*, **5**, 561, (1993)
[40] C. Zhang; D. Braun; A. J. Heeger, *J. Appl. Phys.*, **76**, 5177, (1993)
[41] H. Roex, *PhD Dissertation*, Limburgs Universitair Centrum, Diepenbeek, (2003)

[42] H. Roex; P. Adriaensens; D. Vanderzande; J. Gelan, *Macromolecules*, **36**, 5613, (2003)
[43] A. J. J. M. van Breemen, D. J. M. Vanderznade, P. J. Adriaensens; J. M. J. V. Gelan, *Journal of Organic Chemistry*, **64**, 3106, (1999)
[44] F. R. Denton; A. Sarker; P. M. Lahti; R. O. Garay; F. E. Karasz, *J. Polym. Sci. Part A: Polym. Chem.*, **30**, 2233, (1992)
[45] A. Sarker; P. M. Lahti, *Polym. Prepr.*, **35**(1), 790, (1994)
[46] A. Henckens; K. Colladet; S. Fourier; T. J. Cleij; L. Lutsen; J. Gelan, *Macromolecules*, **38**(1),19, (2005)
[47] A. Henckens; I. Duyssens; L. Lutsen; D. Vanderzande; T. J. Cleij, *Polymer*, **47**, 123, (2006)
[48] B. R. Cho; Y. K. Kim; M. S. Han, *Macromolecules*, **31**, 2098, (1998)
[49] B. R. Cho; M. S. Han; Y. S. Suh; K. J. Oh; S. J. Jeon, *J. Chem Soc, Chem Commun*., 564, (1993)
[50] P. M. Lahti; D. A. Modarelli; F. R. Denton; R. W. Lenz; F. E. Karasz, *J. Am. Chem. Soc.*, **110**, 7258, (1988)
[51] A. Issaris; D. Vanderzande; P. A. Adriaensens; J. Gelan, *Macromolecules*, **31** (14), 4426, (1988)
[52] P.M. Lathi; D.A. Moderelli; F.R. Denton II; R.W. Lenz; F.E. Karasz, *J. Am Chem. Soc.*, **30**, 2223, (1988)
[53] B. R. Hsieh; Y. Yu; A. C. VanLaeken; H. Lee, *Macromolecules*, **30**, 8094, (1997)
[54] B. R. Hsieh; Y. Yu; E. W. Forsythe; G. M. Schaaf; W. A. Feld, *J. Am. Chem. Soc.*, **120**, 231, (1998)
[55] C. J. Neef; J. P. Ferraris, *Macromolecules*, **33**, 2311, (2000)
[56] C. J. Neef; J. P. Ferraris, *Macromolecules*, **37**, 2671, (2004)
[57] L. Hontis; L. Lutsen; D. Vanderzande; J. Gelan, Synthetic Metals, **119**, 135, (2001)
[58] L. Hontis; V. Vrindts; D. Vanderzande; L. Lutsen, *Macromolecules*, **36** (9), 3035, (2003)
[59] J. Wiesecke; M. Rehahn, *Angew. Chem. Ind. Ed.*, **42** (5), 567, (2003)
[60] J. Wiesecke; M. Rehahn, *Polymer Preprints*, **45** (1), 174, (2004)
[61] F. Louwet; D. Vanderzande; J. Gelan, *Synthetic Metals*, **69**, 509, (1995)

[62] L. Hontis; M. Van Der Borght; D. Vanderzande; J. Gelan, *Polymer*, **40**, 6615, (1999)
[63] M. Van Der Borght; D. J. M. Vanderzande; P. Adriaensens; J. Gelan, *Polymer*, **41** (8), 2743, (2000)
[64] P. Adriaensens; M. Van Der Borght; L. Hontis; A. Issaris; A. van Breemen; M. de Kok; D. Vanderzande; J. Gelan, *Polymer*, **41**, 7003, (2000)
[65] D. Vanderzande; L. Hontis; A. Palmaerts; D. Van Den Berghe; J. Wouters; L. Lutsen; T. Cleij, *SPIE*, **5937**, 59370Q, (2005)
[66] "Principles of polymerization", fourth edition, George Odian, Wiley-Interscience
[67] L. Hontis, *PhD dissertation*, Limburgs Universitair Centrum, Diepenbeek, (2002)
[68] M. Gerard; A. Chaubey; B. D. Malhotra, *Biosensors and Bioelectronics*, **17**, 345-359, (2002)
[69] G. G. Wallace; M. Smyth; H. Zhao, *Trends in Analytical Chemistry*, **18**(4), 245-251, (1999)
[70] P. Cooreman; R. Thoelen; J. Manca; M. vandeVen; V. Vermeeren; L. Michiels; M. Ameloot; P. Wagner, *Biosensors and Bioelectronics*, **20**, 2151-2156, (2005)
[71] I. Van Severen; P. Cooreman; R. Thoelen; L. Lutsen; P. Wagner; D. Vanderzande; T. Cleij, *American Chemical Society*, (2006)
[72] T. Schwalm; M. Rehahn, *Macromolecular Rapid Communications*, **29**, 207-213, (2008)

# Chapter 2

# Mechanistic study on the sulfinyl route towards MDMO-PPV

*Abstract: This chapter focuses on the synthesis of MDMO-PPV via an anionic polymerization mechanism. First a short description of the research done by Lieve Hontis is given. During her research into the reaction mechanism of the sulfinyl route, a polymerization procedure was found where anionic and radical polymerization occurs simultaneously. From this starting point we commence the search for a fully anionic polymerization of PPV.*

*The use of lithium diisopropylamide (LDA) and lithium hexamethyldisilazide (LHMDS) as the base in the polymerization of MDMO-PPV is elaborated. Higher molecular weight and more pure polymer is obtained when LHMDS is used. The structure of the polymer obtained using LHMDS was investigated using a $^{13}C$-labeled monomer. This investigation leads to the conclusion that the premonomer purity plays a crucial role in the polymerization and determination of the maximum molecular weight that can be obtained. This combined with the fact that MDMO-monomer cannot be easily purified, leads to the conclusion that a new premonomer should be chosen for the further study of the anionic polymerization of PPVs.*

# 2.1 Introduction

For the sulfinyl route, our group has clearly shown that the high molecular weight material originates from a self-initiating radical polymerization, and this for different solvents in which the polymerization is performed.[1] Low molecular weight material, when observed, originates from an anionic polymerization. For example, when the polymerization is performed in dry NMP using Na*t*BuO as the base, a bimodal distribution is found. It was proven that the high molecular weight material originated from a radical polymerization and the low molecular weight material on the other hand from an anionic polymerization.[2-4] In this case both polymerization mechanisms compete with each other during the polymerization reaction as represented in Figure 2-1.

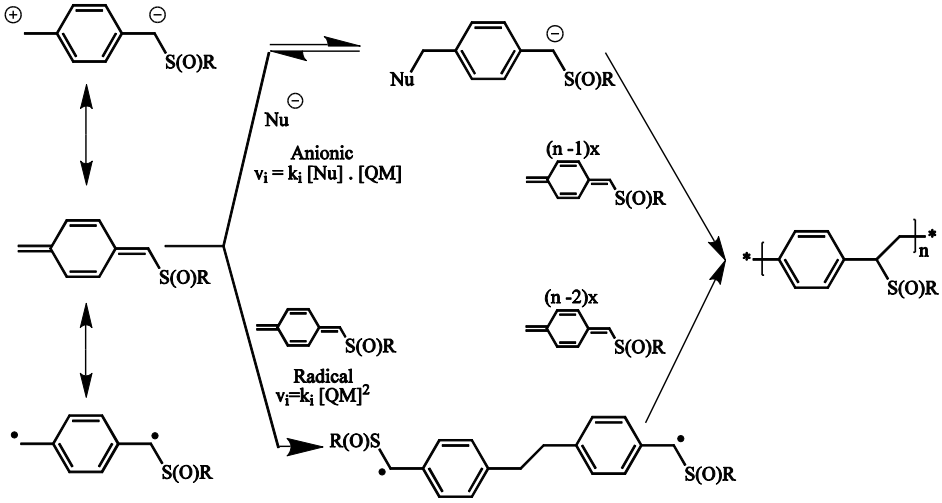


**Figure 2-1: Radical and anionic polymerization mechanism for the sulfinyl route**

It is exactly this double mechanism that we wish to explore further. By changing the polymerization parameters, we hope to achieve fully anionic polymerization of PPVs.

In this chapter the synthesis of poly[2-(3,7-dimethyloctyloxy)-5-methoxy-1,4-phenylene vinylene] is investigated. This PPV-derivative is commercially known as $OC_1C_{10}$-PPV or MDMO-PPV - the abbreviations are derived from the alkoxy side-chains. In this thesis the later abbreviation will be used. These

side-chains on the aromatic ring give the conjugated polymer the property of solubility in common organic solvents and lead together with the backbone to a material that emits an orange color of light, when used in polymer LEDs.

A reason for the industrial interest in this polymer lies in its solubility in the conjugated state. As such, drawbacks of film conversion, such as remaining elimination products or degradation of the ITO electrode - connected to the use of the insoluble and intractable regular PPV - are bypassed. On top of this, MDMO-PPV exhibits very good properties - such as luminescence efficiency, high brightness at low voltage - and therefore finds common use as active layer in polymer LEDs.[5] Even more recently, promising results are obtained for its use in photovoltaic devices.[6,7]

## *2.2 The premonomer synthesis*

The premonomer synthesis was already established[8] and was only slightly modified to accommodate synthesis of larger amounts (Figure 2-2). To synthesize the sulfinyl MDMO-PPV premonomer, first the Gilch MDMO-PPV premonomer **(4)** had to be synthesized. The core of the Gilch premonomer (**3**) was synthesized using a Williamson etherification with *p*-methoxyphenol and 1-chloro-3,7-dimethyloctane (**2**). Compound (**2**) was prepared from the corresponding alcohol in a high yield. These first two synthesis steps were scaled up and the purification was modified to a distillation, as column chromatography limits the practical amount that could be synthesized in one batch. The Gilch MDMO-PPV premonomer, 2,5-bis(chloromethyl)-1-(3,7-dimethyloctyloxy)-4-methoxy-benzene (**4**) was synthesized according to an adapted literature procedure using concentrated HCl and *p*-formaldehyde in acetic anhydride. This step (Figure 2-2) could also be up-scaled easily by using double recrystallization as purification method instead of column chromatography.

The synthesis from the Gilch premonomer to the sulfinyl premonomer consists of three steps, of which the first two are both straightforward to perform and have high yields (Figure 2-3). The last step comprises an oxidation reaction using Tellurium-oxide as catalyst and hydrogen peroxide as oxidant. This reaction is slow and can be sped up by adding a few drops

of concentrated HCl. Over-oxidation is possible, and therefore the reaction has to be monitored by use of TLC. Wrong interpretation of the TLC means a loss in product and yield. An attempt was made to find alternatives to this reaction that do not suffer from over-oxidation and have high yield, but no good alternative was found. The oxidation with periodic acid ($H_5IO_6$) catalyzed by $FeCl_3$ in MeCN[9] resulted in loss of product during the purification step. Oxidation in glacial acetic acid by hydrogen peroxide[10] did yield the sulfoxide, but many side products were found in the $^1H$ NMR analysis and therefore this route was abandoned. Oxidation with 30% aqueous $H_2O_2$ in phenol at room temperature[11] proceeded very quickly in excellent yields, however, the complete removal of the phenol proved to be rather difficult. The bulk of the phenol could easily be removed by distillation and washing with 10 % solution of NaOH in water, but a small amount of phenol always remained. This oxidation method seems the most promising, however a method for a quick and complete removal of the remaining phenol still needs to be found without use of column chromatography, as the sulfinyl premonomer is rather unstable. To conclude, better oxidation methods could be found, but purification then became more difficult. A large batch was synthesized and used for following polymerizations.

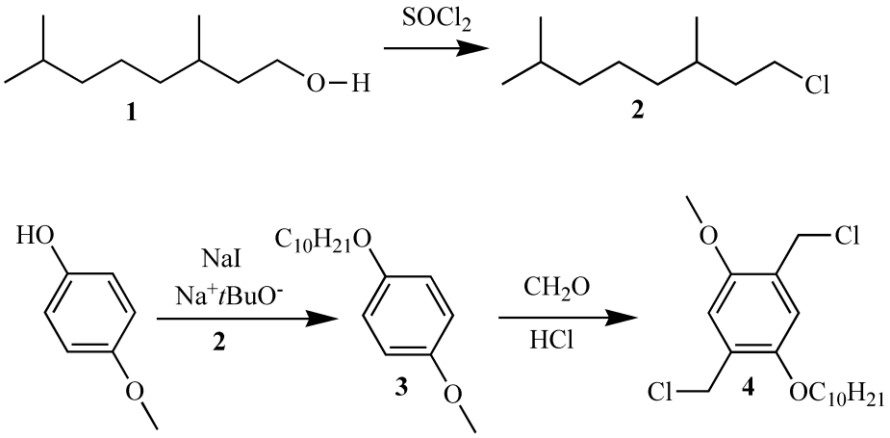


**Figure 2-2: Synthesis of Gilch MDMO-PPV premonomer**

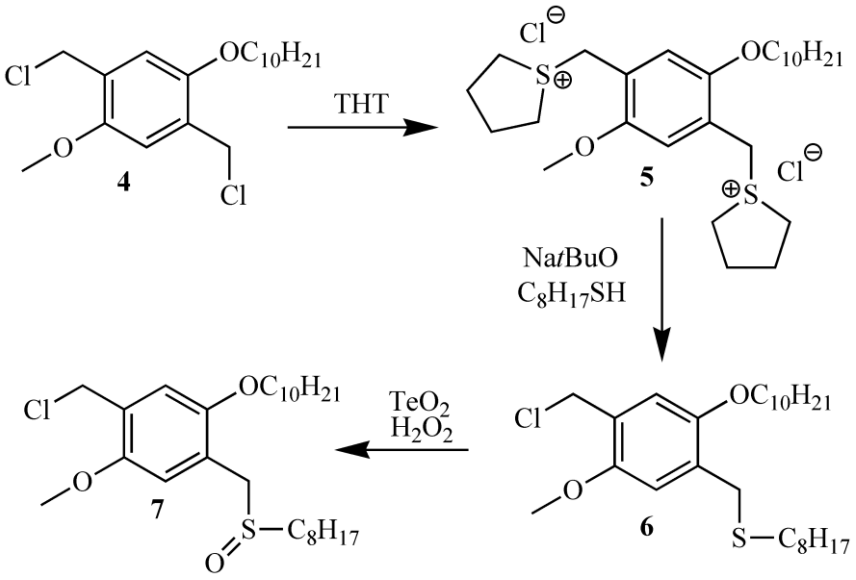


**Figure 2-3: Synthesis of sulfinyl MDMO-PPV premonomer**

# 2.3 Synthesis of MDMO-PPV using LDA as the base

## 2.3.1 Influence of temperature on the polymerization

The temperature dependency of the polymerization was already discussed in chapter 1. Lowering the temperature promotes the anionic polymerization in case of competition between the radical and anionic mechanism. The molecular weight of the high molecular weight fraction (radical) lowers because of lack of monomer; the oligomer fraction keeps roughly its molecular weight. We now want to investigate this effect in another solvent, namely Tetrahydrofuran (THF) and with another base. Like N-methyl-2-pyrrolidone (NMP), tetrahydrofuran (THF) is also an aprotic solvent, allowing for a competition between radical and anionic polymerization. Furthermore, by using a much stronger base, such as Lithium di(isopropyl)amide (LDA), we hope to promote the anionic polymerization in this competition.

The polymerizations at different temperatures were performed in dry THF, which was degassed by passing through a flow of nitrogen gas prior to use.

A premonomer (**7**) solution (0.2 M in THF) was added slowly over the course of 1 hour by an automatic syringe to diluted base (0.17 M solution of LDA in THF; 2.5 equivalent). After complete addition of the premonomer the reaction was left to stir for 20 minutes, after which water was added to the reaction mixture to stop the reaction. The obtained polymer was precipitated in water and the water layer was neutralized with HCl (1N) before extraction with chloroform or dichloromethane. The solvent of the combined organic layers was evaporated under reduced pressure. The thus obtained polymer was dried in vacuum. Molecular weight was determined by GPC against polystyrene standards using THF as eluent. All the data depicted in Table 2-1 are average values of *duplo* experiments, which showed good reproducibility.

| *Temp (°C)* | *$M_n$ (kD)* | *PD* | *Yield (%)* |
|---|---|---|---|
| -78 | 1.4 | 1.99 | 8 |
| -30 | 1.3 | 1.98 | 13 |
| 0 | 1.4 | 2.10 | 45 |
| 30 | 2.0 | 2.43 | n.a. |
| 55 | 1.9 | 2.40 | 46 |

**Table 2-1: Molecular weight in function of temperature (Sulfinyl MDMO-PPV premonomer, LDA, THF)**

The results of the polymerizations at different temperature show only very small variations in molecular weight. Low molecular weight oligomers are formed with a polydispersity of around 2. The very low molecular weights obtained are indicative of an exclusively anionic polymerization. Unlike the polymerization done in NMP previously by dr. Hontis, no radical polymerization seems to be present as there is no high molecular weight material to be found, indicative of a radical polymerization. The observed color of the oligomers is orange, indicative of a partial base induced elimination reaction.

### 2.3.2 Changing order and speed of addition

Previous work done in NMP as solvent and Na*t*BuO as the base, showed a large effect on the order of addition.[2-4] Polymerization of **7** in NMP gives rise to a bimodal distribution of the molecular weight. When base was added to a premonomer solution, more high molecular weight polymer was obtained

than when the premonomer was added to a base solution. In the latter case, significantly more low molecular weight material was found.

To further analyze the importance of the slow reversed addition employed in previous polymerization, some variations of the polymerization procedure were attempted. Although no large differences are observed between the polymerizations in Table 2-2, some remarks can be made. None of the polymers have high molecular weight fractions, indicating that no radical polymerization takes place even if the order and speed of addition is changed. Using fast addition rather than slow, lower polydispersities are obtained. The higher polydispersity observed with the slow addition of base is not surprising as there is a strong change in base concentration during the entire reaction.

| | $M_n$ (kD) | PD |
|---|---|---|
| Slow addition of premonomer to base | 1.5 | 2.08 |
| Fast addition of premonomer to base | 1.6 | 1.37 |
| Slow addition of base to premonomer | 1.4 | 3.19 |
| Fast addition of base to premonomer | 1.8 | 1.32 |

**Table 2-2: Effect of order and speed of addition on the molecular weight obtained (Sulfinyl MDMO-PPV premonomer, LDA, THF, 0°C)**

### 2.3.3 Degradation tests

When we have a closer look at the structure of the polymer formed, we can notice that this polymer still has protons with some acidity. There is a possibility for proton abstraction next to the polarizer on the polymer backbone. This anion could break the chain in a 1,6-elimination, creating on the one hand a part of polymer with a quinoid structure, and on the other hand a part containing an anion chain end. Attack of a nucleophile in the reaction mixture to the quinoid structure is possible.

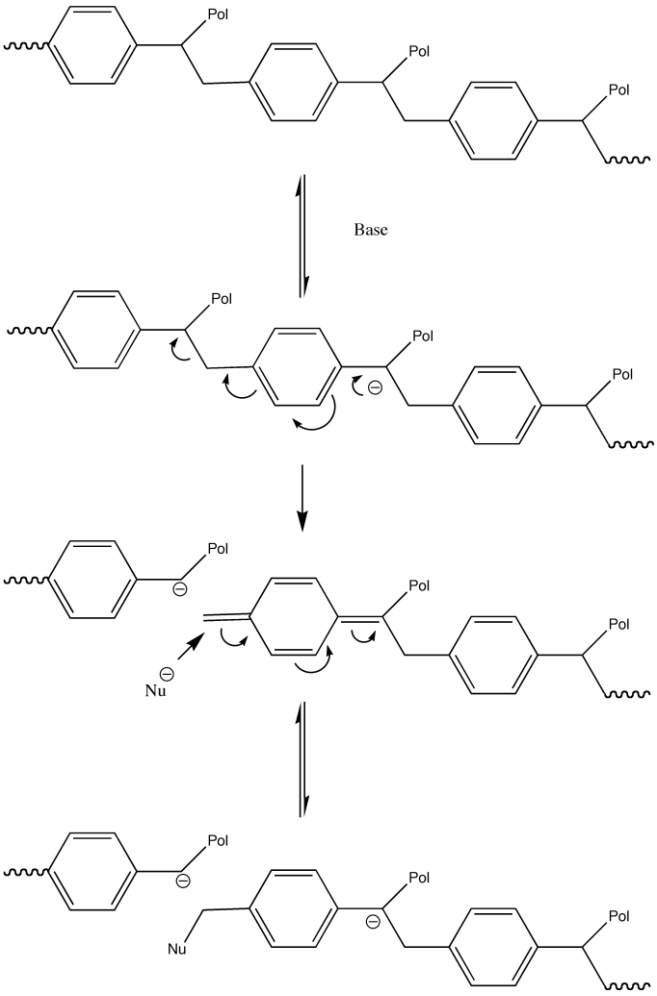


**Figure 2-4: Degradation of the polymer**

Hence, it was checked whether it is possible that the formed polymer degraded under influence of LDA. To this end, a precursor synthesized under standard conditions with Na*t*BuO in s-BuOH was exposed to a solution of LDA in THF. Samples were taken after certain time intervals. The samples were neutralized in water with HCl and extracted with dichloromethane. After removal of the solvent of the combined organic layers, a GPC was taken.

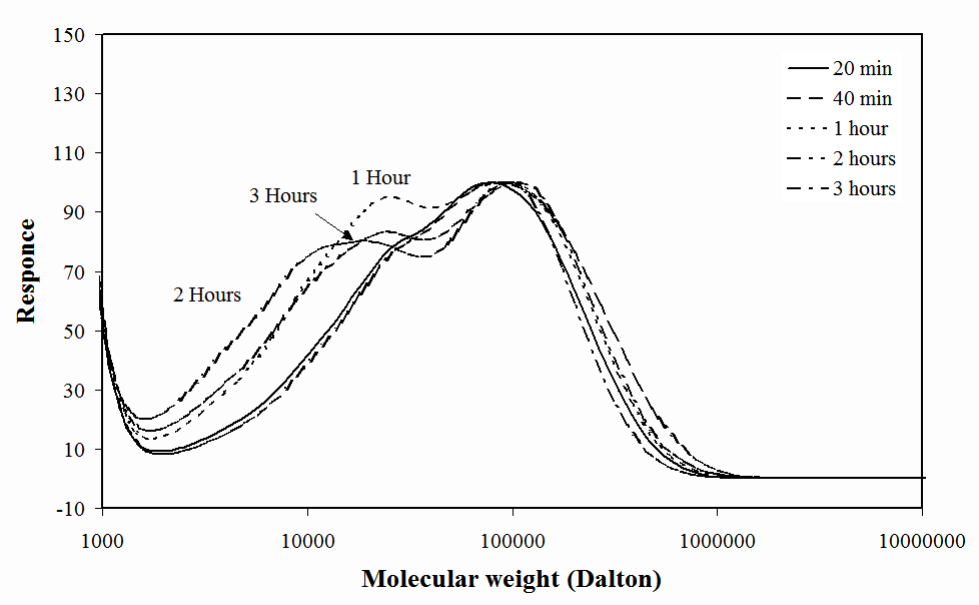


**Figure 2-5: Degradation of high molecular weight polymer by LDA**

In the figure above (Figure 2-5) a shoulder in the high molecular weight part of the graph appears and separates in function of time. There is not much change to the highest molecular weight material. The development of this shoulder is not enough to explain the low molecular weight material obtained with the polymerization using LDA as the base. The experiment shows that degradation might indeed be occurring, but not to such an extent that the formation of high molecular weight material is hindered. The change in molecular weight might also be explained by aggregation–disaggregating effects. Negative charges on the polymer chain would theoretically enhance the de-aggregation of the chains.

### 2.3.4 End group detection

One of the questions that can be asked now is whether the very low molecular weight originates from LDA acting as initiator for the anionic polymerization. Although LDA is sterically hindered, it is not impossible for this nucleophile to react with a quinodimethane system, thereby starting the anionic polymerization.

To have a good idea where one might expect the carbon resonance signals of an LDA molecule attached to a monomer unit in a $^{13}C$ NMR spectrum, the $^{13}C$ NMR signals of some common similar chemicals were looked up on the Spectral database for Organic compounds (‘http://riodb01.ibase.aist.go.jp/sdbs/’). If LDA acts as an initiator, we expect that a structure similar as N,N-diisopropylbenzylamine would be formed. The $^{13}C$ NMR spectrum of N,N-diisopropylbenzylamine was not available, but by combining the spectra of diisopropylamine and N,N-diethylbenzylamine an idea can be formed of the likely chemical shifts that can be expected for N,N-diisopropylbenzylamine. Diisopropylamine has two distinct shifts at 45.3 ppm and 23.5 ppm. N,N-diethylbenzylamine has besides the shifts for the aromatic carbons also signals at 57.6, 46.8 and 11.8 ppm. Therefore we can expect that if LDA acts as initiator, shifts close to 57.6, 46 and 23.5 ppm would be present in the spectrum of the obtained polymer.

Since $^{13}C$ NMR will be used more often to check for defects and end groups, an overview is given in Figure 2-6 of the $^{13}C$-assignments of all possible defects ever observed for this class of $^{13}C$ labeled polymers obtained *via* monomers of which the $\alpha$-$CH_2$ position is $^{13}C$ labeled.

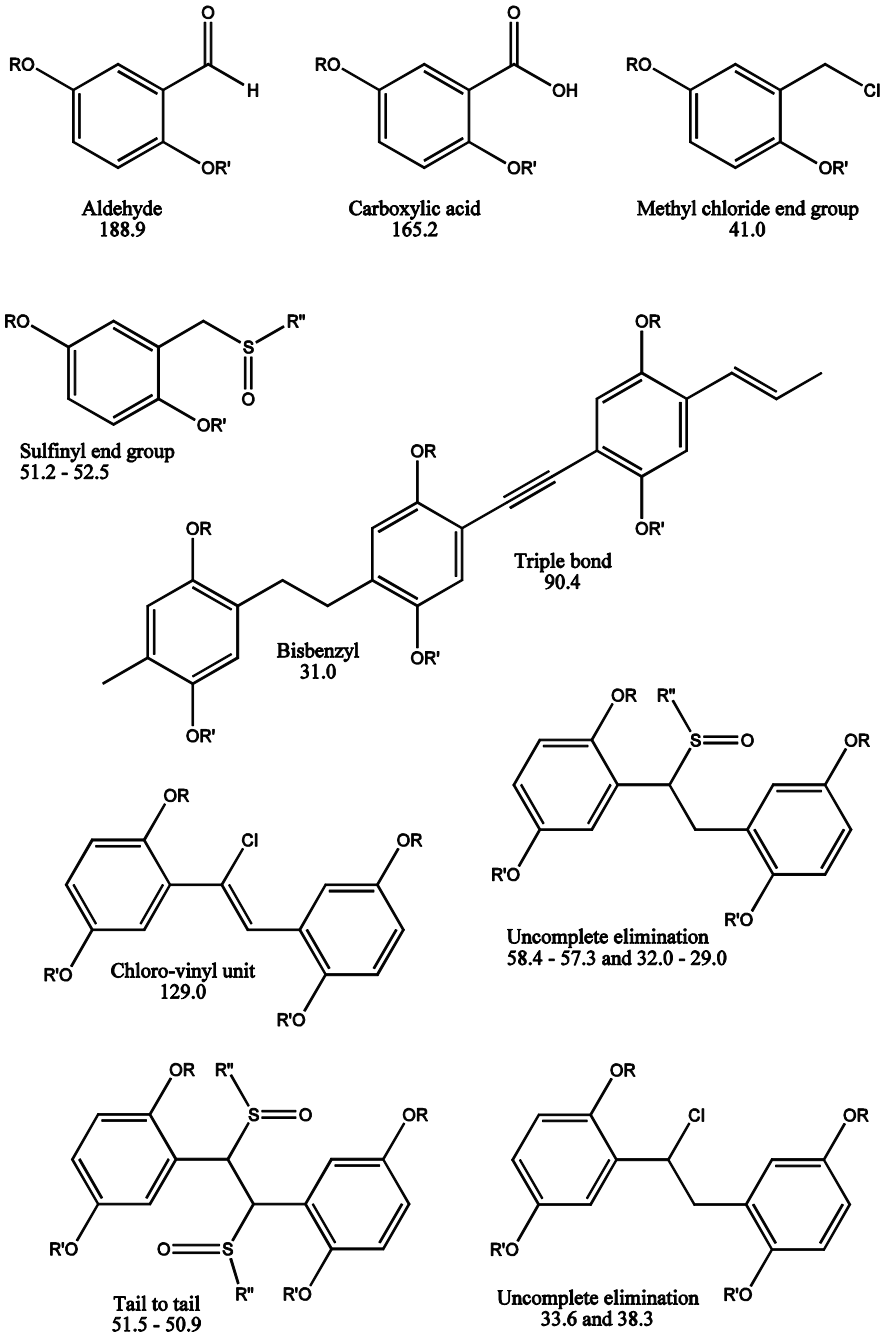


**Figure 2-6: Possible end groups and defects for the sulfinyl route**

To get a better idea of the nature of the end-groups, a small quantity of oligomers was synthesized using LDA as the base in THF. The oligomers were separated by size on BioBeads®. Bio-Beads® beads are neutral, porous cross-linked polystyrene divinylbenzene copolymer beads used for gel permeation separations of lipophilic polymers and low molecular weight, hydrophobic materials in the presence of organic solvents. These non-aqueous spherical beads are used in much the same way aqueous gels are used, except that they are swollen with organic solvents during the separation. The beads chosen for the separation/purification of the polymers had an exclusion limit of 14000 Daltons. The amount of divinylbenzene cross linkage determines the pore size, and hence the molecular weight exclusion limit.

| *Fraction* | $M_n$ *(kD)* | *PD* |
|---|---|---|
| 1 | 2.6 | 1.33 |
| 2 | 1.6 | 1.17 |
| 3 | 0.73 | 1.26 |

**Table 2-3: Molecular weights measured by GPC after separation on BioBead Column**

After the separation of the oligomers by BioBeads®, the different fractions were investigated by $^{13}C$ NMR.

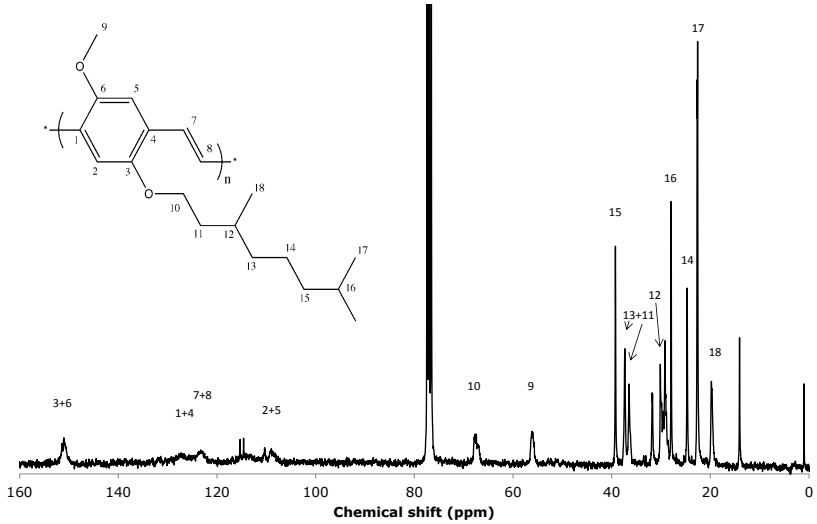


**Figure 2-7: $^{13}C$ Spectrum of sulfinyl MDMO PPV after elimination and separation on biobeads. High molecular weight fraction.**

Detailed analysis showed that LDA does not act as initiator as there was no signal found at 46 ppm or 23 ppm, which would be expected in case LDA would be build in the polymer chain. There was no signal found around 165 ppm (carboxylic acid), but there was a small signal at 188 ppm, indicating the presence of an aldehyde. The signal of the aldehyde end functionality was not visible in the higher molecular weight fraction, but was clearly visible in the lower molecular weight fraction. There it was even present at a concentration of 14%, indicating that it must be one of the main end groups of the oligomers. Further analysis of the $^{13}C$ NMR showed no sign of triple bonds, bisbenzyl unit, methyl chloride end group or chloro-vinyl group. There were signals found at the location where sulfinyl end groups would be expected, however, signals overlap with the $OC_{10}H_{21}$ side group on the polymer backbone.

The separation by BioBeads and analysis by $^{13}C$ NMR was repeated on a different sample, and confirmed the results of the first analysis. The second analysis however showed more clear signals that could be assigned to a sulfinyl end group and in a lesser extent the signal of the aldehyde was found.

From this study, we can conclude that the oligomers synthesized anionicly show no mayor defects in the polymer backbone, and are probably end capped with either an aldehyde or sulfinyl end group.

## *2.4 Use of other bases*

Clearly the base changes the polymerization from a predominantly radical polymerization when Na*t*BuO was used as the base to an anionic polymerization in the case of LDA. To further investigate the effect of the base, the use of three bases was compared under exactly the same conditions. A solution of sulfinyl premonomer (**7**) was added slowly during 1 hour to 1.1 equivalents of base dissolved in THF at 30 °C. The fraction of oligomer and polymer in the samples was calculated by dividing the surface under the respective peak by the total surface under the GPC curve.

| *Base* | *Distribution* | *$M_n$ (kD)* | *PD* | *Fraction* |
|---|---|---|---|---|
| LDA | bimodal | 1.9 | 1.59 | 92.4% |
| | | 29 | 1.26 | 7.6% |
| NaH | - | Monomer | | |
| K*t*BuO | bimodal | 1.7 | 1.35 | 79.3% |
| | | 23 | 1.81 | 20.7% |

**Table 2-4: Influence of the base on the polymerization**

| *Description* | *Reaction time* | *$M_n$ (kD)* | *PD* |
|---|---|---|---|
| 1.1 eq. NaH | 1 hour | Monomer | |
| | 4 hours | Monomer | |
| | 24 hours | 2.8 | 1.9 |
| 5.0 eq. NaH | 1 hour | Monomer | |
| | 4 hours | Monomer | |
| | 24 hours | 2.4 | 1.3 |

**Table 2-5: Influence of the reaction time when using NaH as the base**

No polymer was found after the reaction of the MDMO-monomer **7** with NaH using slow reversed addition in THF (Table 2-4). Only after 24 hours, some low molecular weight oligomers could be found (Table 2-5). NaH forms a suspension in THF and does not fully dissolve; therefore the reactivity is limited to the surface of the particle. Using a larger quantity of NaH did not improve the situation and only oligomers were formed after 24 hours (Table 2-5).

In the past, an attempt was made to polymerize α-chloro-α'-n.butylsulfonyl-*p*-xyleen in THF at 20 °C using fast normal addition and 1 equivalent of NaH.[12] After 5 hours no polymer was formed. Only after 1 day polymerization time, some low molecular weight polymer could be found. UV-Vis experiments confirmed that the quinodimethane system could be formed, but that initiation and propagation did not occur. In other solvents such as DMF and NMP, polymerization was possible.

Using K*t*BuO, a bimodal distribution of molecular weights is obtained. Many years ago this phenomenon has also been observed when using NMP as

solvent. This bimodal distribution was also observed when polymerizing this premonomer using slow reversed addition in THF. [13]

It is clear that the choice of the base plays a significant role in the outcome of the polymerization. It is however remarkable that the molecular weight of the oligomer fraction does not change much using different bases. If we however wish to gain more control over the anionic polymerization, high molecular weights are necessary. Only then specific initiators can be added to regulate the molecular weight.

## 2.5 The use of LHMDS as the base for the synthesis of MDMO-PPV

Although lithium diisopropylamide (LDA) is commonly thought of in terms of its basic and weak nucleophilic properties, it has been shown to behave as a single-electron transfer (SET) donor in several types of reactions.[14-17] LDA is also known to reduce certain haloarenes by donating an $\alpha$-hydrogen to the aryne intermediate in these reactions.[18] A competing radical, carbanion and carbene pathway has been found in reactions with hindered primary alkyl halides with LDA.[19] LDA is even used for the initiation of anionic polymerizations.[20] Consequently the question arises to what extent the observed behavior of the sulfinyl polymerization in THF relates to the base used. It can be envisioned that the observed polymerization behavior is a consequence of side reactions induced by LDA. Therefore the use of a more sterically hindered amide base such as Lithium bis(trimethylsilyl)amide (LHMDS) is of interest (Figure 2-8).

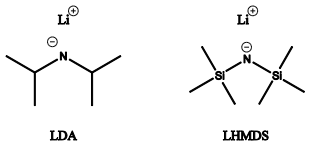


LDA LHMDS

**Figure 2-8: Structure of LDA and LHMDS**

LHMDS can be acquired in a THF solution and therefore, is very easy to transfer from shipping container to storage or a reactor. LHMDS is a more stable base than LDA, but it has a lower $pK_a$ (Table 2-6). Furthermore,

LHMDS is a base that starts to crystallize on cooling the solution below 5 °C giving rise to large colorless crystals, which can be redissolved by warming to ambient temperature. Pure LHMDS is rather stable: it starts to decompose only above 300 °C. LHMDS is a non-pyrophoric strong base, widely employed in organic synthesis as a metalation agent. The principle advantages of this reagent are the improved selectivity obtained in deprotonation reactions and the enhanced thermal stability. It is employed as a base in generating enolates for the preparation of lactone precursors.[21-22]

| *Base* | *$pK_a$* |
|---|---|
| LDA | 35.7 in THF [23] |
| LHMDS | 29.5 in THF [24] |
| K*t*BuO | ~16 in water |
| K*t*BuO | 32.2 in DMSO [25] |
| NaH | ~30 in water |

**Table 2-6: $pK_a$'s of the different bases used**

Initial results of the synthesis of MDMO-PPV by using LHMDS as the base, shows that again oligomers are formed with a reasonable yield. (Table 2-7) Compared to using LDA as the base, LHMDS yields higher molecular weight oligomers.

| *Amount base used (Eq.)* | *$M_n$ (kD)* | *PD* | *Yield (%)* |
|---|---|---|---|
| 1.1 | 4.7 | 1.99 | 39 |
| 2.5 | 5.8 | 2.35 | ~60 |

**Table 2-7: Initial results when using LHMDS as the base**

### 2.5.1 Comparison of characteristics

When we compare the converted polymer synthesized using LDA as the base, with the polymer synthesized using LHMDS as the base, we can see that the FT-IR-spectrum of both polymers is not the same. (Figure 2-9) We find all the usual signals that are known for MDMO-PPV, but for the LDA synthesized oligomer, new vibrations appear between 1800-1720 $cm^{-1}$. These vibrations are usually associated with degradation of the MDMO-PPV.[26]

This suggests that LDA not only acts as the base, but that it also induces side reactions, changing the structure of the oligomer formed.

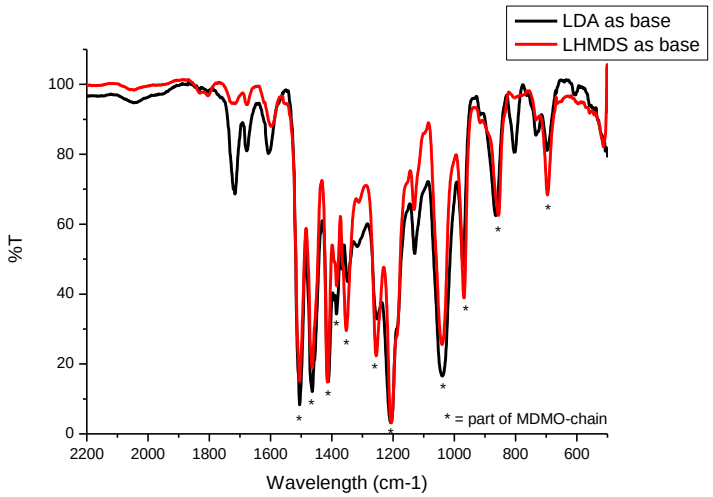


**Figure 2-9: FT-IR spectra of MDMO-oligomers synthesized with either LDA or LHMDS**

These defects, noted in the FT-IR spectrum, are also responsible for the lower $\lambda_{max}$ found after thermal conversion when analyzing the two oligomers using UV-Vis spectroscopy. (Figure 2-10)

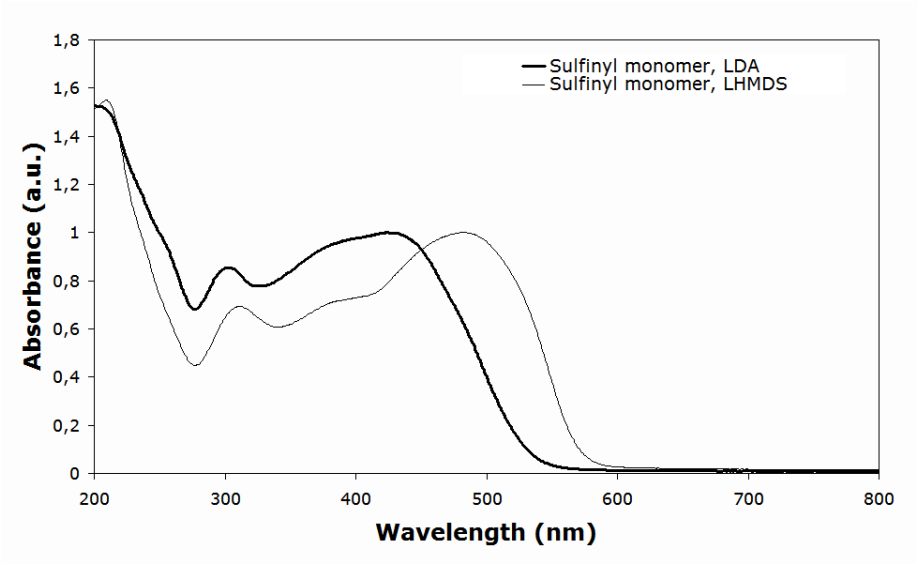


**Figure 2-10: UV-Vis spectra of MDMO-oligomer synthesized using LDA or LHMDS as the base**

From the UV-Vis spectra the optical bandgap can be calculated. (Table 2-8)

| *Base used* | $\lambda_{max}$ *(nm)* | $E_g$ *(eV)* |
|---|---|---|
| LDA | 425 | 2.33 |
| LHMDS | 484 | 2.17 |

**Table 2-8: Comparison of the $\lambda_{max}$ and the optical bandgap**

From this comparison, we can conclude that LHMDS is a better base for the synthesis of MDMO-PPV *via* an anionic polymerization mechanism. The obtained oligomer has a higher $\lambda_{max}$, lower $E_g$ and less visible defects in its FT-IR spectrum, compared to the oligomer obtained using LDA as the base.

### 2.5.2 Influence of temperature

Due to the lower activation energy required for the anionic polymerization, we again expect that the anionic polymerization is promoted at lower temperatures, *versus* the radical polymerization at higher temperatures. Three polymerizations were performed at different temperatures in duplicate using slow addition of the premonomer to an excess of base in THF.

| *Temperature (°C)* | $M_n$ *(kD)* | *PD* | *Yield (%)* |
|---|---|---|---|
| -78 | 3.8 | 2.11 | n.a. |
| 0 | 4.0 | 2.08 | 60 |
| 30 | 4.4 | 2.61 | 65 |

**Table 2-9: Molecular weight in function of temperature (Sulfinyl, LHMDS)**

The results are similar to the experiments with LDA, with the exception that the obtained molecular weight is significantly higher (LDA: Table 2-1 page 40 and LHMDS: Table 2-9). Although that a small rise in molecular weight can be noticed when polymerizing at higher temperatures similar as seen when using LDA, this rise is too low to be of much significance.

When performing the polymerization at 0 °C, the molecular weight does not seem to change much when we prolong the reaction time. (Table 2-10) Only a small rise in $M_n$ can be observed when we analyze the polymers before elimination of the sulfinyl group. After the elimination step, the polymers obtained after different reaction times all have about the same molecular weight. The increase noticed before elimination is due to partial base induced

conversion. When the polymer is partially converted into the conjugated form, the chain becomes stiffer, therefore the hydrodynamic volume of the chain rises, and the GPC will report a shorter retention time. It is clear from the yields that the polymerization is finished after 80 minutes. As we add the premonomer slowly during 1 hour, and then let the polymerization continue for an extra 20 minutes, this means that the last premonomer added has reacted within 20 minutes.

Before elimination:

| *Time* | $M_n$ *(kD)* | *PD* |
|---|---|---|
| 80 min | 4.0 | 2.08 |
| 2h | 4.1 | 2.11 |
| 4h | 4.3 | 2.14 |
| 24h | 5.7 | 2.86 |

**Table 2-10: Molecular weight of the precursor polymer in function of time (Sulfinyl, LHMDS, 0 °C)**

After elimination:

| *Time* | $M_n$ *(kD)* | *PD* | *Yield (%)* |
|---|---|---|---|
| 80 min | 5.8 | 2.35 | 60 |
| 2h | 3.7 | 2.93 | 60 |
| 4h | 4.4 | 2.30 | 61 |
| 24h | 5.0 | 2.63 | 73 |

**Table 2-11: Molecular weight of the converted polymer in function of time (Sulfinyl, LHMDS)**

The base induced elimination can also be seen in the FT-IR of the precursor polymer taken after different polymerization times (Figure 2-11). The absorption at 1045 $cm^{-1}$ is indicative of the sulfinyl group. As the reaction time becomes longer, this absorption lowers, and the absorption at 975 $cm^{-1}$, indicative of the double bond, rises.

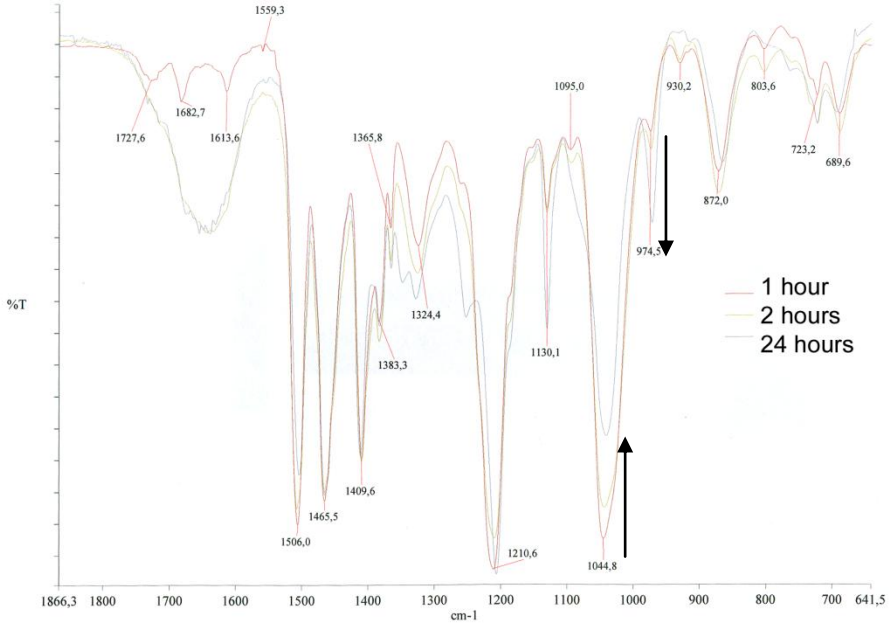


**Figure 2-11: FT-IR-spectrum after different polymerization times (before thermal elimination)**

After elimination in toluene and precipitation in methanol, the polymer was analyzed by dropcasting on a quarts glass and measuring by UV-Vis spectroscopy. Even though that the molecular weight does not change with increasing reaction time, the $\lambda_{max}$ lowers. (Figure 2-12) The maxima found are 501 nm, 492 nm, 483 nm, 443 nm after 1, 2, 4 and 24 hours respectively. This decrease in $\lambda_{max}$ is an indication for a shortening of the conjugation length, alternatively it can be explained by changes in the aggregation behavior of the polymer.

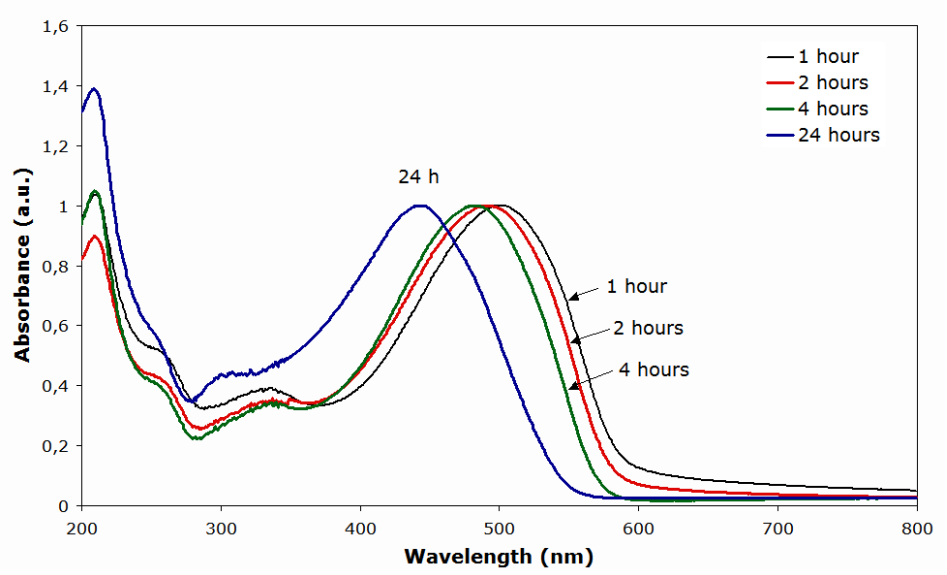


**Figure 2-12: UV-Vis specta after elimination of the polymer**

### 2.5.3 Verifying anionic polymerization

To verify the anionic character of the polymerization using LHMDS in THF, the effect of TEMPO on the polymerization was studied. Using LHMDS as a base in THF without further additives, material is obtained of moderate molecular weight (Table 2-12, entry 1). When this experiment was repeated with the addition of 0.5 equivalents of TEMPO, only a small change in $M_n$ is observed and the yield stays very high. If the polymerizations were radical in nature, the expected change in $M_n$ and yield would be much larger. This clearly confirms that when LHMDS is used as the base in THF, the oligomers are obtained through an anionic mechanism.

| *Additive* | *$M_n$ (kD)* | *PD* | *Yield (%)* |
|---|---|---|---|
| none | 17.0 | 2.45 | ~90 |
| TEMPO | 11.8 | 2.24 | ~82 |

**Table 2-12: Effect of TEMPO on the polymerization of 7 using LHMDS**

The obtained results in Table 2-12 show a much higher $M_n$ then the previous results (Table 2-9 to 2-11). The reason for the dissimilar result was the use

of a new batch of premonomer. The batch used to synthesize the polymers presented in table 2-12 had been purified twice by column chromatography. Apparently, the higher purity influenced the polymerization results directly by producing high molecular weight polymer. This sensitivity to purity of the premonomer is also a telltale sign of anionic polymerization. This suggests that the higher purity is vital in order to have higher molecular weight polymer.

### 2.5.4 Detection of end groups

In order to investigate the end groups present on the polymers obtained *via* anionic polymerization, Bio-Beads® S-X were used. They are neutral porous styrene divinylbenzene copolymer beads for the separation/purification of the polymers with an exclusion limit of 14000 Daltons.

A small batch of oligomers was synthesized using LHMDS as the base in THF. The sulfinyl premonomer was polymerized at 0 °C for 1 hour. After extraction of the precursor polymer, the polymer was converted in toluene (110 °C, 3h) and purified by precipitation and filtration. After drying under vacuum overnight, the polymer was dissolved in THF and separated on Bio-Beads. The different fractions (20 mL) were quickly analyzed by using UV-Vis spectroscopy, to verify that a good separation was obtained (Figure 2-13). The UV-Vis spectrum was taken of the oligomers dissolved in THF, since the UV-Vis measurement of the oligomers after dropcasting on quartz caused significant broadening of the measured absorption. This broadening is most likely caused by aggregation phenomena. The resulting fractions were combined according to their UV-Vis characteristics in 5 fractions. These fractions were analyzed by GPC to confirm that the molecular weight of the oligomers was sufficiently separated (Table 2-13).

| *Fraction* | *Mn (kD)* | *PD* | *Collected weight (mg)* |
|---|---|---|---|
| 1 | 10.2 | 1.99 | 85.4 |
| 2 | 3.58 | 1.56 | 19.2 |
| 3 | 2.07 | 1.17 | 6.3 |
| 4 | 1.57 | 1.13 | 4.9 |
| 5 | 1.22 | 1.11 | 2.9 |

**Table 2-13: Molecular weight of by Bio-Beads separated fractions**

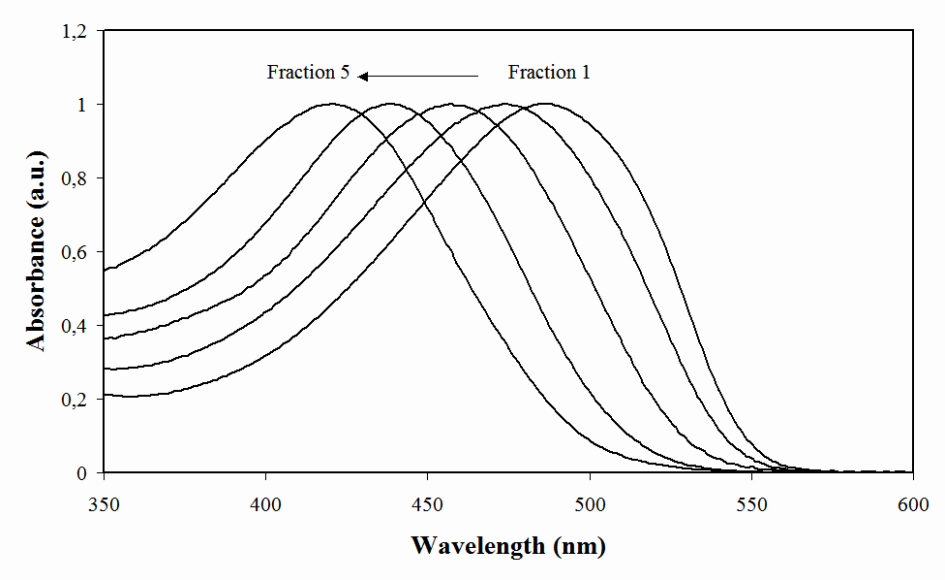


**Figure 2-13: UV-Vis spectra of the collected oligomers**

After careful analysis of the $^{13}C$ NMR spectra of the different fractions, we can conclude that all signals become sharper at lower molecular weights. The sulfinyl end group that we expected to see is however not visible. It is not clear why the carbons next to the sulfinyl group are not visible, especially since there is no clear sign of any other end group in the $^{13}C$ NMR spectra. It should be noted that the signal at 188 ppm was too weak to be significant. This is surprising since when LDA was used as the base to obtain MDMO-PPV oligomers, sulfinyl end groups were found. The same result was expected when using LHMDS, however, $^{13}C$ NMR cannot clearly verify this. A more sensitive method that can be used to detect the end groups and possibly defects in the polymer chain is the use of a $^{13}C$-labeled premonomer.

### 2.5.5 $^{13}$C-labeling of the MDMO-PPV premonomer

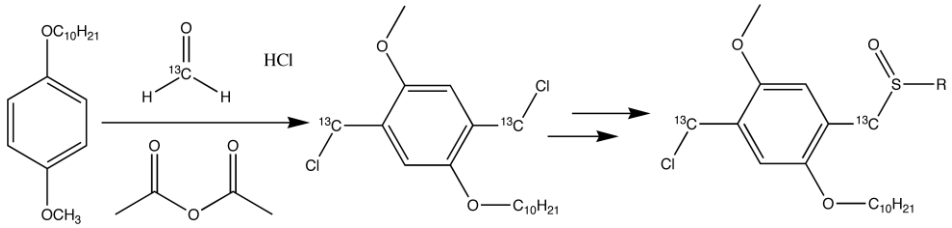


**Figure 2-14: Synthesis of labeled sulfinyl MDMO-PPV premonomer**

$^{13}$C-labeling is an effective way to see the end groups in an oligomer as the signals of the end groups together with the double bounds and possible defects will be increased by a factor of about 100. Dr. Hilde Roex has done $^{13}$C-labeling of the MDMO-PPV premonomer in the past in order to compare the sulfinyl polymerization route to the Gilch route. The premonomer was synthesized again, but this time using an octyl side chain on the sulfinyl group, as opposed to a butyl side chain employed previously. Both the Gilch and the sulfinyl $^{13}$C-labeled premonomers were analyzed using $^{1}$H and $^{13}$C NMR for later reference. The synthesis of the premonomer is described in chapter 5, where a more broad comparison is made between this polymerization route and other routes.

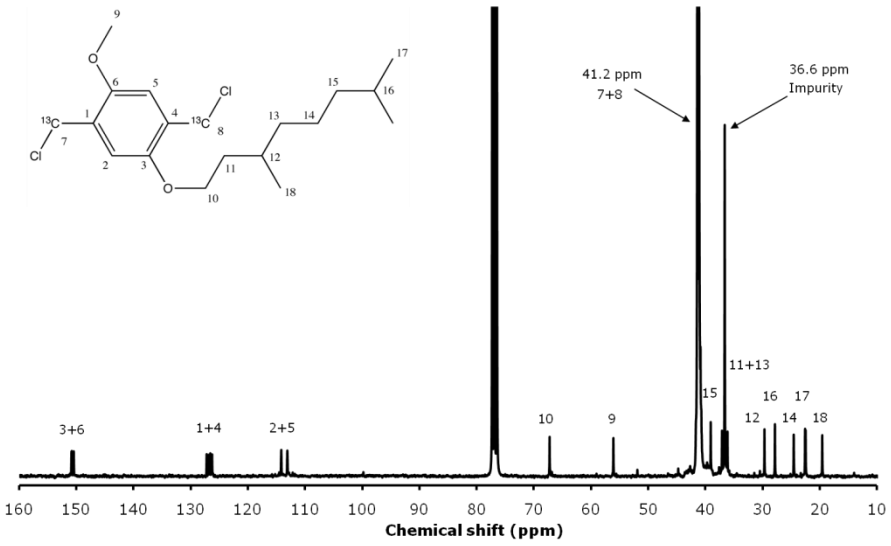


**Figure 2-15: $^{13}$C Spectrum of labeled Gilch MDMO-PPV premonomer**

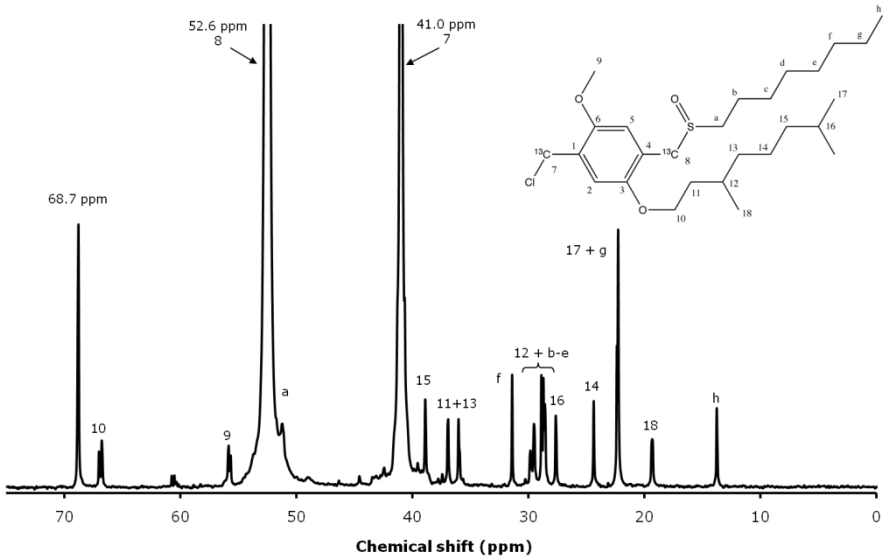


**Figure 2-16: $^{13}$C Spectrum of labeled sulfinyl MDMO-PPV premonomer**

The sulfinyl premonomer was polymerized anionicly using LHMDS as the base at 0 °C in THF. After two eliminations and precipitations, the obtained polymer was analyzed using $^{13}$C NMR. More detail on the method of recording the $^{13}$C-spectrum can be found in chapter 5.

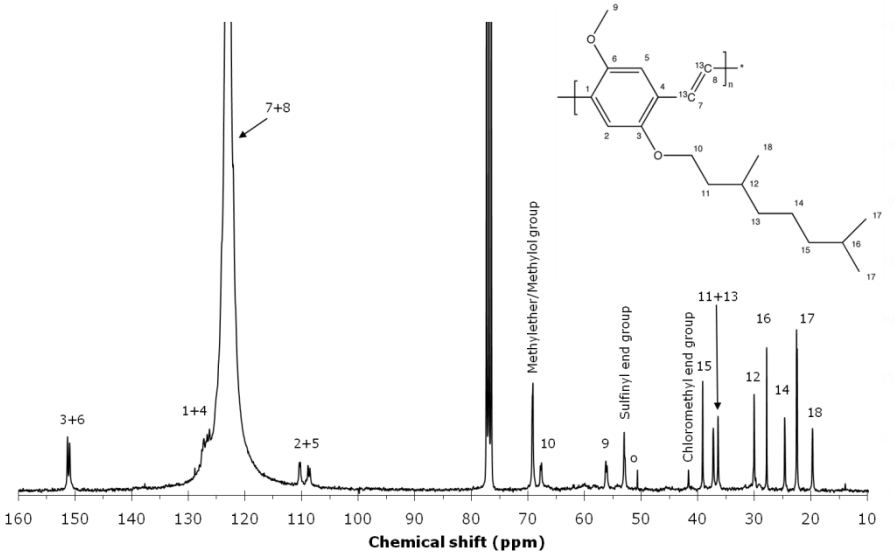


**Figure 2-17: $^{13}$C Spectrum of converted labeled MDMO-PPV polymer**

The signal of the double bond at 123 ppm is the most prominent signal in the spectrum. After one elimination, the only signals that do not conform to the polymer are originating from an aldehyde, a sulfinyl end group, a chloromethyl end group, and an unknown group, probably an methylether or methylol end group.

| | *First elimination* | *Second elimination* |
|---|---|---|
| Incomplete elimination | 0 % | 0 % |
| Aldehyde | 0.96 % | 1 % |
| Sulfinyl end group (53.0 ppm) | 1.4 % | 1.3 % |
| Chloromethyl end group (41.7 ppm) | 0.2 % | 0.3 % |
| Ether/methylol end group (69.2 ppm) | 2.8 % | 2.9 % |

**Table 2-14: Defects found in MDMO-polymer synthesized using LHMDS**

| *Description* | *$M_n$ (kD)* | *PD* |
|---|---|---|
| Precursor | 10.5 | 2.56 |
| 2nd elimination | 17.7 | 3.26 |

**Table 2-15: GPC of precursor and converted labeled polymer**

The obtained results were rather surprising. As expected the sulfinyl end group that would be formed in an ideal anionic polymerization was detected. In addition, the aldehyde had been found in the analysis of MDMO-PPV previously. It has been proposed that the aldehyde originated from an oxidation reaction that occurs during the work-up of the polymer. Oxygen is excluded systematically during the polymerization reaction, and this should prevent the creation of the aldehyde end group during polymerization. However, when we look at the obtained amount of end groups, we note that the amount of ether/alcohol end group is about equal to the sum of the other end groups. The first question that has to be asked is where these ether groups originate from.

The answer to this question could be found in the $^{13}C$ NMR of the premonomer. The premonomer contained exactly the same signal as was found in the oligomer. The impurity was already present before the oxidation of the sulfanyl functionality. There was also a labeled impurity found in the labeled Gilch premonomer. Past research was done on the effect of impurities on the polymerization, and in case of the radical polymerization, impurities were not build into the polymer chain. We now have to conclude that this is not valid for the anionic polymerization. It seems that the impurities can act as initiators for the anionic polymerization, explaining the low molecular weight obtained.

We now face a problem that the sulfinyl MDMO-PPV premonomer could not be purified easily. The premonomer could not be recrystallized. Normally the premonomer is purified by column chromatography, but also here care has to be taken that the product does not stay too long in contact with the column, as degradation occurs during the purification. An attempt was made to separate the two isomers of the premonomer by column chromatography and recrystallize the isomers separately, however, although that separation was possible, no appropriate recrystallization solvent could be found.

This leads us to a profound conclusion, that by using the MDMO-monomer, impurities are difficult to avoid, and thereby it will be difficult to obtain oligomers with high molecular weight. The highest molecular weight obtained was 40 kD (Mw), using a premonomer that was purified 3 times by column chromatography. If higher molecular weights are wanted, then perhaps another premonomer has to be chosen, which can be purified by recrystallization, in order to avoid degradation on the silica column.

# 2.6 Comparison with the Gilch premonomer

## 2.6.1 Polymerization using LDA as the base

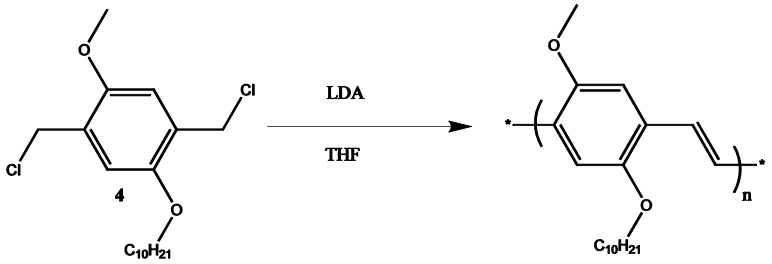


**Figure 2-18: Polymerization of Gilch MDMO premonomer**

The question can be raised whether the procedure described in previous section to achieve anionic polymerization with the sulfinyl route can be transferred to the Gilch route. In order to shed light on this question, the same reaction conditions were repeated for the Gilch premonomer. First a set of polymerizations was performed at different temperatures using LDA as the base (4.8 equivalents) and THF as solvent (Figure 2-18).

The results in Table 2-16 show low molecular weight at all temperatures, indicating anionic polymerization also for the Gilch premonomer. Only in the case of -78 °C, a bimodal distribution is found. There is a high molecular weight fraction, originating from a radical polymerization and a relatively larger fraction of low molecular weight material.

| *Temp (°C)* | *$M_n$ (kD)* | *PD* | *Yield (%)* |
|---|---|---|---|
| -78 (bimodal) | 85* | 2.18 | 14 |
| | 1.8** | 1.15 | |
| -20 | 1.7 | 1.21 | 34 |
| 0 | 1.7 | 1.14 | 49 |
| 35 | 1.1 | 1.15 | 10 |

*** High molecular weight fraction ** Low molecular weight fraction**

**Table 2-16: Molecular weight for different polymerization temperatures (Gilch MDMO, LDA)**

There is no easy explanation why, only at very low temperatures, a bimodal distribution is found. We would expect that the anionic polymerization is dominant at lower temperatures, as the expected activation energy for the initiation for the radical polymerization should be higher. To make sure that the radical polymerization was not caused by the workup, *i.e.* pouring the reaction mixture in water, the workup was slightly altered for the duplicate reaction, by adding the water to the cold reaction mixture. This had no effect on the result *i.e.* again a bimodal distribution was obtained.

Rehahn *et al*. reported that the radical Gilch polymerization typically produces 1,2-dichloro-[2,2]paracyclophane as a side reaction (Figure 2-19). [27] We also investigated the filtrate of the precipitated polymer, and found the signals described in said article. This verifies that indeed in this case, a radical polymerization mechanism is present. The same signals were not found in the filtrate of the polymerization at higher temperatures, in which no high molecular weight material was found.

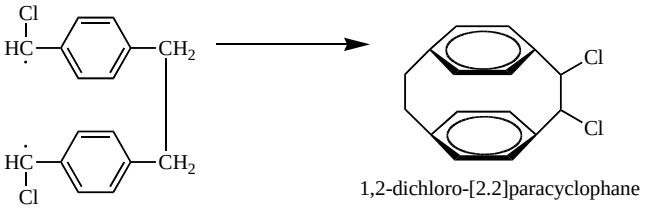


**Figure 2-19: Formation of 1,2-dichloro-[2,2]paracyclophane**

We cannot find a good explanation why the radical polymerization appears at very low temperature, but we must conclude that there must be some buildup of quinodimethane system as the radical polymerization needs a minimum concentration of quinodimethane systems to initiate. Maybe this buildup originates from a low anionic polymerization rate at very low temperatures.

To make sure that the low molecular weight material does not originate from a reaction time that is too short, an experiment was performed in which samples of the polymerization mixture were taken over time. The result clearly shows that the molecular weight does not increase with reaction time. $^{1}$H NMR confirms that no premonomer is left after 1 hour 20 minutes.

| *Reaction time* | *$M_n$ (kD)* | *PD* |
|---|---|---|
| 1h 20 min | 1.1 | 1.15 |
| 2h 20 min | 1.1 | 1.14 |
| 3h 20 min | 1.1 | 1.14 |
| 4h 20 min | 1.1 | 1.13 |

**Table 2-17: Samples taken at different times. (Gilch MDMO, LDA, 35 °C)**

Ferraris [28] claims to achieve better control (lower PD) by applying the technique of slow reversed addition. From the previous result we can conclude that the reaction is very fast. To investigate the effect of the speed of addition of the premonomer, the faster addition of the premonomer was compared to the slow addition. The result in Table 2-18 shows that adding the premonomer faster does not change the result.

| *Description* | *$M_n$ (kD)* | *PD* |
|---|---|---|
| slow addition (60 min) | 1.7 | 1.14 |
| faster addition (20 min) | 1.6 | 1.17 |

**Table 2-18: Exploring different premonomer addition speeds (Gilch MDMO, LDA, 0 °C)**

### 2.6.2 Polymerization using LHMDS as the base

When the Gilch monomer is polymerized using LHMDS as the base and THF as solvent, only high molecular weight material is obtained. (Table 2-19). This is in sharp contrast to the results using LDA, where only low molecular weight material is obtained. Based on previous experience, this tells us that the polymerization in this case is radical in nature. There seems to be a relationship between the molecular weight, yield and temperature.

| *Temperature (°C)* | *$M_n$ (kD)* | *PD* | *Yield (%)* |
|---|---|---|---|
| -78 | Monomer | | 0 |
| 0 | 45 | 7.34 | 3.1 |
| 30 | 91 | 7.94 | 44.5 |

**Table 2-19: Molecular weight in function of temperature (Gilch, LHMDS)**

$^1$H NMR analysis shows that a significant amount of premonomer is left after one hour of polymerization. This explains the low yields obtained at 0 °C. By

taking samples after different polymerization times an increase was found in the yield over time. (Table 2-20 and Table 2-21) While taking the samples great care was taken to avoid contamination of the reaction mixture by water or air. The polymerization rates seems very slow at low temperatures, probably due to slow deprotonation of the premonomer.

| *Time* | *$M_n$ (kD)* | *PD* | *Yield (%)* |
|---|---|---|---|
| 1h 20 min | 45 | 7.34 | 3.1 |
| 2h 20 min | 56 | 6.81 | 16.0 |
| 4h 20 min | 34 | 10.31 | 40.2 |
| 23h | 12 | 16.08 | 73.7 |

**Table 2-20: Molecular weight in function of time (Gilch MDMO, LHMDS, 0 °C)**

| *Time* | *$M_n$ (kD)* | *PD* | *Yield (%)* |
|---|---|---|---|
| 1 hour | 91 | 7.94 | 44.5 |
| 2 hours | 46 | 6.09 | 50.7 |
| 4 hours | 51 | 4.59 | 68.1 |

**Table 2-21: Molecular weight in function of time (Gilch MDMO, LHMDS, 30 °C)**

### 2.6.3 Comparison of characteristics

When we compare the optical absorption of the converted polymer synthesized using LDA as the base, with the polymer synthesized using LHMDS as the base, then we note a lower $\lambda_{max}$ after thermal conversion for the oligomer synthesized using LDA compared to the oligomer synthesized using LHMDS. This is probably due to the much lower molecular weight obtained when using LDA as the base. LHMDS yields high molecular weight material through a radical polymerization mechanism.

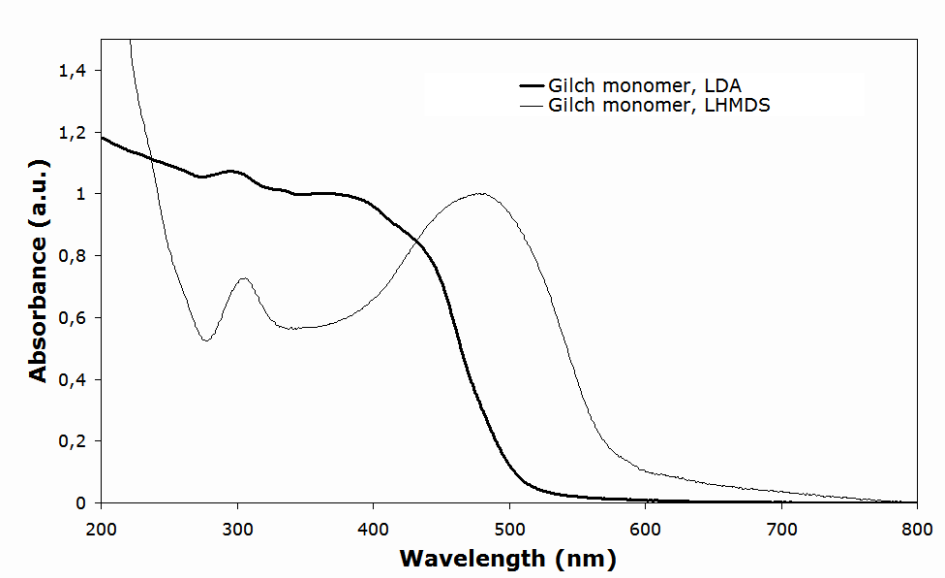


**Figure 2-20: UV-Vis spectra of Gilch MDMO-oligomer synthesized using LDA or LHMDS as the base**

### 2.6.4 Conclusion comparison sulfinyl with Gilch monomer

To explain the large difference between polymerizing the Gilch premonomer with LDA or LHMDS, it seems that the anionic polymerization in the former case is induced by the characteristics of LDA beyond just being a base. When we compare the behavior of the Gilch premonomer in the presence of LHMDS to the sulfinyl premonomer with LHMDS, then the surprising observation is that when using LHMDS in THF, the sulfinyl premonomer gives rise exclusively to an anionic polymerization where the Gilch premonomer gives exclusively rise to a radical polymerization. It is not clear what the reason is for this extreme difference in behavior. Possibly it relates to a difference in the ability of a sulfinyl functional group to stabilize a carbanion compared to a chlorine functional group. The sulfinyl route seems to be unique as anionic polymerization by using LHMDS as base seems only possible by this route.

## 2.7 Conclusions

In this chapter, we report the anionic polymerization of MDMO-PPV *via* the sulfinyl route. At first LDA was used as a strong base to achieve anionic polymerization. However, with this base oligomers were obtained with very low molecular weight. LHMDS is a superior base in this case, as polymers with not only a higher molecular weight were obtained, but also with a longer average conjugation length after elimination of the sulfinyl group. Some polymerization parameters were explored in order to increase the comparatively low molecular weight, but impurities in the premonomer sample were found to be detrimental to the molecular weight. As the premonomer purity is the most important factor, solutions have to be found to improve the premonomer purity. Due to the good solubility of MDMO-PPV premonomer in many solvents, no recrystallization solvent could be found. This leads us to the conclusion that we indeed have a good method to synthesize PPVs *via* an anionic polymerization mechanism. However, if we want to further investigate the possibilities of this polymerization, we have to find a different premonomer, which can be purified to a higher level of purity. Furthermore it seems that the Gilch MDMO-PPV premonomer in the same conditions gives rise to a purely radical polymerization mechanism. It is possible to invoke an anionic polymerization of the Gilch premonomer by using LDA as the base, however this gives rise to the formation of oligomers with a low conjugation length.

## 2.8 Experimental part

**Chemical and optical characterization.**

NMR spectra were recorded with a Varian Inova Spectrometer at 300 MHz for $^{1}H$ NMR and at 75 MHz for $^{13}C$ NMR. Analytical Size Exclusion Chromatography (SEC) was performed using a Spectra series P100 (Spectra Physics) pump equipped with a pre-column (5 μm, 50 mm*7.5 mm, guard, Polymer Labs) and two mixed-B columns (10 μm, 2x300 mm*7.5 mm, Polymer Labs) and a Refractive Index (RI) detector (Shodex) at 40 °C. THF was used as the eluent at a flow rate of 1.0 mL/min. Molecular weight distributions are given relative to polystyrene standards. GC-MS data were obtained with a Varian TSQ 3400 Gas Chromatograph and a TSQ 700 Finnigan Mat mass spectrometer. UV-Vis measurements were performed on a Cary 500 UV-Vis-NIR spectrophotometer (scan rate 600 nm/min, continuous run from 200 to 800 nm). FT-IR spectra were collected with a Perkin Elmer Spectrum One FT-IR spectrometer (nominal resolution 4 $cm^{-1}$, summation of 16 scans). *In situ* elimination reactions were performed in a variable temperature oven (Harrick). This oven can be positioned in the beam of either the FT-IR spectrometer or the UV-Vis-NIR-spectrophotometer.

**Chemicals**

All chemicals were purchased from Aldrich or Acros and used without further purification unless otherwise stated. LDA was purchased as a 2 M solution in THF, LHMDS as a 1 M solution in THF and used as such. THF was dried over sodium/benzophenone and distilled under nitrogen prior to use. All polymerizations were performed under a nitrogen atmosphere. All glassware used for the polymerizations was dried overnight in a drying oven at 110 °C prior to use.

**Preparation of 1-chloro-3,7-dimethyloctane (2)**

To a mixture of 3,7-dimethyl-1-octanol (62 g, 0.40 mol) and pyridine (1 mL) as a catalyst at 15 °C, freshly distilled $SOCl_2$ (62 g, 0.52 mol) was added

dropwise over a period of 1 hours, keeping the internal temperature below 30 °C. This mixture was heated at 100 °C for 1.5 hours. After cooling to room temperature, 30 mL of water was carefully added. The organic layer was washed 2 times with water (30 mL) and 2 times with an aqueous solution of $NaHCO_3$ (10 %, 30 mL), after which it was dried over $MgSO_4$. After distillation under reduced pressure (80 °C/10 mbar) a colorless liquid was obtained (55.76 g, 80 % yield); $^1$H NMR (300 MHz, $CDCl_3$, ppm): 3.54 (m, 2H), 1.77 (m, 1H), 1.53 (m, 3H), 1.30-1.10 (m, 6H), 0.86 (t, 9H, J=6.79); MS (EI, m/e): 176 ($M^+$), 161 ($M^+$-$CH_3$), 133 ($M^+$-$C_3H_7$), 113, 105.

**Preparation of 1-(3,7-dimethyloctyloxy)-4-methoxybenzene (3)**

In a three-neck round-bottom flask 15 g *p*-methoxyphenol (120 mmol), 13.9 g Na*t*BuO (145 mmol) were dissolved in 125 mL ethanol under $N_2$ atmosphere at room temperature, after which 1-chloro-3,7-dimethyloctane (23.33 g, 132 mmol) and 0.5 g sodium iodide (3.3 mmol) were added. The resulting solution was stirred for 72 h at reflux temperature. The reaction was quenched with water, and then extracted with $CH_2Cl_2$ (3x with 50 mL). The combined organic extracts were dried over anhydrous $MgSO_4$. $CH_2Cl_2$ was evaporated under reduced pressure. The pure product was obtained by flash chromatography over silica using n-hexane/ethylacetate 6/4 as effluent. The product could also be purified by Kugelrohr distillation. Pure product was obtained as a second fraction at 110 °C ($10^{-2}$ mbar). The first fraction consists of pure 1-chloro-3,7-dimethyloctane (**2**). A yield of 27.82 g (87 %) of **2** was obtained. $^1$H NMR (300 MHz, $CDCl_3$, ppm): 6.84 (4H, $H_{arom}$); 3.94 (m, 2H, $OCH_2$); 3.76 (s, 3H, $OCH_3$); 1.8(1H); 1.7 (1H); 1.6 (2H); 1.4 (2H); 1.3 (1H); 1.2 (3H); 0.95 (d, J=6.5Hz, 3H, $CH_3$); 0.89 (d, J=6.6Hz, 6H; 2 x $CH_3$). MS (EI, m/z): 264 ($M^+$), 124 ($M^+$-$C_{10}H_{20}$), 109 ($M^+$-$C_{11}H_{23}$).

**Preparation of 2,5-bis(chloromethyl)-1-(3,7-dimethyloctyloxy)-4-methoxy-benzene (4)**

27.82 g (0.105 mol) of **3** and 26.0 g (0.866 mol) of paraformaldehyde were placed in a three-neck round bottom flask in an ice bath. After dropwise addition of 80 mL of 37 % HCl under $N_2$ a white suspension was formed. 213 g (1.77 mol) of acetic anhydride was added dropwise at such a rate that the internal temperature did not exceed 70 °C. After stirring for 12 h at 75 °C,

the mixture was cooled and poured in 500 mL of water. The resulting white precipitate was collected by filtration and dissolved in hexane. The organic layer was washed with an aqueous solution of $NaHCO_3$ (100 mL), washed three times with water (100 mL) and dried over anhydrous $MgSO_4$. Hexane was evaporated under reduced pressure. (Yield: 94.5%) Pure product was obtained by recrystallization in hexane (Final yield: 72%). $^1$H NMR (300 MHz, $CDCl_3$, ppm): 6.91 (d, 2H, $H_{arom}$); 4.62 (d, 4H, $CH_2Cl$, J=2.07 Hz); 4.0 (m, 2H, $OCH_2$); 3.84 (s, 3H, $OCH_3$); 1.9-1.4 (4H); 1.4-1.1 (6H); 0.93 (d, 3H, J=6.45); 0.86 (d, 3H, 2x$CH_3$, J=6.6Hz). MS(CI, m/z): 360 ($M^+$), 220 ($M^+$-$C_{10}H_{20}$), 184.

**Preparation of bis-tetrahydrothiophenium salt of 2,5-bis(chloromethyl)-1-(3,7-dimethyl-octyloxy)-4-methoxybenzene (5)**

A solution of 40 g (0.11 mol) of **4** and 50 g (0.58 mol) of tetrahydrothiophene in MeOH (80 mL) was stirred for 70 h at ambient temperature under $N_2$ atmosphere. After precipitation in cold acetone (1000 mL, 0 °C), the precipitate was filtered off and washed with cold hexane. The product was dried under reduced pressure at room temperature. (88.7 g, 76 %) $^1$H NMR (300 MHz, $D_2O$, ppm): 7.12 (s, 2H, $H_{arom}$); 4.41 (s, 4H, Ar$\underline{CH_2}$S, J=2.07 Hz); 4.07 (m, 2H, $OCH_2$); 3.80 (s, 3H, $OCH_3$); 3.40 (m, 8H, $SCH_2$); 2.21 (m, 8H, $SCH_2C\underline{H_2}$); 1.9-1.4 (4H); 1.4-1.1 (6H); 0.93 (d, 3H, J=6.45); 0.82 (d, J=3.0 Hz).

**Preparation of 2-(octylsulfanyl)methyl)-5-(chloromethyl)-1-(3,7-dimethyloctyloxy)-4-methoxybenzene (6)**

A mixture of NaO*t*Bu (5.0 g, 52.1 mmol) and n-octanethiol (7.464 g, 51.05 mmol) in MeOH (100 mL) was stirred for 30 min at room temperature. The clear solution was added in one portion to a stirred solution of **5** (28.9 g, 52.1 mmol) in MeOH (160 mL). After three hours the reaction mixture was neutralized with aqueous HCl, if necessary, and concentrated in vacuo. The crude product was diluted with $CHCl_3$ (25 mL), the precipitate was filtered off and the solvent was evaporated. The obtained oil was diluted with octane (25 mL) and concentrated again to remove the tetrahydrothiophene by azeotropic distillation [29]. This sequence was repeated three times to afford light yellow viscous oil. A 23.1 g (49.0 mmol) of crude product was formed.

$^1$H NMR (300 MHz, $CDCl_3$, ppm): 6.89/6.79 (2H, $H_{ar}$); 4.58 (s, 2H, $CH_2Cl$); 4.0 (m, 2H, $OCH_2$); 3.76 (s, 2H, $CH_2S(R)$); 2.58 (t, 2H, $SC\underline{H}_2R$); 1.9-1.2 (14H, $H_{alif.}$); 0.89 (d, 3H, $CH_3$, J=6.43); 0.82 (d, 9H, 3x$CH_3$, J=6.51). MS(EI, m/z): 470.5 $[M]^+$, 330 $[M\text{-}C_{10}H_{21}]^+$, 185 $[M\text{-}C_{10}H_{21}\text{-}SC_8H_{17}]^+$.

**Preparation of 2-(octylsulfinyl)methyl)-5-(chloromethyl)-1-(3,7-dime-thyloctyloxy)-4-methoxybenzene (7)**

An aqueous (35 wt%) solution of $H_2O_2$ (8.8 g, 90.5 mmol) was added dropwise to a solution of crude thioether **6** (25.08 g, 53.23 mmol), $TeO_2$ (1.06 g, 6.65 mmol) and ten drops of diluted HCl (1N) in methanol (200 mL). The reaction was followed on TLC (time: 2.5 h) and as soon as the overoxidation took place, it was quenched by a saturated aqueous NaCl solution (30 mL). After extraction with $CHCl_3$ (3 x 30 mL), the organic layers were dried over $MgSO_4$ and concentrated in *vacuo*. (22.08 g) The reaction mixture was purified by fast column chromatography ($SiO_2$, eluent hexane/ethylacetate 60/40) to give pure **7** (65 % yield starting from the tetrahydrothiophenium salt) as light yellow viscous oil. $^1$H NMR (300 MHz, $CDCl_3$, ppm): 6.9 (d, 1H, $H_{ar}$); 6.8 (d, 1H, $H_{ar}$); 4.56 (s, 2H, $CH_2Cl$); 3.93+3.95 (dd, 2H, $CH_2S(O)R$); 3.9 (m, 2H, $OCH_2$); 3.8 (s,3H, $OCH_3$); 1.9 (1H); 1.7 (1H); 1.6 (2H); 1.4 (2H); 1.3 (1H); 1.12 (m, 2H); 0.90 (d, J=6.3Hz, 3H, $CH_3$); 0.83 (d, J=6.6Hz, 6H; 2 x $CH_3$). $^{13}$C NMR (300 MHz, $CDCl_3$, ppm): 13.87 (1C, $CH_2C\underline{H}_3$); 19.50 (1C, $CHC\underline{H}_3$); 22.4 (1C); 22.5 (2C); 24.5 (2C); 27.7 (1C); 30.2 (1C); 36.1 (1C); 37.1 (1C); 39.0 (1C); 41.1 (1C); 51.3 (d, 1C, $S(O)\underline{C}H_2CH_2$); 52.6 (d, 1C, $\underline{C}H_2S(O)$); 55.9 (d, 1C, $OCH_3$); 67.0 (d, 1C, $OCH_2$); 113.0 (1C); 115.0 (1C); 119.6 (1C); 126.4 (1C); 150.7 (2C). MS(CI, m/z): 487 $[M+1]^+$, 470 $[M\text{-}O]^+$, 325 $[M\text{-}S(O)C_8H_{17}]^+$, 289, 185, 151

**General procedure for sulfinyl precursor route polymerization using slow reversed addition**

All glassware was dried overnight in a drying oven at 110 °C and flamed under vacuum prior to use. The premonomer **7** (974 mg, 2.0 mmol) was placed in a 50 mL three-necked flask equipped with a Teflon stirrer and the flask was degassed by 3 consecutive vacuum/nitrogen cyclings. Dry, degassed THF (10 mL) was transferred to the monomer flask by use of a

glass syringe. In a second flask, the base (2.5 equivalents) was diluted in 25 mL of dry THF under nitrogen atmosphere and brought to the appropriate reaction temperature. The premonomer was transferred to a glass syringe, and the polymerization was started by slow addition of this premonomer (10 mL/hour) to the second flask. The reaction was stopped 20 minutes after complete addition of the premonomer. The excess of base was neutralized by addition of a 1.0 M aqueous hydrochloric acid solution, followed by extraction with dichloromethane. The combined organic layers were concentrated under reduced pressure. The polymers were analyzed by size exclusion chromatography (SEC) without further purification.

**General procedure for the conversion of precursor polymer to conjugated polymer**

A solution of precursor polymer (2.0 mmol, 0.9 g) in toluene (10 mL) was degassed for 1h by passing through a continuous stream of nitrogen. The solution was heated to 110 °C and stirred for 3 h. After cooling to room temperature, the solution was added dropwise to cold methanol (100 mL) resulting in the precipitation of the polymer. The polymer was filtered off on a Teflon filter, washed with cold methanol and dried at room temperature under reduced pressure. The conjugated MDMO-PPV was obtained as a red polymer. Yields were quantitative.

**The influence of temperature on the polymerization**

The general polymerization procedure for slow reversed addition was followed. The different polymerization temperatures were obtained as follows: 0 °C with an ice/water mixture; -78 °C using a mixture of acetone and solid $CO_2$. The polymerizations at 30 °C and 55 °C were performed in a thermostatic flask.

**Changing the order and speed of addition**

For the test using fast reversed addition, the general procedure was followed, with the exception that the premonomer **7** was added as fast as possible by syringe, as opposed to adding over a course of one hour. In case of slow addition of the base, the premonomer was diluted in 25 mL of THF

and the base (LDA 2N, 2.5 equivalents) was added slowly over the course of one hour. In case of fast addition of the base, the base was injected in one shot (LDA 2N, 2.5 equivalents)

**Degradation tests**

A precursor polymer was synthesized using a radical polymerization.[30,31] The premonomer **7** (1 g, 2.1 mmol) was dissolved in 16 mL of s-butanol. Na*t*BuO (0.28 g, 2.91 mmol) was dissolved in 10 mL s-butanol, and both solutions were degassed for 30 min using a continuous $N_2$ flow. The polymerization starts after addition of the base to the premonomer solution. The reaction time was 1 hour at 30 °C. After stopping the polymerization by addition of water and extraction of the polymer with chloroform, the solvent was evaporated. The obtained precursor polymer was dissolved in 17mL of THF and exposed to 1.4 mmol LDA (2 N). Samples (2 mL) were taken after 20 minutes, 40 minutes, 1 hour, 2 hours and 3 hours. All samples were poured into water, neutralized with HCl (1 N) and extracted with chloroform. After evaporation of the solvent, the samples were analyzed using GPC.

**End group detection (LDA or LHMDS)**

Oligomers synthesized at 0 °C using 2.5 eq. LDA or LHMDS were used for the end group detection. The precursor oligomers were converted into the conjugated polymer by the general procedure for the conversion of precursor polymer to conjugated polymer. The conjugated polymer was dissolved in THF and separated on a column filled with BioBeads S-X. The BioBeads column was rinsed with distilled THF prior to use to remove possible impurities on the column. After evaporation of the solvent the fractions were analyzed using $^{13}C$ NMR.

**Use of other bases**

The general procedure for the synthesis of sulfinyl precursor polymer using slow reversed addition was used. The amount of base was changed to 1.1 equivalents compared to the monomer. In case of NaH, a 40% dispersion of NaH in oil was used. The oil was removed by dissolving the base in hexane and removal of the hexane after precipitation. This procedure was performed

three times without exposing the base to air. The final remains of hexane were removed under vacuum.

**Verifying anionic polymerization**

Sulfinyl premonomer (0.244 g, 0.5 mmol) was dissolved in 8.75 mL dry THF. TEMPO (39.1 mg, 0.25 mmol) was added to the premonomer solution. The solution was cooled to 0 °C and the polymerization started by adding the base (LHMDS 1N: 1.25 mmol). After 1 hour the polymerization was stopped as described in the general procedure. The polymers were further purified by precipitation from chloroform (4 mL) in cold methanol (40 mL). After filtration, the obtained polymers were analyzed using GPC.

**Preparation of 2,5-bis(chloro-$^{13}$C-methyl)-1-(3,7-dimethyloctyloxy)-4-methoxy-benzene**

A 3.16 g (12 mmol) of **2** and 1.0 g (33.3 mol) of paraformaldehyde-$^{13}$C (isotopic purity of 99%, Cambridge Isotope Laboratory, Inc., Andover) were placed in a 100 mL three-neck round bottom flask in an ice bath. After dropwise addition of 19.5 g of 37 % HCl (198 mmol) under $N_2$ a white suspension was formed. 36.78 g (360 mmol) of acetic anhydride was added dropwise at such a rate that the internal temperature did not exceed 70 °C. After stirring for 3.5 h at 75 °C, the mixture was cooled and poured in 60 mL of water. The resulting white precipitate is collected by filtration. The product was dissolved in hexane and dried over anhydrous $MgSO_4$. After recrystallization in hexane, pure product was obtained. $^1$H NMR (300 MHz, $CDCl_3$, ppm): 6.91 (dd, 1H, $H_{arom}$); 6.89 (dd, 1H, $H_{arom}$); 4.62 (dd, 4H, $CH_2Cl$,$^1$J=152 Hz, J=2.09 Hz); 4.0 (m, 2H, $OCH_2$); 3.84 (s, 3H, $OCH_3$); 1.9-1.4 (4H); 1.4-1.1 (6H); 0.93 (d, 3H, J=6.51); 0.85 (d, 3H, 2x$CH_3$, J=6.5Hz). $^{13}$C NMR (300 MHz, $CDCl_3$, ppm): 19.68 (1C, CHC$\underline{H}_3$); 22.58 (1C); 22.69 (1C); 24.68 (1C); 27.96 (1C); 29.79 (1C); 36.26 (1C); 37.22 (1C); 39.18 (1C); 41.4 (1C); 36.74+41.3 (1C, Cl$^{13}\underline{C}H_2$); 56.21 (1C, $OCH_3$); 67.37 (1C, $OCH_2$); 113.22 (1C); 114.3 (1C); 126.4-127.4 (2C); 150.7 (2C). MS(CI, m/z): 362 ($M^+$), 222 ($M^+$-$C_{10}H_{20}$), 186.

**Preparation of 2-($^{13}$C-octylsulfinyl)methyl)-5-($^{13}$C-chloromethyl)-1-(3,7-dime-thyloctyloxy)-4-methoxybenzene.**

The reactions were analogous to the synthesis of **5**, **6** and **7**. Yield 49% calculated starting from 2,5-bis(chloro-$^{13}$C-methyl)-1-(3,7-dimethyloctyloxy)-4-methoxy-benzene. $^{1}$H NMR (300 MHz, $CDCl_3$, ppm): 6.86 (d, 1H, $H_{ar}$); 6.77 (d, 1H, $H_{ar}$); 4.54 (d, 2H, $^{1}$J=154Hz, J=2.7 Hz, $CH_2Cl$); 4.2+3.7 (dd, 2H, $CH_2S(O)R$); 3.9 (m, 2H, $OCH_2$); 3.7 (d,3H, OCH3); 2.5 (m, 2H); 1.60–1.85 (m, 2H), 1.38– 1.58 (m, 2H), 1.05–1.30 (m, 6H), 0.86 (dd, 3H, $CH_3$); 0.79 (m, 6H; 2 x $CH_3$). $^{13}$C NMR (100 MHz, $CDCl_3$, ppm): 13.8 (1C); 19.4 (1C); 22.3 (2C); 22.4 (1C); 24.4 (1C); 27.7 (1C); 28.6 (1C); 28.8 (1C); 28.9 (1C); 29.6 (1C); 29.9 (1C); 31.5 (1C); 36.0 (1C); 37.0 (1C); 39.0 (1C); 41.1 (1C $^{13}CH_2Cl$); 51.5 (1C); 52.4+52.7 (1C $^{13}CH_2S(O)R$); 55.9 (d, 1C); 66.8 (d, 1C); 68.9 (Impurity); 113.5 (1C); 114.4 (1C); 119.7 (1C); 126.1 (1C); 150.6 (2C). MS(CI, m/z, rel.int. (%)): 489 $[M+1]^+$.

## 2.9 References

[1] A. Issaris; D. Vanderzande; J. Gelan, *Polymer*, **38** (10), 2571, (1997)

[2] L. Hontis; M. Van Der Borght; D. Vanderzande; J. Gelan, *Polymer*, **40**, 6615, (1999)

[3] M. Van Der Borght; D. J. M. Vanderzande; P. Adriaensens; J. Gelan, *Polymer*, **41** (8), 2743, (2000)

[4] P. Adriaensens; M. Van Der Borght; L. Hontis; A. Issaris; A. van Breemen; M. de Kok; D. Vanderzande; J. Gelan, *Polymer*, **41**, 7003, (2000)

[5] H. Becker; H. Spreitzer; W. Kreuder; E. Kluge; H. Schenk; I. Parker; Yong Cao, *Adv. Mater.*, **12**(1), 42, (2000)

[6] G. H. Gelinck; J. M. Warman; E. G. J. Staring, *J. Phys. Chem.*, **100,** 5485, (1996)

[7] C. J. Brabec; N. S. Sariciftci; J. C. Hummelen, *Adv. Funct. Mater.*, **11**(1), 15, (2001)

[8] H. Becker; H. Spreitzer; K. Ibrom; W. Kreuder, *Macromolecules*, ***32***, 4925, (1999)

[9] S. Soo, K.; K. Nehru; S. Soo Kim; D. Won Kim; H. Chul Jung, *Synthesis*, ***17***, 2484-2486 (2002)

[10] a) Leo A. Paquette; Richard V. C. Carr, *Organic Synthesis*, **Coll. Vol. 7**, 453 (1990); b) Leo A. Paquette; Richard V. C. Carr, *Organic Synthesis*, **Vol. 64**, 157 (1986)

[11] Wei Liang Xu; Yun Zheng Li; Qing Shan Zhang; He Sun Zhu, *Synthesis*, **2**, 227-232, (2004)

[12] F. Louwet, *Phd Thesis: Synthese van poly(p-xylyleen)-derivaten via een anionische polymerisatieroute: mechanisme en perspectieven*, LUC, (1993)

[13] V. Royen, *Master thesis*, KHLim, (2004)

[14] E. C. Ashby; A. K. Deshpande; G. S. Patil, *J. Org. Chem.*, **60**, 663, (1995)

[15] G. R. Newkome; D. C. Hager, *J. Org. Chem.*, **47**, 599, (1982)

[16] N. D. Kimpe; Z. P. Yao; N. Schamp, *Tetrahedron Lett.*, **27**, 1707, (1986)

[17] C. Shen; C. Ainsworth, *Tetrahedron Lett.*, **20**, 89, (1979)

[18] G. Wittig; C. N. Rentzea; M. Rentzea, *Liebigs Ann.*, 744, (1971)

[19] E. C. Ashby; B. Park; G. S. Patil; K. Gadru; R. Gurumurthy, *Journal Of Organic Chemistry*, **58**, 424-437, (1993)

[20] T. E. Long; R. A. Guistina; B. A. Schell; J. E. Mcgrath, *J. Polym.Sci. Part A: Polym. Chem.*, **32**, 2425, (1994)
[21] S. K. Taylor; J. A. Fried; Y. N. Grassl; A. E. Marolewski; E. A. Pelton; T. J. Poel; D. S. Rezanka; M. R. Whittaker, *J. Org. Chem.*, **58**, 7304, (1993)
[22] B. Ye; L. Qiao; Y. Zhang; Y. Wu, *Tetrahedron*, **50**, 9061, (1994)
[23] R.R. Fraser; T.S. Mansour, *J. Org. Chem.*, **49**, 3442, (1984)
[24] U. Wannegat; H. Niederprüm, *Ber. Dtsch. Chem. Ges.*, **94**, 1540, (1961)
[25] W. N. Olmstead; Z. Margolin; F. G. Bordwell, *J. Org. Chem.*, **45**, 3295, (1980)
[26] S. Chambon; A. Rivaton; J. Gardette; M. Firon, *Solar Energy Materials and Solar Cells*, **91**(5), Selected Papers from the European Conference on Hybrid and Organic Solar Cells -- ECHOS '06, European Conference on Hybrid and Organic Solar Cells, 394-398, (2007)
[27] J. Wiesecke; M. Rehahn, *Macromol. Rapid Commun.*, **28**, 78–83, (2007)
[28] C. J. Neef; J. P. Ferraris, *Macromolecules*, **33** (7), 2311–2314, (2000)
[29] CRC Press, *Handbook of chemistry and physics*, **64th edition**, page D-17, (1983-1984)
[30] L. Lutsen; A. Van Breemen; W. Kreuder; D. Vanderzande; J. Gelan, *Helvetica Chimica Acta*, **83**, 3113, (2000)
[31] L. Lutsen; P. Adriaensens; H. Becker; A. J. van Breemen; D. J. M. Vanderzande; J. Gelan, *Macromolecules*, **32** (20), 6517-6525, (1999)

# Chapter 3

# Mechanistic study on the sulfinyl route towards unsubstituted PPV

*This chapter focuses on the synthesis of Poly(p-phenylene vinylene) or 'unsubstituted PPV' via an anionic polymerization mechanism. The previous chapter showed the importance of the purity of the premonomer when using anionic polymerization to synthesize MDMO-PPV. As MDMO-monomer was difficult to purify, 1-(Chloromethyl)-4-[(n-octylsulfinyl)methyl]benzene or 'unsubstituted PPV premonomer' was chosen to further investigate the possibilities of anionic polymerization. After double recrystallization of the premonomer, polymers could be synthesized with relatively high molecular weight. The anionic nature was verified by polymerizing in presents of a radical inhibitor. Various polymerization conditions were explored and the issue of reproducibility was addressed. The new polymerization procedure provides us with a tool to further investigate the anionic polymerization of PPVs. The chapter concludes with a few experiments to see whether the polymerization is living or not. In the next chapter end-capping of the polymer and the use of multifunctional initiators are explored.*

# 3.1 Introduction

This chapter describes the synthesis of Poly(*p*-phenylene vinylene) (PPV) using a strong base in a aprotic solvent such as THF. The previous chapter concluded with the idea that premonomer purity is the most important factor for the result of the polymerization. The polymerization parameters such as temperature and order of addition, did not have much effect on the molecular weight of the oligomers obtained. This is not unexpected for the anionic polymerization, as the molecular weight for living anionic polymerization is only determined by the ratio of monomer to initiator. It was concluded that impurities are built into the polymer and therefore probably acted as initiators. This means that if a higher molecular weight is desired using anionic polymerization, very pure premonomer has to be used. As MDMO-monomer is quite difficult to purify, another premonomer had to be chosen which is much easier to purify, e.g. 1-(Chloromethyl)-4-[(n-octylsulfinyl)methyl]benzene (**1**). This premonomer can be recrystallized in a chloroform/hexane mixture.

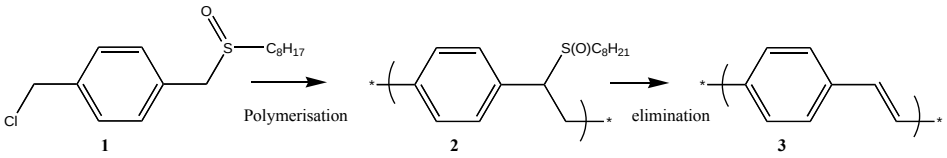


**Figure 3-1: Synthesis of unsubstituted PPV *via* sulfinyl route**

# 3.2 Monomer synthesis and storage

The premonomer (**1**) was synthesized according to a known procedure.[1] Special attention was taken towards the purification of the premonomer, as this is expected to have a great effect in the outcome of the polymerization. The premonomer was recrystallized twice from a hexane/chloroform mixture after purification using column chromatography. The premonomer was obtained as a white powder. $^{1}H$ NMR and $^{13}C$ NMR were used to check for impurities, and within the detection limits, none were found.

During the initial study of the polymerization of **1** in THF using LHMDS as the base, a notable decrease in molecular weight was noted over time for

repeating polymerizations under the same conditions (Table 3-1). In this period the premonomer was always dried under vacuum before use, but not stored under dry nitrogen atmosphere during storage. The decrease in molecular weight when repeating polymerizations under the same conditions shows the importance of keeping the premonomer dry. Therefore a new batch of premonomer was synthesized and kept under dry nitrogen during storage (at -20 °C when stored for several days). After exposure to air, the batch was dried under vacuum for 1 hour and brought back under nitrogen. From time to time a standard polymerization with LHMDS was performed to verify that the premonomer did not change in a period of four months. This clearly shows that premonomer purity is an extremely important factor, as can be expected for anionic polymerizations.

| *Time after synthesis of premonomer* | *Temperature (°C)* | $M_n$ *(kD)* | *PD* |
|---|---|---|---|
| Few days | 0 | 29.8 | 3.89 |
| 1 month | 0 | 22.5 | 2.80 |
| 7 months | 0 | 19.4 | 2.80 |

**Table 3-1: Reproducibility of results over longer period of time when not properly stored**

## *3.3 Comparing base LDA with LHMDS*

First results of premonomer polymerized at various temperatures (-64 °C and 0 °C) on a vacuum line using fast normal addition (base added to the premonomer solution) in THF as solvent and with LDA as the base, indicated the occurrence of exclusively anionic polymerization (Table 3-2, entries 1 & 2). However the polydispersities observed are inconsistent with living polymerization. The presence of exclusively oligomers raised the idea that LDA could act as an anionic initiator: LDA has been already reported in literature as being an initiator for the anionic polymerization of methacrylate monomers and a more steric hindrance base namely LHMDS was preferred which could not act as initiator of the polymerization.[2] In our case, polymers with 10 times higher molecular weight were obtained when polymerizations were repeated using LHMDS as the base instead of LDA. (Table 3-2, entries 3 & 4)

| *Base* | *Temp (°C)* | *$M_n$ (kD)* | *PD* |
|---|---|---|---|
| LDA | -64 | 1.4 | 1.31 |
| LDA | 0 | 1.9 | 1.88 |
| LHMDS | -64 | 22 | 2.10 |
| LHMDS | 0 | 20 | 3.21 |

**Table 3-2: Result of polymerizations of premonomer (1) at -64 °C and 0 °C in THF**

A similar result was observed using the MDMO-PPV monomer (Table 2-1 on page 40 and Table 2-7 on page 50), although only a doubling of molecular weight could be observed when switching from LDA to LHMDS. Clearly also in this case, LHMDS provides a better polymer and therefore will be used for all further polymerizations in this chapter.

### 3.3.1 Evaluation of the conversion process of the precursor polymers towards the conjugated polymer

One of the analytical techniques that gives insight in the elimination and degradation reaction of the precursor polymer and conjugated polymer respectively, is *in situ* UV-Vis spectroscopy. The UV absorption of the conjugated polymer is due to the $\pi$-$\pi^*$ transition in the conjugated backbone and depends on the 'effective' conjugation length.

The UV-Vis experiments are performed using a dynamic heating program of 2 °C/min from room temperature up to 200 °C under a continuous flow of nitrogen. For this purpose a specially designed oven, the Harrick High Temperature cell (HHT cell), containing the precursor polymer spin-coated on a quartz window is placed in the beam of the spectrometer. During the elimination step, a gradual red-shift is observed as oligomeric fragments start to form. At a further stage, the absorption band becomes broad as the conjugation length increases.

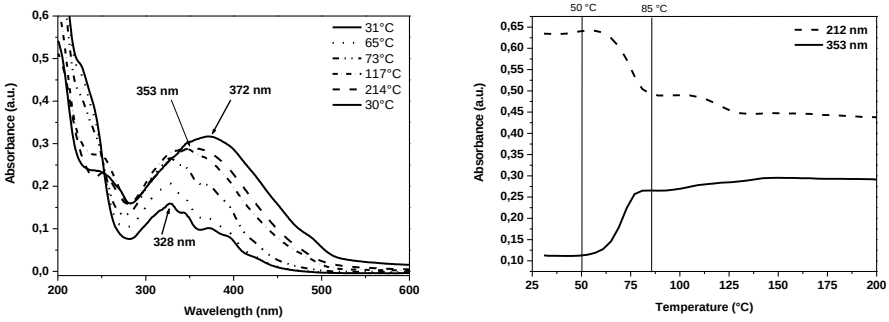


**Figure 3-2: UV-Vis absorption spectra of the polymer synthesized using LDA in function of temperature (left). UV-Vis profile of the maximum absorption peak (max = 353 nm) as a function of the temperature for the polymer synthesized using LDA (right)**

Before heating, the polymer synthesized with LDA showed a strong absorbance at 328 nm as shown in Figure 3-2 (left). As the heating program progressed, a new absorption band appeared that gradually increased in intensity and wavelength with the increasing temperature. This was due to an extension of the average conjugation length. Finally, the maximum absorption peak was obtained at 353 nm. Due to thermochromic effects, this maximum shifts to 372 nm after cooling down to room temperature.

Figure 3-2 (right) shows the formation of the conjugated system in a temperature range of 50 °C to 85 °C, as the absorbance at 353 nm increases. The conjugated structure started to develop around 50 °C and the majority of the conjugated segments were already formed when, at a heating rate of 2 °C/min, the temperature reached 85 °C.

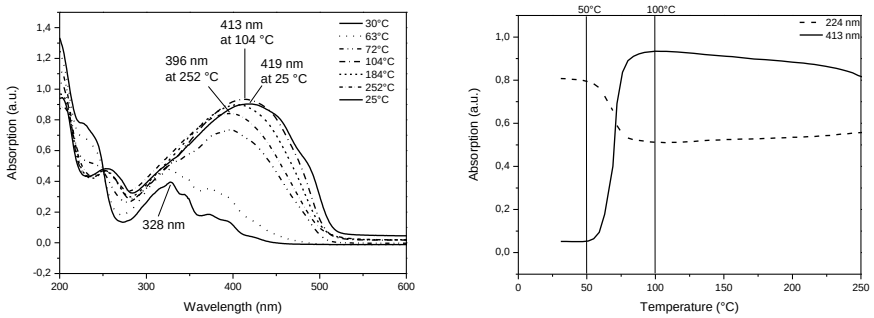


**Figure 3-3: UV-Vis absorption spectra of the polymer synthesized using LHMDS in function of temperature (left). UV-Vis profile of the maximum absorption peak (max = 413 nm) as a function of the temperature for the polymer synthesized using LHMDS (right)**

The precursor polymer synthesized with LHMDS also showed a strong absorbance at 328 nm as shown in Figure 3-3 (left). As the heating program progressed, a new absorption band appeared that gradually red shifted with increasing temperature. The maximum absorption peak was obtained at 413 nm at 104 °C. Due to thermochromic effects, this maximum shifts to 396 nm when the polymer is further heated to 252 °C and to 419 nm after cooling down to room temperature. This is higher than the maximum obtained after cooling of the polymer synthesized with LDA.

Figure 3-3 (right) shows the formation of the conjugated system in a temperature range of 50 °C to 100 °C, as the absorbance at 413 nm increases. The conjugated structure started to develop around 50 °C and the majority of the conjugated segments were already formed when, at a heating rate of 2 °C/min, the temperature reached 100 °C.

Compared to LDA, the oligomer synthesized using LHMDS had a much higher $\lambda_{max}$. The starting temperature for the elimination as well as the temperature at full conversion was rather similar in both cases. The reason for the lower $\lambda_{max}$ when using LDA can be either explained by the presence of a higher amount of defects in the polymer chain or by the fact that the oligomer length is shorter.

### 3.3.2 *In situ* infrared spectroscopy (FTIR)

To obtain additional information about the temperature range in which the elimination and degradation reactions take place, an *in situ* heating reaction on the polymers synthesized using LDA or LHMDS was performed under continuous flow of nitrogen at 2 °C/min starting from ambient temperature up to 350 °C. A film of the precursor polymer was spin-coated on a KBr pellet and inserted into the HHT-cell, in which the elimination reaction was carried out.

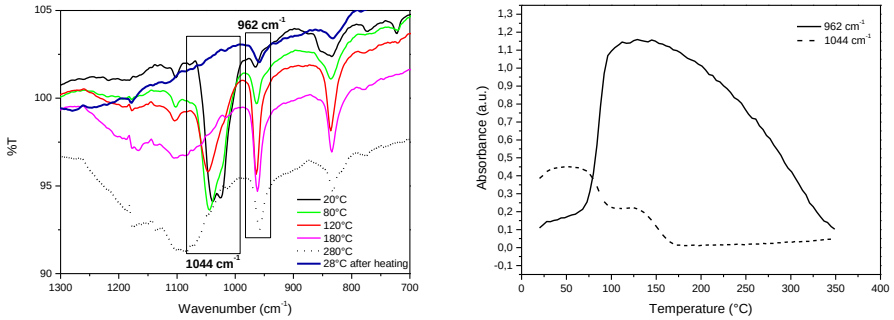


**Figure 3-4: Overlay of FT-IR spectra of PPV obtained by using LDA as the base at different temperatures during thermal conversion (left). Absorbance profile at 962 cm$^{-1}$ and 1044 cm$^{-1}$ *versus* temperature for the sulfinyl precursor polymer (right).**

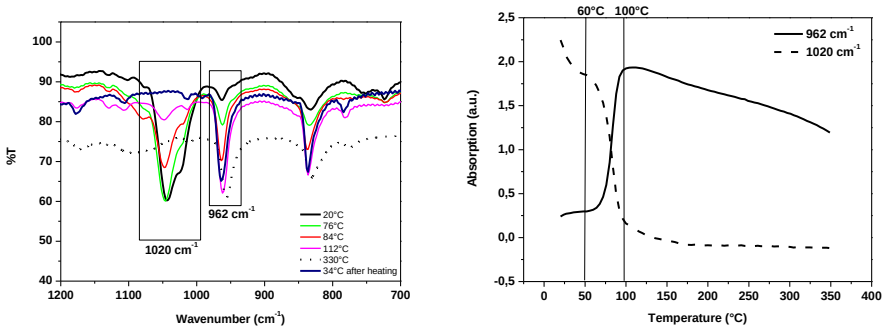


**Figure 3-5: Overlay of FT-IR spectra of PPV obtained by using LHMDS as the base at different temperatures during thermal conversion (left). Absorbance profile at 962 cm$^{-1}$ and 1020 cm$^{-1}$ *versus* temperature for the sulfinyl precursor polymer (right).**

During elimination, we monitored the IR absorbance at a certain wavenumber *versus* time. The increase and decrease of the *trans* vinylene double bond absorption at 962 cm$^{-1}$, and the decrease of the sulfinyl

absorption at 1044/1020 $cm^{-1}$ (elimination) *versus* increasing temperature are displayed in Figure 3-4 and Figure 3-5. The elimination of the sulfinyl leaving group started already at 65 °C and was completed at 110 °C using these heating conditions for both the oligomer synthesized using LDA and the oligomer synthesized using LHMDS. As expected, the IR absorbance of the *trans* vinylene double bond increased in this temperature range, whereas the sulfinyl absorption signal decreased. In the region between 110 °C and 180 °C, there was a slight decrease in the absorbance of the double bond. This was not due to decomposition of the conjugated polymer material, but was related to a thermochromic effect as was already demonstrated by *in situ* UV-Vis experiments. At higher temperatures a fast decrease in the absorbance at 962 $cm^{-1}$ could be observed indicating the degradation of the conjugated polymer. This degradation was much more pronounced for the material synthesized using LDA as compared to the oligomer synthesized using LHMDS. These observations are in excellent agreement with the UV-Vis data.

## 3.4 Verification of the anionic nature of the polymerization

To verify the anionic versus radical character of the polymerization using LHMDS in THF, the effect of 2,2,6,6-Tetramethylpiperidine-1-oxyl (TEMPO) was studied on the new polymerization procedure, and compared to a classic radical polymerization of PPV. TEMPO is a stable radical and is widely used as a radical trap in organic synthesis and free radical polymerizations. For the Wessling precursor route, the radical trapping reagent TEMPO in some cases completely suppressed the formation of high molecular weight poly(α-tetrahydrothiophenio para-xylylene). UV-Vis spectral analysis showed that the radical trap did not affect the equilibrium production of the para-xylylene, hence TEMPO must affect the subsequent polymerization chain propagation steps, which is strong evidence that the mechanism is radical in nature.[3]

Using Na*t*BuO as a base in s-butanol, high molecular weight material was obtained (Table 3-3, entry 1) *via* a radical polymerization mechanism.[4] When this experiment was repeated with the addition of 0.5 equivalents of TEMPO,

the molecular weight lowered dramatically, and almost no polymer could be recovered after precipitation in methanol (entry 2). When the same experiments were conducted using LHMDS as the base in THF, with (entry 6) and without TEMPO (entry 5), no change was observed on the molecular weights, nor in the yields of the reactions. This nicely verified that the polymers were not obtained through a radical mechanism. To further prove that the base is responsible for the change to an anionic mechanism, the effect of TEMPO was also attempted on a polymerization in THF using Na*t*BuO as the base. Again high molecular weight material was obtained in absence of radical inhibitor TEMPO, and a drastic decrease of both yield and molecular weight in presence of TEMPO (Table 3-3, entry 3 and 4 and Figure 3-6). Concerning the Gilch route, Rehahn *et al.* investigated the addition of TEMPO to suppress the radical polymerization of PPV, and came to the conclusion that one equivalent of TEMPO is necessary to completely stop the radical polymerization.[5] This could explain the fact that only a reduced molecular weight was observed (entry 4) when 0.5 equivalents of TEMPO were used to suppress the radical polymerization.

| *Entry* | *Base* | *Solvent* | *Additive* | $M_n$ *(kD)* | *PD* | *Yield (%)* |
|---|---|---|---|---|---|---|
| 1 | Na*t*BuO | s-butanol | None | 52 | 4.02 | 52 |
| 2 | Na*t*BuO | s-butanol | TEMPO | 7.0 | 1.43 | < 1 |
| 3 | Na*t*BuO | THF | None | 191.9 | 6.87 | 79 |
| 4 | Na*t*BuO | THF | TEMPO | 41.4 | 2.73 | 21 |
| 5 | LHMDS | THF | None | 17.3 | 2.50 | 84 |
| 6 | LHMDS | THF | TEMPO | 14.1 | 3.47 | 82 |

**Table 3-3: Verification of anionic nature of polymerization**

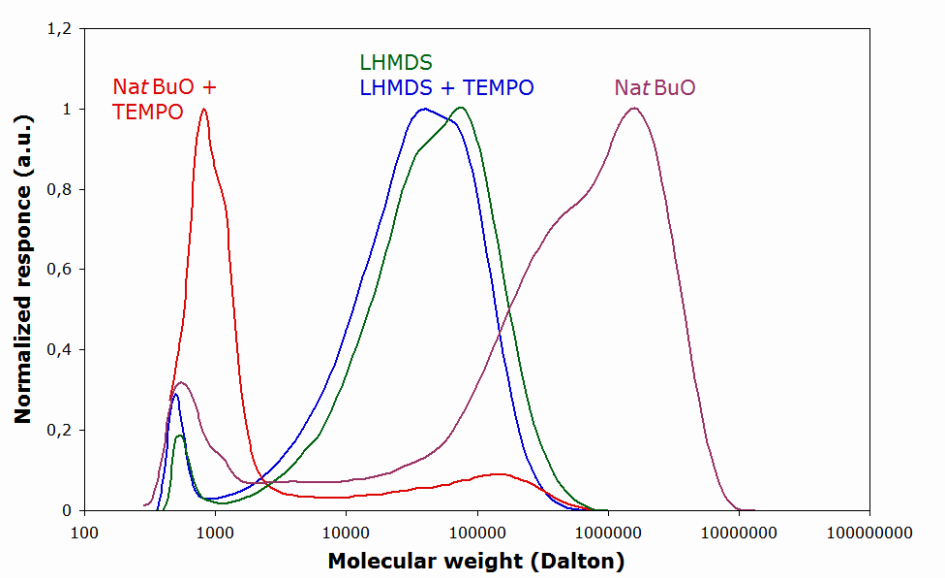


**Figure 3-6: Verification of anionic nature of polymerization**

## *3.5 Exploring reaction conditions*

A small set of experiments was performed to investigate the effect of the different polymerization parameters on the molecular weight of the obtained polymer. In these experiments, the effect of the monomer concentration, the amount of base and the polymerization temperature were investigated. Comparing entry 1, 2 and 3 in Table 3-4 one can see little effect of the premonomer concentration on the molecular weight. This is in contrast to the radical polymerization of PPV, in which a doubling of the concentration roughly results in a doubling of the molecular weight.[6] The polydispersity however did seem to increase when increasing the monomer concentration.

By comparing entry 1 with entry 4, we can see the effect of doubling the amount of base. The effect of temperature is visible by comparing entry 1 with entry 5 and 6. There does not seem to be any change in molecular weight or polydispersity when the amount of base was doubled. Furthermore, increasing the temperature did not seem to have any effect. Lowering the temperature to -64 °C had an effect on the solubility of the premonomer in THF which might explain the lower molecular weight

obtained at - 64 °C. Possibly the premonomer was not fully dissolved during the polymerization resulting in a lower molecular weight.

| *Entry* | *Concentration Monomer (M)* | *Eq base* | *Temperature (°C)* | *$M_n$ (kD)* | *PD* |
|---|---|---|---|---|---|
| 1 | 0.1 | 1.1 | 0 | 22.5 | 2.80 |
| 2 | 0.5 | 1.1 | 0 | 16.7 | 4.56 |
| 3 | 0.05 | 1.1 | 0 | 27.5 | 2.33 |
| 4 | 0.1 | 2.0 | 0 | 26.4 | 2.48 |
| 5 | 0.1 | 1.1 | -64 | 17.4 | 1.96 |
| 6 | 0.1 | 1.1 | 30 | 16.4 | 3.64 |

**Table 3-4: Exploring different reaction conditions**

In general, it is evident that there is little effect of the polymerization parameters on the outcome of the polymerization. Concentration does seem to have an effect on the polydispersity, but not on the obtained molecular weights. These results are very different from the results expected for a radical polymerization of PPV, in which especially the concentration has a large effect 6. On the other hand, the results are not unexpected for an anionic polymerization.

### 3.5.1 Change of reaction medium: aprotic apolar solvent

Both the solvating power and the dielectric constant of the reaction medium considerably increase the reactivity of initiators, compared to that of aprotic apolar hydrocarbons. This occurs as a result of disaggregation of aggregates, solvation of active species and even by dissociation of ion pairs into free ions. The data in Table 3-5 show the pronounced effect of the solvent in the polymerization of styrene by sodium naphthalate ($3x10^{-3}$ M) at 25 °C.[7] The apparent propagation rate constant is increased by 2 and 3 orders of magnitude in tetrahydrofuran and 1,2-dimethoxyethane, respectively, compared to the rate constants in benzene and dioxane. Hence, to slow down the reaction speed in order to better investigate the kinetics of the polymerization reaction, a polymerization solvent with a lower dielectric constant was chosen. Since the dielectric constant of toluene (Toluene: 2.38 THF: 7.58)[8] is similar to that of benzene and dioxane, toluene should be able

to slow down the polymerization rate. In addition, the solubility parameter is similar to that of THF (Toluene: 18.2 $J^{1/2}cm^{-3/2}$, THF: 20.3 $J^{1/2}cm^{-3/2}$).

| *Solvent* | *Dielectric Constant ($\varepsilon$)* | *$K_p^{App}$ (L $mol^{-1}$ $s^{-1}$)* |
|---|---|---|
| Benzene | 2.2 | 2 |
| Dioxane | 2.2 | 5 |
| Tetrahydrofuran | 7.6 | 550 |
| 1,2-dimethoxyethane | 5.5 | 3800 |

**Table 3-5: Effect of solvent on anionic polymerization of styrene. Data taken from reference 7**

It was observed that the polymers obtained in toluene had the same molecular weight as the polymers obtained in THF (Table 3-6). It was also evident that the type of polymerization was anionic, since the addition of TEMPO had no effect on the result obtained. When the polymerization was performed in toluene, an immediate color change to yellow was observed on addition of the base. Precipitation of polymer was visible within minutes. Even though that toluene should slow down the polymerization rate, it still seems that the polymerization is very fast, too fast for kinetic studies. Lowering the temperature further to decrease the kinetics would result in precipitation of the premonomer and the obtained yield. We therefore abandoned the idea to perform kinetic studies on the anionic polymerization of PPVs.

| *Solvent* | *Additive* | *Eq base* | *$M_n$ (kD)* | *PD* |
|---|---|---|---|---|
| Toluene | none | 1.2 | 9.9 | 4.10 |
| Toluene | TEMPO | 1.2 | 12.0 | 3.38 |
| Toluene | none | 2.4 | 13.1 | 2.41 |
| Toluene | TEMPO | 2.4 | 8.4 | 2.20 |

**Table 3-6: Polymerization of 1 in Toluene using LHMDS as the base**

### 3.5.2 Effect of monomer concentration

The initial exploration of the polymerization parameters showed little effect of the monomer concentration on the obtained molecular weight. This is in contrast to the radical polymerization of PPV, in which the concentration has a large effect.6 In the anionic polymerization of MDMO-monomer also little effect of the monomer concentration was observed. To further verify this

effect, the concentration was changed from 0.01 M to 0.1 M. The observed result at 0 °C was somewhat surprising, since we did not see a clear linear relationship between concentration and molecular weight but rather a large difference between the experiments done in duplicate (Table 3-7). After precipitation, the filtrate was analyzed by $^{1}$H NMR, and some remaining premonomer was found. Yield of the polymerization was found to be typically around 80-90%. In case of entry 1, more premonomer was found in the filtrate compared to entries 2 to 4. The reason for finding some premonomer left after the reaction may be found in the amount of base used (1.1 equivalents) in these polymerizations.

| *Entry* | *Conc. (M)* | *$M_n$ (kD)* | *PD* | *Yield (%)* |
|---|---|---|---|---|
| 1 | 0.010 | 8.2 (8.9) | 2.45 (2.34) | 82 (54) |
| 2 | 0.025 | 8.7 (8.8) | 2.51 (2.53) | 90 (85) |
| 3 | 0.075 | 16.0 (13.0) | 3.20 (3.02) | 94 (75) |
| 4 | 0.100 | 11.2 (13.9) | 2.80 (2.83) | 68 (79) |

**Table 3-7: Effect of monomer concentration. Duplicate in brackets.**

The extent of variation is more apparent when five polymerizations were compared, which were performed under the same conditions. The polymerization was performed five times using the same batch of premonomer at 0 °C, with a premonomer concentration of 0.05 M and 1.2 equivalents of base.

| *Experiment* | *$M_n$* | *PD* |
|---|---|---|
| 1 | 14.9 | 3.96 |
| 2 | 15.4 | 3.82 |
| 3 | 9.8 | 2.99 |
| 4 | 14.1 | 2.71 |
| 5 | 9.3 | 2.20 |
| **Avg.** | 12.7 ±2.9 | 3.14 |

**Table 3-8: Variation of polymerization results**

The data in Table 3-8 show a variation of the results which is larger than the change of molecular weight at different monomer concentrations, making it impossible to make any claims on the effect of monomer concentration on the polymerization, other than the claim that the resulting molecular weight

does not change more than the apparent standard deviation of the experiment.

### 3.5.3 Change of base concentration

One possible explanation for the apparent variation of the molecular weight seen in the previous paragraph would be that the base might be too concentrated and would create small, but significant inhomogeneities in the reaction mixture. This possible source of irreproducibility could be avoided by injecting the base in a more diluted form. In the standard procedure, the base is injected in a 1 M concentration in dry THF, but in order to study the effect of base concentration, the base was diluted to a 0.1 M concentration. The monomer concentration after injection of base was 0.05 M, the temperature was 0 °C and 1.2 equivalents of base were used.

The results in Table 3-9 show that the same variation exists when the base was diluted. Apparently, the base concentration has no effect on the reproducibility of the experiments.

| *Experiment* | $M_n$ *(kD)* | *PD* |
|---|---|---|
| 1 | 9.2 | 2.26 |
| 2 | 22.2 | 3.34 |
| 3 | 19.1 | 3.44 |
| 4 | 18.6 | 2.68 |
| **Avg.** | 17±5.6 | 2.93 |

**Table 3-9: Variation by using diluted base**

### 3.5.4 The use of a base with a different cation

Another way of improving the reproducibility might be a change of the cation of the base. The cation can have many effects on the polymerization. Lithium is generally better solvatated in aprotic polar solvents, such as THF, than the larger Sodium ion. Therefore less free ion pairs are present when using $Na^+$ as counterion, and the polymerization should go slower. In an aprotic apolar solvent such as dioxane, in which there is no solvatation of the cation, larger cations are less strongly linked to the anion, and therefore larger cations speed up the reaction.

The result in Table 3-10 show that there was not much change in the molecular weight obtained when NaHMDS was used as the base. If we compare the results of the previous experiments using LHMDS with this experiment, we notice that the reproducibility is not good in both cases. The average yield of the polymerizations with NaHMDS as the base was 85.1 %.

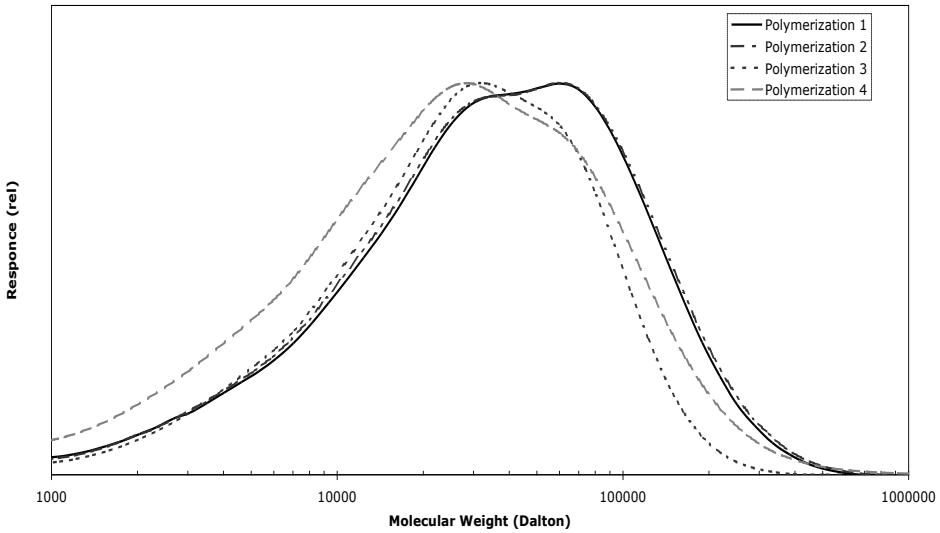


**Figure 3-7 : Polymerization results using NaHMDS as the base**

| *Base* | *Number of experiments* | $M_n$ *(kD)* | *PD* |
|---|---|---|---|
| LHMDS (1.0 M) | 5 | 13±2.9 | 3.14 |
| LHMDS (0.1 M) | 4 | 17±5.6 | 2.93 |
| NaHMDS (1.0 M) | 4 | 14±2.6 | 3.67 |

**Table 3-10: Effect of base on the reproducibility of the polymerization**

### 3.5.5 Characterization of polymers synthesized using NaHMDS by means of UV-Vis

The UV-Vis spectrum of the polymer obtained by polymerization using NaHMDS (1.0 M) (previous paragraph) was measured using a dynamic heating program of 2 °C/min from room temperature up to 200 °C under a continuous flow of nitrogen. During the elimination step, a gradual red-shift was observed concomitant with the formation of oligomeric fragments.

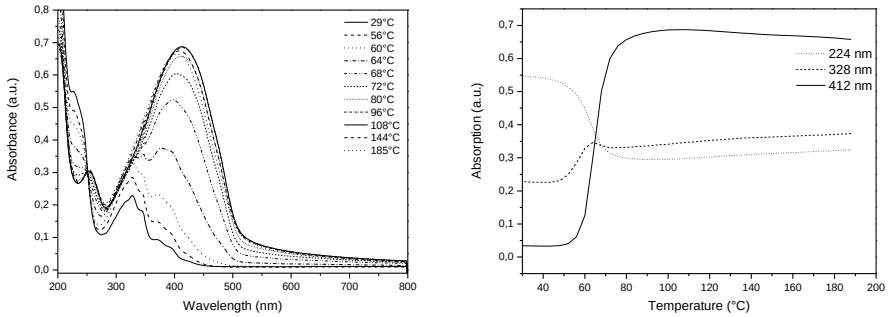


**Figure 3-8: UV-Vis absorption spectra of the polymer synthesized using NaHMDS in function of temperature (left). UV-Vis profile of the maximum absorption peak (max = 412 nm) as a function of the temperature for the polymer synthesized using NaHMDS (right)**

Before heating, the polymer showed a strong absorbance at 328 nm as shown in figure 3-8 (left). As the heating program progressed, a new absorption band appeared that gradually increased in intensity with increasing temperature. This was due to an extension of the average conjugation length. Finally, the maximum absorption peak was obtained at 412 nm.

Figure 3-8 (right) shows the formation of the conjugated system in a temperature range from 55 °C to 80 °C, as the absorbance at 412 nm increases. The conjugated structure started to develop around 55 °C and the majority of the conjugated segments had already been formed when, at a heating rate of 2 °C/min, the temperature reached 80 °C. This is similar to the result obtained with the polymers synthesized using LHMDS as the base (Figure 3-3, page 84).

### 3.5.6 Characterization of polymers synthesized using NaHMDS by means of FT-IR

To obtain additional information about the temperature range in which the conversion and degradation reactions take place, an *in situ* heating reaction on the polymers synthesized using NaHMDS was performed under continuous flow of nitrogen at 2 °C/min starting from ambient temperature up to 350 °C, in a similar way as was done for the polymers prepared using LHMDS (paragraph 3.3.2)

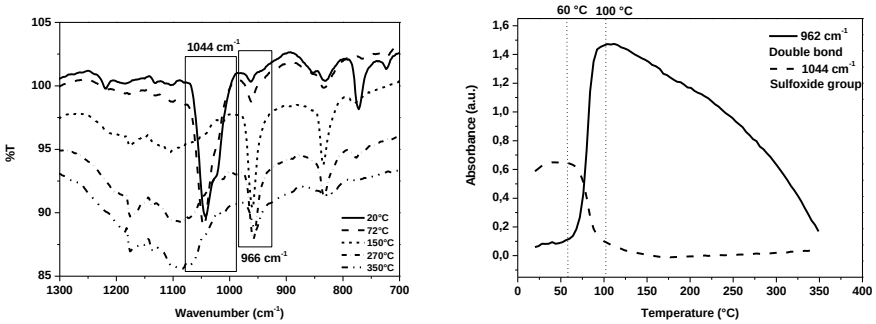


**Figure 3-9: Overlay of FT-IR spectra of PPV obtained by using NaHMDS as the base at different temperatures during thermal conversion (left). Absorbance profile at 962 $cm^{-1}$ and 1044 $cm^{-1}$ *versus* temperature for the sulfinyl precursor polymer (right).**

During conversion, we monitored the IR absorbance at a certain wavelength *versus* time. The increase and decrease of the *trans* vinylene double bond absorption at 962 $cm^{-1}$, and the decrease of the sulfinyl absorption at 1044 $cm^{-1}$ (elimination) *versus* increasing temperature are displayed in Figure 3-9.

Also in this case the results obtained were similar to the results obtained with the polymers synthesized using LHMDS.

### 3.5.7 Reaction rate

All previous polymerization times were fixed at 60 minutes. However, when the base is added, a red color usually appears within 1 minute, and in some cases precipitation was seen shortly thereafter. This suggests that the polymerization is complete after much less time than 60 minutes. If enough

base is used for the polymerization, no premonomer can be found in the filtrate after precipitation.

In order to investigate the rate of the polymerization, an experiment was set up in duplicate, from which samples were taken after 10, 20 and 40 minutes. The samples were precipitated in water, extracted and analyzed without further purification.

Monomer concentration was found to be less than 1% according to $^{1}$H NMR after 10 minutes and thereafter. This is in contrast to the experiments in which the concentration was varied and 10% premonomer was found after 1 hour reaction time (paragraph 3.5.2, page 90). The reason for this difference can be found in the low amount of excess base that was used in those experiments. Furthermore the molecular weights of the samples taken over time shown in table 11 indicate that the polymerization is completely finished after 10 minutes. This result verifies that the polymerization is very fast, making kinetic studies more difficult.

| *Time (min)* | *$M_n$ (kD)* | *PD* | *Monomer concentration in the filtrate* |
|---|---|---|---|
| 10 | 13.5 | 2.69 | < 1% |
| 20 | 15.7 | 2.86 | < 1% |
| 40 | 15.0 | 3.25 | < 1% |

**Table 3-11: Properties of samples taken after specific reaction times**

## *3.6 Conclusions*

In chapter 2 we concluded that the lack of purity of the premonomer explained the formation of oligomers. Because of difficulties in purifying MDMO-PPV premonomer, a different premonomer was investigated in this chapter. Poly(*p*-phenylene vinylene) or 'unsubstituted PPV' can be synthesized anionicly starting from a highly purified unsubstituted PPV premonomer. This premonomer was recrystallized twice to achieve this high purity. The obtained molecular weight was low in the case that LDA was used, and moderate in the case that LHMDS was used. LHMDS produces polymer with higher conjugation length compared to LDA, which is similar as the results observed when using MDMO-PPV premonomer. The anionic nature of the polymerization was verified and typical polymerization parameters were investigated. There seems to be a significant variation in the obtained molecular weight when repeating the same polymerization conditions. Although the origin of this problem of irreproducibility of the molecular weight was investigated, it could not be solved or explained. However, this was not the aim of this chapter. Instead, the goal of this chapter was to find a good polymerization procedure and the influence of the different polymerization parameters. In next chapter the use of initiators and end cappers will be investigated.

## 3.7 Experimental part

**Chemical and optical characterization.**

NMR spectra were recorded with a Varian Inova Spectrometer at 300 MHz for $^{1}H$ NMR and at 75 MHz for $^{13}C$ NMR. Analytical Size Exclusion Chromatography (SEC) was performed using a Spectra series P100 (Spectra Physics) pump equipped with a pre-column (5 μm, 50 mm*7.5 mm, guard, Polymer Labs) and two mixed-B columns (10 μm, 2x300 mm*7.5 mm, Polymer Labs) and a SpectraSYSTEM RI-150 Refractive Index (RI) detector (Shodex) at 40 °C. HPLC grade tetrahydrofuran (THF) was used as the eluent at a flow rate of 1.0 mL/min. Toluene was used as flow rate marker. Molecular weight distributions are given relative to polystyrene standards with a narrow polydispersity. GC-MS data were obtained with a Varian TSQ 3400 Gas Chromatograph and a TSQ 700 Finnigan Mat mass spectrometer. UV-Vis measurements were performed on a Cary 500 UV-Vis-NIR spectrophotometer (scan rate 600 nm/min, continuous run from 200 to 800 nm). FT-IR spectra were collected with a Perkin Elmer Spectrum One FT-IR spectrometer (nominal resolution 4 $cm^{-1}$, summation of 16 scans). *In situ* elimination reactions were performed in a variable temperature oven (Harrick). This oven can be positioned in the beam of either the FT-IR spectrometer or the UV-Vis-NIR-spectrophotometer.

**Chemicals**

Commercially available chemicals (Aldrich and Acros) were used without further purification unless stated otherwise. LDA was purchased as a 2 M solution in THF, LHMDS as a 1 M solution in THF and used as such. THF was dried over sodium/benzophenone and distilled under nitrogen prior to use. All polymerization reactions were performed under a nitrogen atmosphere. All glassware used for the polymerization reaction was dried overnight in a drying oven at 110 °C prior to use.

**Synthesis of chloromethyl-4-(n-octylsulfinyl)methylbenzene (1)**

The premonomer chloromethyl-4-(n-octylsulfinyl)methylbenzene was synthesized according to a literature procedure.[9] The premonomer was recrystallized twice in a hexane – chloroform mixture and dried overnight in a dessicator. Chemical purity was verified with $^{1}H$ NMR and $^{13}C$ NMR.

Yield: 50.3 %. $^{1}H$ NMR (300 MHz, $CDCl_3$, ppm): 7.38+7.28 (dd, 2H), 4.57, (s, 2H), 4.11+3.98 (dd, 2H), 3.92+3.84 (m, 2H), 3.64 (m, 2H), 3.61 (m, 2H), 3.51 (m, 2H), 3.33 (s, 3H), 2.90+2.70 (m, 2H).

**Standard sulfinyl polymerization procedure in THF at ambient temperature**

All glassware was dried overnight in a drying oven at 110 °C prior to use. A 100 mL three-neck flask with Teflon stirrer was dried by flaming it under vacuum. After weighing the premonomer (200mg, 0.66 mmol) and adding it to the flask, all air was removed by applying sequentially vacuum and nitrogen to the flask. Dry THF was transferred to the reaction flask by use of a glass syringe. Normal premonomer concentration was 0.05 M unless stated otherwise. The flask was brought to the appropriate reaction temperature and adding the base (1.2 eq) by syringe started the polymerization. The base was not cooled before addition to avoid precipitation of the base. After 1 hour the reaction was stopped by adding water to the reaction mixture. Excess of base was neutralized by addition of 1.0 M aqueous hydrochloric acid, followed by extraction with dichloromethane. The combined organic layers were concentrated under reduced pressure. The polymers were analyzed by SEC without further purification.

**Comparing base LDA with LHMDS**

The general polymerization procedure was followed. Prior to the addition of the base, the reaction flask with the premonomer (200 mg, 0.665 mmol in 13.5 mL THF) was cooled to –64 °C using a chloroform/liquid nitrogen bath or to 0 °C using a water/ice bath. The base was added in one addition (0.399 mL LDA 2N or 0.798 mL LHMDS 1N). The reaction was stopped after 1 hour and the polymer extracted as described in the general procedure.

**Verification of anionic mechanism**

The general polymerization procedure was followed. In case of LHMDS as the base: The premonomer (200 mg, 0.665 mmol) was dissolved in 12.5 mL THF and cooled to 0 °C using a water/ice bath. The base was added in one shot (0.865 mL LHMDS 1N, 1.3 equivalents). The reaction was stopped after 1 hour and the polymer extracted as described in the general procedure. In a parallel reaction 0.5 equivalents of TEMPO (52 mg, 0.333 mmol) were added to the premonomer solution prior to polymerization. In case of Na*t*BuO as the base the base (83 mg, 0.864 mmol) was dissolved in 10 mL of dry THF in a separate flask. The premonomer was dissolved in 3.3 mL of THF at 0 °C. The dissolved base was transferred by glass syringe to the reaction vessel in one addition.

**Use of toluene as solvent**

The general polymerization procedure was followed. Dry toluene was used as solvent instead of dry THF. Toluene was dried over Na/benzophenone under $N_2$ atmosphere until blue, and distilled into a dry three-necked flask.

**Effect of concentration**

The general polymerization procedure was followed. In four separate flasks, premonomer (4x 200 mg; 4x 0.66 mmol) was added dissolved in THF to following concentrations: 0.1 M, 0.075 M 0.025 M and 0.01 M. The reaction was performed at 0 °C with 1.1 equivalents of LHMDS. After extraction and removing solvent, the polymer was first dissolved in 5 mL $CHCl_3$ and then precipitated in a hexane/diethyl ether mixture (20 mL/20 mL). Yellow polymer was obtained in all cased with a yield of 80-90%

**Change of base concentration**

The general polymerization procedure was followed. 200 mg premonomer was dissolved in 6.5 mL of THF. The base was diluted to a 0.1 M solution and added by syringe in one shot.

**The use of a base with a different cation**

The general polymerization procedure was followed. Sodium bis(trimethylsilyl)amide (NaHMDS, 1N) was used as the base instead of Lithium bis(trimethylsilyl)amide (LHMDS, 1N). The premonomer (200 mg, 0.665 mmol) was dissolved in 12.5 mL THF and cooled to 0 °C using a water/ice bath. The base was added in one shot (0.8 mL NaHMDS 1N, 1.2 equivalents). The reaction was stopped after 1 hour and the polymer extracted as described in the general procedure. The reaction was performed 4 times. The average yield of the polymerizations was 85.1 %.

**Reaction rate**

The general polymerization procedure was followed. The premonomer (200 mg, 0.665 mmol) was dissolved in 13.3 mL THF and cooled to 0 °C using a water/ice bath. The base was added in one shot (0.732 mL LHMDS 1N, 1.1 equivalents). Samples were taken after 10, 20 and 40 minutes using a dry syringe. Care was taken that no moisture or air entered the reaction vessel. The samples were precipitated in water, extracted and analyzed without further purification.

## 3.8 References

[1] L. J. Lutsen; A. J. van Breemen; W. Kreuder; D. J. M. Vanderzande; J. M. J. V. Gelan, *Helvetica Chimica Acta*, **83** (12), 3113-3121, (2000)

[2] S. Anton; Ph Teyssié; R. Jérôme, *Journal of Polymer Science: Part A*, **35**, 3637-3644, (1997)

[3] F. R. Denton III; Paul M. Lahti; F. E. Karasz, Journal of Polymer Science Part A: Polymer Chemistry, **30** (10), 2223–2231, (1992)

[4] A. Issaris; D. J. M. Vanderzande; J. M. J. V. Gelan, *Polymer*, **38** (10), 2571, (1997)

[5] J. Wiesecke; M. Rehahn, *Macromolecular Rapid Communications*, **28**, 78-83, (2007)

[6] D. J. M. Vanderzande; L. Hontis; A. Palmaerts; D. Van Den Berghe; J. Wouters; L. Luts; T. Clije, *SPIE*; 59370Q, (2005)

[7] G. Odian, *Principles of polymerization*, Fourth edition, Wiley-Interscience Publication, (2004)

[8] J. A. Riddick; W.B. Bunger; T. K. Sakano, *Organic solvents: Physical properties and purification*, **Fourth edition**, Wiley-Interscience Publication, (1986)

[9] A. J. J. M. Van Breemen; D. J. M. Vanderzande; P. J. Adriaensens; J. M. J. V. Gelan, *J. Org. Chem.*, 64, 3106-3112, (1999)

# Chapter 4

# End functionalization of unsubstituted PPV

*The mechanistic study on the sulfinyl route in chapters 2 and 3 led to the conclusion that an exclusively anionic polymerization of PPV is possible. In case of unsubstituted PPV, a moderate molecular weight is obtained. The use of anionic initiators should therefore be possible. Four similar initiators were synthesized and tested in different concentrations with the polymerization. The results indicate that indeed the initiators work as expected and are incorporated in the polymer chain. This opens up many new possibilities to synthesize conjugated polymers bearing functional end groups. Theoretically, block-co-polymers could be obtained by performing a reaction at these chain ends (e.g. coupling of polymers, or by using the functional PPV as macroinitiators). An even more simple method of obtaining block-co-polymers, is by adding a second monomer at the end of the anionic polymerization of PPV. Clearly the use of initiators opens up many new possibilities for specific polymer architectures.*

## *4.1 Introduction*

Chapter 3 concluded with a new method to synthesize PPV *via* an anionic mechanism. Using 'unsubstituted PPV' premonomer **1** (1-(Chloromethyl)-4-[(n-octylsulfinyl)methyl]benzene), polymers with moderate molecular weights can be obtained (Figure 4-1). We have verified that we indeed have

a fully anionic mechanism under these conditions. In addition, the phenomenon is reasonably reproducible, even though some variation on the obtained molecular weight in successive polymerizations remains present.

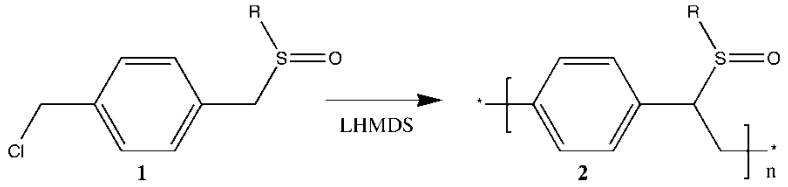


**Figure 4-1: Anionic polymerization of unsubstituted PPV**

The next step is to gain more control over the polymerization by using anionic initiators. For the initiation to be successful, the free energy of the initiation step must be favorable, and in order to have a narrow polymer dispersity, the initiation has to be faster than the propagation, and no transfer reactions should be present. For the classical anionic polymerization, it is necessary that the $pK_a$ of the initiator is higher than the $pK_a$ of the propagating anion, so that the first addition is energetically favorable. If the propagating anion is not very strongly stabilized, a powerful nucleophile is required as initiator. On the other hand, if the propagating anion is strongly stabilized, a rather weak nucleophile will be successful as initiator, although more powerful nucleophiles would work too. In the case of the anionic polymerization of PPV, there is an energy gain when the quinodimethane system of the monomer becomes aromatic. It was calculated by Schwalm et al. that although direct attack of K*t*BuO to the *p*-quinodimethane monomer in THF is exothermic, the bimolecular process is calculated to be slightly endergonic at room temperature ($\Delta G_{calcd} \approx +8$ kJ $mol^{-1}$) despite the aromatization of the $\pi$-system.[1] For the polymerization to take place, it is therefore necessary that the initiator is a stronger nucleophile then K*t*BuO although that a slightly less strong nucleofile than the propagating anion would probably also be energetically favorable. The anionic polymerization of PPVs is however more complicated. A strong nucleophile, such as s-butyl lithium, would be immediately protonated by the rather acid protons of the premonomer. We therefore cannot use an initiator that is a stronger base than the deprotonated premonomer, however the initiator anion must still react efficiently with the quinodimethane system. Therefore we looked for an initiator similar to the growing chain end. To this end we have synthesized

four very similar initiators, bearing a sulfinyl group on one side and a different functional group on the other. (Figure 4-2) After deprotonation of the position next to the sulfinyl group, these additives could act as initiators for the anionic polymerization. The four different substituents on the ring will influence the acidity of this proton. We expect that an initiator with higher acidity of the protons in benzylic position, will be deprotonated faster, but the initiation speed will be lower.

## *4.2 Synthesis of initiators*

The synthesis of the initiators, which are presented here, is quite straightforward. In contrast to the synthesis of the premonomer, the bissulfonium salt is not needed as an intermediate step, and direct substitution with an excess of octanethiol is possible. Oxidation was done on the unpurified thioether, resulting in a mixture of products in the last step. After column chromatography and two recrystallizations, very pure initiator was obtained.

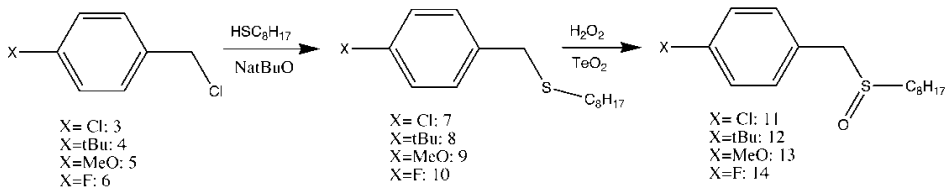


**Figure 4-2: The four initiators used in the study**

During the re-crystallizations, we encountered some problems. An unknown black powder seemed to form during the re-crystallization. In order to investigate the reason for this problem, a simple test was performed. Pure initiator (with fluorine group) was tested for the resistance against water or oxygen at elevated temperature (60 °C) in the re-crystallization solvent. The test showed that the initiator quickly degraded when water was present in the solvent at elevated temperature. As a result, all solvent and product should be dried in order to avoid degradation of the initiators. When dryness is ensured, no black powder was observed during re-crystallizations. The initiators were always stored in a desiccator.

Another question is whether the initiators will be consumed in side reactions because of the strong basic environment present during the polymerization. In order to test for this possibility, fluorine initiator was dissolved in THF and deprotonated using 2 equivalents of LHMDS for 1 hour. After normal workup, the initiator was found unchanged as established by $^1$H NMR.

## 4.3 The polymerization procedure

The polymerization procedure used for this study is based on the polymerization procedure of previous chapter. The polymerization was performed in a three-necked flask with Teflon stirrer. Prior to the reaction all glassware was dried overnight in an oven, and before use by heating with a flame under vacuum. To degas the solvent, a flask was charged with dry THF and $N_2$ gas was passed through the liquid for 15-30 minutes. After the unsubstituted PPV premonomer (200 mg) and the initiator were added to the reaction vessel, the flask was again brought under vacuum for 15 minutes. Afterwards an exact amount of THF was transferred to the reaction vessel by syringe, providing a premonomer concentration of 0.05 M. The polymerization was started by adding 1.2 equivalents of LHMDS (1 M) by syringe. After 1 hour at 0 °C, the reaction mixture was precipitated in water, extracted and analyzed without further purification. In selected cases the polymer was afterwards precipitated in a mixture of hexane-diethylether (1/1). The precipitated polymer was recovered by filtration, washed with hexane and dried under reduced pressure at room temperature. Residual fractions were concentrated *in vacuo*. A preliminary study was done using the four different initiators **11, 12, 13** and **14** at 0 mol%, 5 mol% and 10 mol%. Afterwards a more detailed study was performed to verify this result using a lower amount of initiators (1 mol% and 2 mol%).

## 4.4 Results and discussion

The experimental results obtained in the presence of the initiators show many interesting results. The results of the initial study presented in Figure 4-3 and the results of the more detailed study revealed in Table 4-1 show that the initiators had a strong effect on the molecular weight. The numerical

molecular weight lowered in the initial study from 12 kilodalton when no additive was used to 6 kDa when 5% initiator was used and 4 kDa when 10% initiator was used. Clearly the effect was very reproducible as the more detailed study showed similar effects. When the inverse molecular weight was plotted *versus* the amount of additive used, a clear linear relationship was found (Figure 4-4).

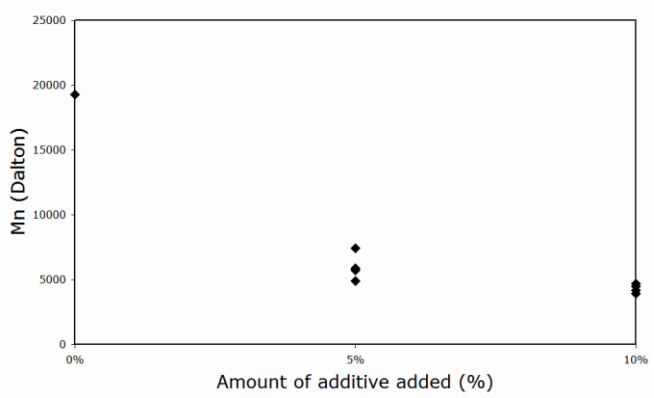


**Figure 4-3: Initial study of the effects of the different additives**

| *Initiator* | *Amount initiator (mol%)* | *$M_n$ (kD)* | *PD* | *St dev (kD)* |
|---|---|---|---|---|
| - | 0 | 12.1 | 2.88 | 17.38 |
| 11 | 1 | 11.6 | 2.83 | 6.42 |
| (Cl-) | 2 | 9.8 | 2.83 | 8.77 |
| | 5 | 6.1 | 2.29 | 1.15 |
| | 10 | 4.1 | 1.93 | 0.30 |
| 12 | 1 | 11.7 | 3.38 | 5.81 |
| (*t*.butyl-) | 2 | 10.6 | 3.12 | 2.57 |
| | 5 | 5.9 | 2.77 | 0.84 |
| | 10 | 4.1 | 2.29 | 0.70 |
| 13 | 1 | 10.3 | 4.33 | 8.30 |
| ($CH_3O$-) | 2 | 9.2 | 3.58 | 5.52 |
| | 5 | 6.7 | 2.51 | 2.21 |
| | 10 | 4.7 | 2.23 | 0.72 |
| 14 | 1 | 10.4 | 2.73 | 0.20 |
| (F-) | 2 | 9.1 | 2.61 | 2.63 |
| | 5 | 5.7 | 2.14 | 0.24 |
| | 10 | 3.9 | 1.89 | 0.05 |

*** Additive 14 and 13 in duplicate, 11 and 12 in triplicate.**

**Table 4-1: Detailed study of the effect of the additives**

In literature, additives have been used before in order to gain control over the molecular weight of PPV-derivatives. [2-6] However, as far as we know, this is the first time that a linear relationship between inverse molecular weight and amount of additive has been found (cf. Chapter 1). This is strong evidence that our initiators indeed work in the initiation step of the polymerization and that an anionic polymerization occurs.

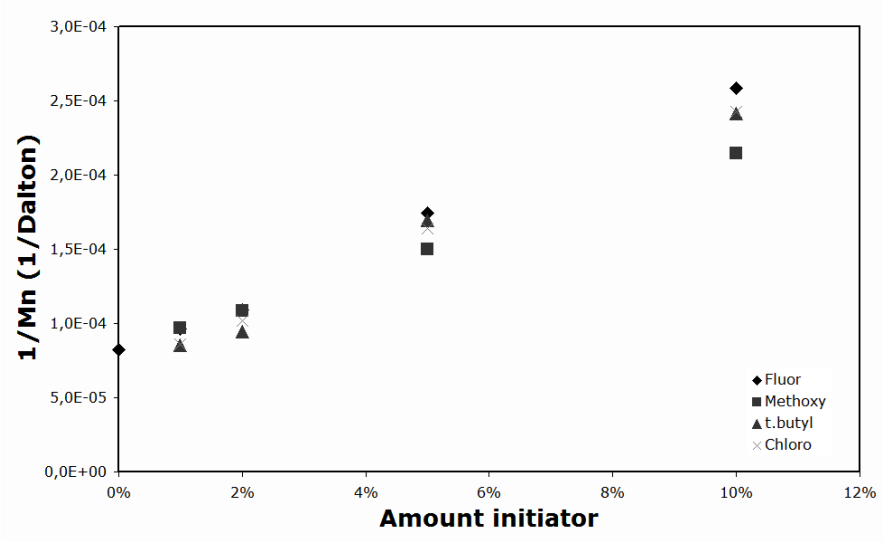


**Figure 4-4: Plot $1/M_n$ *versus* amount of additive added to polymerization**

For a living anionic polymerization, the degree of polymerization DP, can be predicted by the formula below.

$$DP = \frac{[M]_0}{[I]_0} \rho$$

where $[M]_0$ and $[I]_0$ are the initial molar concentrations of the monomer and initiator, respectively and $\rho$ is the conversion percentage.

In the case of the synthesis of PPVs *via* an anionic polymerization, we have to take into account that "impurities" probably also act as initiator moieties. Indeed we have to note that the polymerization is spontaneous when we add base to the premonomer. This implies that there must be some initiator present in order to start the polymerization. The amount of this spontaneous

initiation is relatively high; as only polymers with moderate molecular weight are formed. This means that the formula needs to be adapted to accommodate for a certain amount of "impurities". The formulas below assume the presence of a living anionic polymerization with full consumption of the monomer.

$$\mathrm{DP} = \frac{[\mathrm{M}]_0}{[\mathrm{Impurities}] + [\mathrm{Initiator}]_0}$$

$$\mathrm{M}_n = Const \times \mathrm{DP}$$

$$\frac{1}{\mathrm{M}_n} \propto \frac{1}{\mathrm{DP}} = \frac{[\mathrm{Impurities}]}{[\mathrm{M}]_0} + \frac{[\mathrm{Initiator}]_0}{[\mathrm{M}]_0}$$

$$\frac{1}{\mathrm{M}_n} = a \times b. \frac{[\mathrm{Initiator}]_0}{[\mathrm{M}]_0}$$

The identity of said "impurities" can be real "impurities" as referred to in chapter 2 or are maybe intrinsic initiators present as a consequence of *p*-quinodimethane system formation. Indeed possibly the benzylic anion formed after deprotonation of the premonomer may act as an initiator (Figure 4-5). This would imply that in this case a competition exists between formation of the *p*-quinodimethane system and the initiation of the anionic polymerization. For the moment we do not know if the benzylic anion acts as an initiator or not, however if the benzylic anion presented in the figure below would be an efficient initiator, we would expect much lower molecular weights.

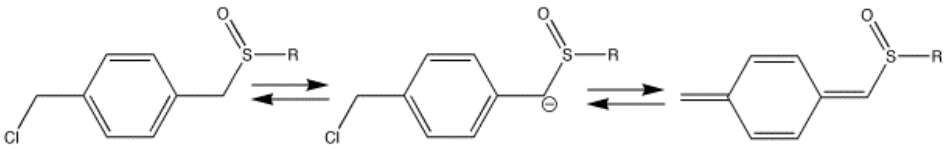


**Figure 4-5: formation of the true monomer from the premonomer**

Closer inspection of the results presented in table 4-1 reveals that there is no significant effect of the substituents on the initiator on the obtained molecular weight. All initiators seem to have a similar effect on the molecular weight. This is interesting for the development of future initiators,

knowing that both electron withdrawing and electron donating groups can be incorporated.

### 4.4.1 Verification of anionic polymerization mechanism

| *Initiator* | *Additive* | *Amount initiator (mol%)* | *$M_n$ (kD)* | *PD* |
|---|---|---|---|---|
| **12** (*t*.butyl) | none | 10 | 4.1 | 2.24 |
| **13** (methoxy) | none | 10 | 4.7 | 2.28 |
| **12** (*t*.butyl) | TEMPO | 10 | 4.0 | 1.83 |
| **13** (methoxy) | TEMPO | 10 | 4.2 | 2.09 |

**Table 4-2: Effect of TEMPO on the polymerization**

To confirm the occurrence of an anionic mechanism, the effect of radical inhibitor TEMPO was investigated using either a *t*.butyl or a methoxy functionalized initiator. As expected, there was no notable effect of the radical inhibitor, confirming that when an initiator is used, the polymerization mechanism remains anionic in nature.

### 4.4.2 Detection of initiator in the polymer chain

To verify that the additive acted as initiator, a $^{19}$F-NMR of the polymer synthesized in presence of 10 mol% of additive **14** was examined. The only natural occurring isotope of fluorine, $^{19}$F, is a spin ½ nucleus as the hydrogen nucleus. Its g-value is also not very different from a proton. The NMR frequency in a 1 Tesla field being 40.055 MHz, as compared to 42.576 MHz for the proton. Observation of $^{19}$F NMR is therefore comparatively straightforward accessible with standard equipment. The polymer was purified by dissolving it in a minimal amount of good solvent (chloroform) and adding a poor solvent (hexane) until precipitation occurred. By doing so, the higher molecular weight polymer precipitated first, leaving all impurities, and possible left over initiator in the liquid phase. The absence of additive or low molecular weight material was verified using GPC and $^{1}$H NMR. The $^{19}$F-NMR clearly showed a peak of a fluorine atom attached to a benzene ring (Figure 4-7). In addition, $^{13}$C NMR verifies the presence of the additive **14** build into the polymer (signals 161 ppm, 163 ppm and 115 ppm). Using $^{13}$C NMR with Fluorine decoupling, the doublet at 163-161 changes to a singulet,

again verifying the origin of this signal as being a carbon next to a fluorine atom (Figure 4-6)

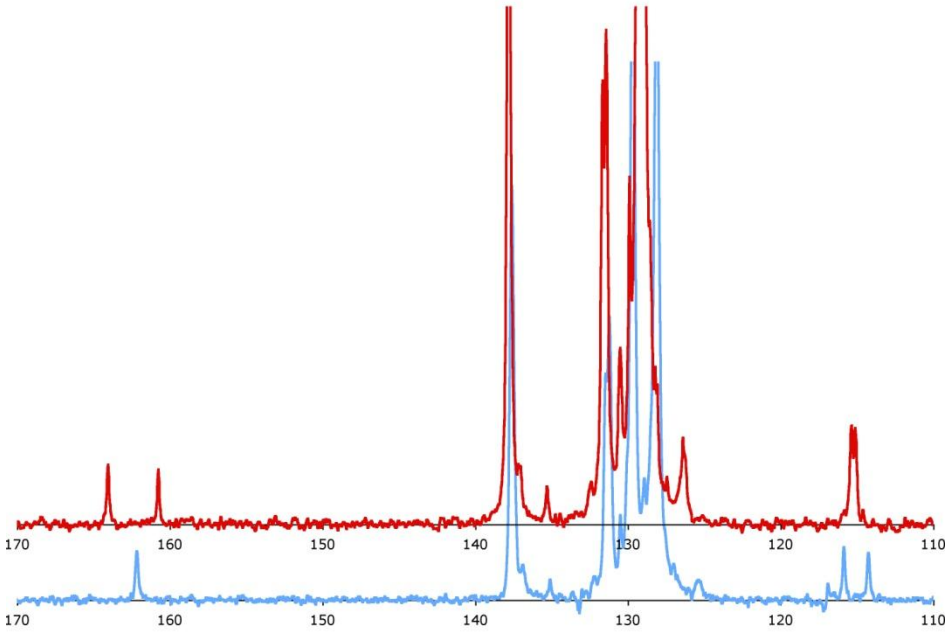


**Figure 4-6: Above: $^{13}$C NMR of polymer initiated with 14 with H-decoupling. Below: $^{13}$C NMR of polymer initiated with 14 with F-decoupling.**

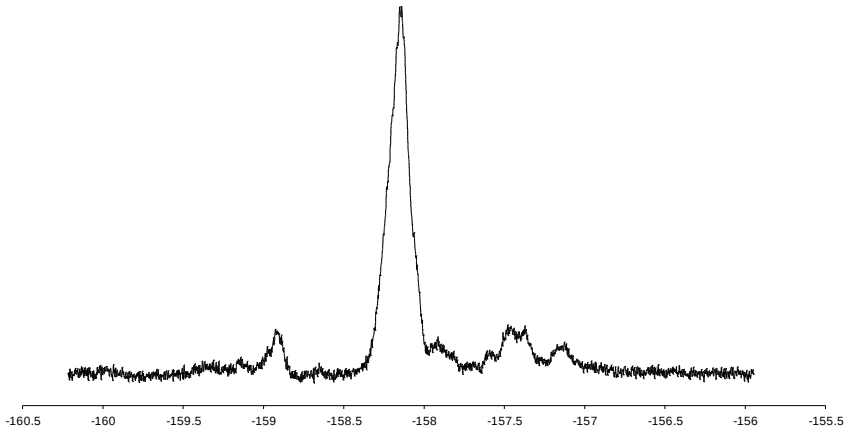


**Figure 4-7: $^{19}$F-NMR of the polymer initiated with additive 14**

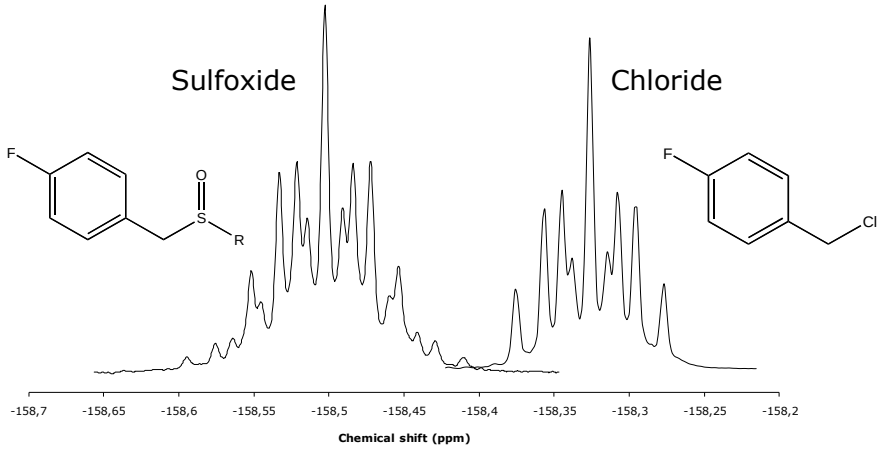


**Figure 4-8: $^{19}$F-NMR of the initiator and the starting product for the synthesis of the initiator**

Analysis of the fluorine initiator and 1-(chloromethyl)-4-fluorobenzene shows clearly the coupling between fluorine and the protons on the benzene ring. The fluorine signal from the oligomer is broader as is expected for polymer due to the reduced mobility of the chain.

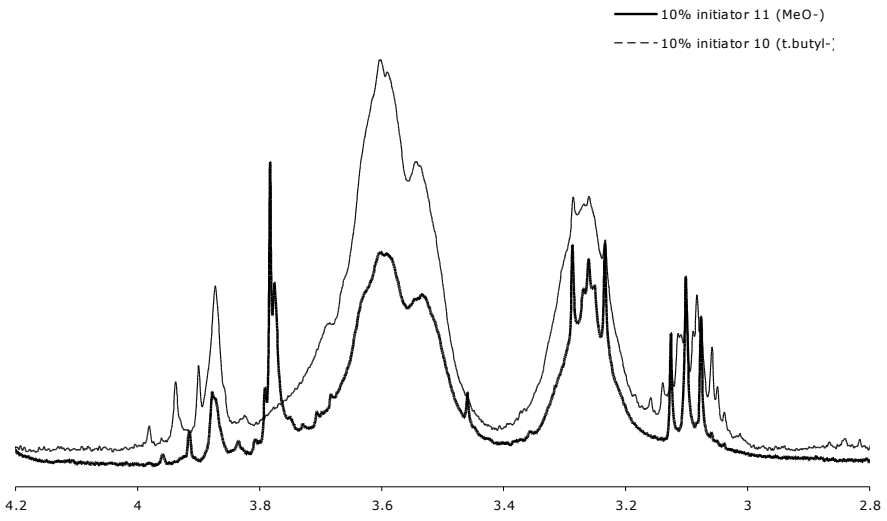


**Figure 4-9: Comparison of $^{1}$H NMR of polymer synthesized with 10% of initiator 12 vs. 10% initiator 13**

Due to overcrowding, the build-in initiators are difficult to identify in $^1$H NMR spectra of the polymers. Only in the spectrum of the polymer initiated with the methoxy-initiator, a distinct methoxy peak could be found at 3.77 ppm (Figure 4-9).

### 4.4.3 Effect of reversed addition

We still notice a large polydispersity for the polymerizations, even when high amounts of initiator are used. Possible reasons for this high polydispersity might be that the initiation speed is not faster than the propagation speed or that not all initiator is used completely. In order to try to improve the initiation reaction, the order of the addition of the chemicals to the reaction was changed. The initiator **14** and the base were cooled to 0 °C, after which the premonomer was added slowly over a period of 20 minutes. After complete addition of the premonomer, the polymerization mixture was allowed to react for an additional 20 minutes.

| | *Amount of initiator (mol%)* | *$M_n$ (kD)* | *PD* |
|---|---|---|---|
| Normal addition | 0 | 7.2 | 2.99 |
| Normal addition | 5 | 5.1 | 2.58 |
| Normal addition | 10 | 3.0 | 1.96 |
| Reversed addition | 5 | 6.0 | 2.52 |
| Reversed addition | 10 | 4.2 | 2.18 |

**Table 4-3: Effect of reversed addition when using initiator 14**

We see no effect of the reversed addition on the polydispersity. It remains relatively high compared to what would be expected for a controlled living polymerization. This however does not mean that this is not living polymerization. Most likely the initiation step is not efficient enough to obtain the very low polydispersities that can be expected when using controlled living polymerization.

Some other small tests were done to improve the polydispersity, involving complexation of the lithium ion (LiCl and $LiClO_4$), but the results did not show any improvement, so further testing was abandoned.

# 4.5 The use of multi-functional initiators

To verify that the additives really act as initiator, the following experiments were performed: three different initiators, with one, two or four initiation sites were synthesized (Figure 4-10). The additive with 2 initiation sites was used in half the amount as the one with one site, and the additive with four initiator sites was used in a quarter amount as the one with one initiation site. 10 mol% of initiator **14** was used in the first polymerization. In this case, one initiator was available for every ten monomer units. The expected polymerization degree is then 11 (the initiator is counted as one unit). Initiator **15** was present in a ratio of 1/20. The expected polymerization degree is therefore 21, a doubling of the previous polymerization.

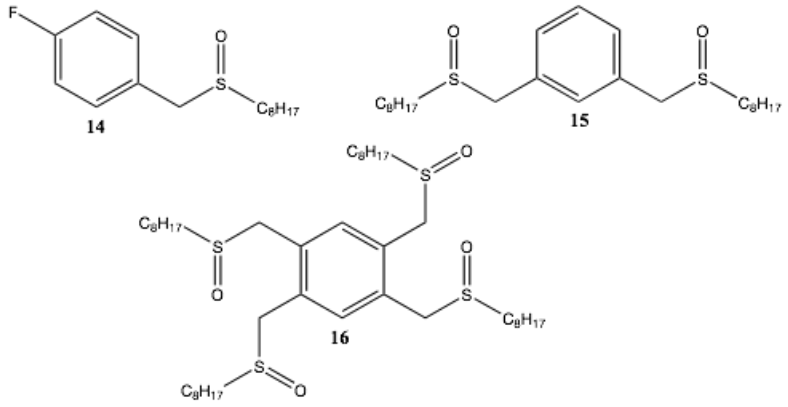


**Figure 4-10: Multifunctional initiators**

The results in table 5 clearly show this trend as expected. Clearly the additives work as initiators, even for the more sterically hindered additive (**16**).

| *Additive* | *Eq. add* | *$M_n$ (kD)* | *PD* |
|---|---|---|---|
| 14 | 0.1 | 3.96 (3.78) | 1.89 (1.96) |
| 15 | 0.05 | 6.63 (6.85) | 2.09 (2.24) |
| 16 | 0.025 | 13.21 | 2.90 |

**Table 4-4: Use of multifunctional initiators**

## 4.6 The use of end cappers

When carried out under the appropriate conditions, termination reactions do not occur in anionic polymerization. One usually adds a compound such as water or alcohol to terminate the process, since the resulting new anionic species ($HO^-$ or $RO^-$) are too weak to reinitiate.

Compounds such as water, alcohols, molecular oxygen, carbon dioxide, etc. react very quickly with the carbanions at the chain ends, terminating the propagation. Therefore, one must scrupulously dry and de-aerate the polymerization ingredients to be able to get a truly living system.

The standard polymerization using LHMDS typically has a red color during the reaction. This color immediately disappears upon addition of water. This led us to believe that a living anion might still be present on the chain end. Addition of a suitable electrofile would provide the polymer with a chosen end group. This electrofile, which reacts with the anion present at the end of the chain, is typically called an end-capper.

Three end cappers have been tested: Deuterated water, 4-*tert*-butylbenzoyl chloride and methoxy benzylchloride. To test the endcapping process, a 0.05 M solution of **1** in THF was polymerized in presence of 10mol% of **14**. Addition of deuterated water after 1 hour resulted in an immediate color change of the reaction mixture from red to yellow. The polymer was precipitated and analyzed by $^2$D-NMR. A broad signal was found at 4.0 ppm, which could originate from a deuterium attached next to a sulfinyl group (Figure 4-11). This clearly demonstrated that end-capping is potentially possible.

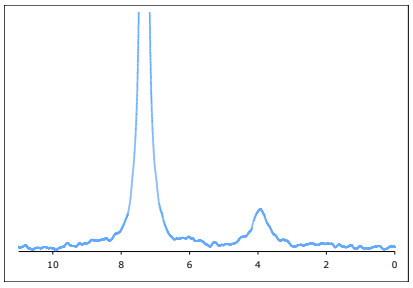


**Figure 4-11: $^2$D-NMR of end capped polymer**

The next end-capper that was tested was 4-*tert*-butylbenzoyl chloride. Benzoyl chlorides are very reactive towards anions, and are therefore good candidates for end-cappers. An extra incentive for this type of molecule is the location of the new signal after addition to the chain end. A keton

typically has a signal between 180 and 230 ppm in $^{13}C$ NMR, at which range no other signals of the polymer are located. This makes detection of the addition more straightforward. The premonomer was polymerized in presence of 10mol% of **14** and the reaction was terminated by a surplus of 4-*tert*-benzoyl chloride. Due to the use of a surplus end-capper and the solubilizing effects of it, the polymer could no longer be precipitated in the standard way. Therefore the polymer was purified by dialysis. The polymer was dissolved in chloroform and brought inside a membrane. After 48 hours of dialysis the polymer was analyzed using $^{13}C$ NMR. *Tert*-butylbenzoyl chloride has a specific signal for the carbonyl chloride at 167.8 ppm. Both the signals of the initiator and the acyl chloride function could be found in roughly the same amount (Figure 4-12).

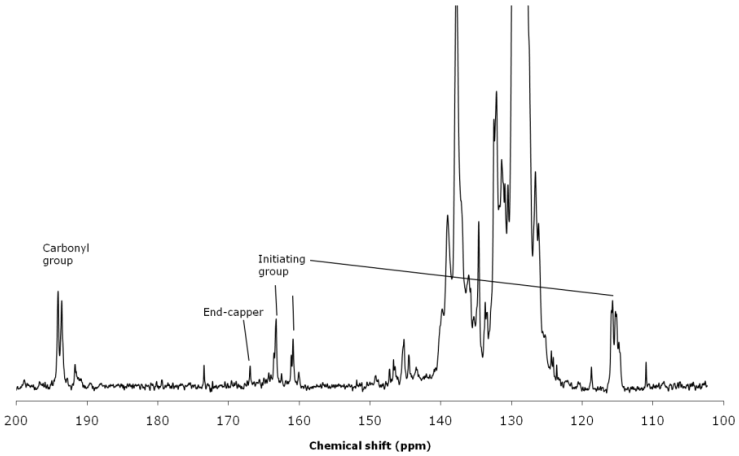


**Figure 4-12: $^{13}C$ NMR of end capped polymer**

The use of a benzoyl chloride as an end-capper has a possible disadvantage, since a keton functional group is introduced in the polymer structure. This keton could later act as an electron trap, reducing the performance of the device in which it would be used. A better end-capper would be a continuation of the conjugation, bearing a functional group that could be later used for further polymerization, or reaction. Therefore another end-capper was used, namely: methoxy benzyl chloride. Analysis of the $^{13}C$ NMR is more difficult as the signal of the methoxy group can easily be confused with the signal of trace amounts of dichloromethane, but the signal of the

methoxy group could also be found in the $^{1}H$ NMR spectrum (Figure 4-13). The signal of the aldehyde group could not be detected.

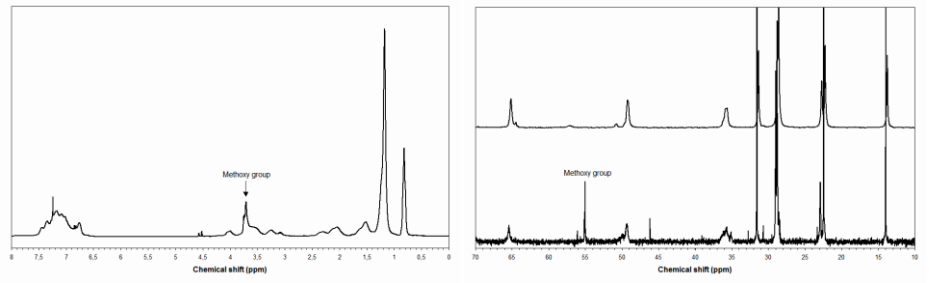


**Figure 4-13: Left: $^{1}H$ NMR of PPV end capped with methoxy benzyl chloride, right: $^{13}C$ NMR of polymer with end capping at bottom, without end capping at top.**

### 4.6.1 Living polymerization

Many anionic polymerizations, especially of non-polar monomers such as styrene and 1,3-butadien, take place under conditions in which there are no effective termination reactions. Propagation occurs with complete consumption of monomer resulting in the formation of living polymers. The propagating anionic centers remain intact since transfer of a proton or other positive species from the solvent does not occur. Living polymers are produced as long as one employs solvents, such as benzene, tetrahydrofuran, and 1,2-dimethoxyethane, which are relatively inactive in chain transfer with carbanions.

The non-terminating character of living anionic polymerization is apparent in several different ways. Many of the propagating carbanions are colored. If a reaction system is highly purified so that impurities are absent, the color of the carbanions is observed to persist throughout the polymerization and does not disappear or change at 100% conversion. Further, after 100% conversion is reached, adding more monomer, either the same monomer or a different monomer, can induce additional polymerization. The added monomer is also polymerized quantitatively and the molecular weight of the living polymer is increased.

The sequential addition of premonomers was also tried for the anionic polymerization. A standard polymerization was started, but after 20 minutes

a sample was taken and a new portion of base and premonomer was added. After mixing of the second portion for 20 minutes, the reaction was terminated with a small quantity of HCl (aq).

The results in table 4-5 show that there was a small decrease in molecular weight after addition of the second portion of base and premonomer. The new premonomer does not seem to attach to the chains already present in the reaction mixture. This however does not necessarily mean that the anion on the end of the chain is not living. When adding the second portion of premonomer, new acidic protons are added to the mixture. The proton next to the sulfinyl group on the premonomer is acid enough to first terminate the living anions. The polymerization would then start again, in presence of the dead chains of the first batch. This would explain why similar molecular weight with a higher polydispersity is obtained after addition of the second batch.

| *Experiment* | $M_n$ *(kD)* | *PD* |
|---|---|---|
| Before second addition of base and premonomer | 16.2 | 3.74 |
| After second polymerization | 9.84 | 5.21 |

**Table 4-5: Sequential addition of sulfinyl premonomer**

Clearly it is not possible to obtain block-co-polymer by sequential addition of two sulfinyl premonomers, since the second batch of premonomer would terminate the first batch of polymer. A block-co-polymer could possibly be obtained with a second monomer that does not contain any acidic protons.

### 4.6.2 End capping to form an ATRP-marcoinitiator

One of the advantages of an anionic polymerization as compared to a radical polymerization, is the relative ease to make block-co-polymers. Blends of nonconjugated polymers with PPV derivatives in certain proportions can result in significant improvements in optoelectronic properties because of exciton confinement.[7,8] Diblock copolymers of poly(*p*-phenylene) (PPP) or polythiophene (PT) with polystyrene (PS) or poly(methyl methacrylate) have been shown to exhibit enhanced PL and EL properties with respect to pure PPP or PT.[9-11] There are two common ways to make block-co-polymers using anionic polymerization. The first option is the end-capping of the polymer

with a functional group, which acts as an initiator in the following polymerization, or by simply adding the second monomer to the first polymerization. The second technique requires that the anionic chain ends remain active (living) until the addition of the second monomer and that the polymerization remains energetically favorable.

ATRP or Atom Transfer Radical Polymerization is a form of pseudo living radical polymerization. It allows the polymerization reaction to be carried out in a controlled way and can be used to obtain polymers with high molecular weight and low polydispersity index. This control result from the use of a transition metal based catalyst. This catalyst provides an equilibrium between the active, and therefore propagating, polymer and the inactive form of the polymer; known as the dormant form. Since the dormant state of the polymer is vastly preferred in this equilibrium, side reactions are suppressed. By lowering the concentration of radicals, termination is suppressed and control is achieved.

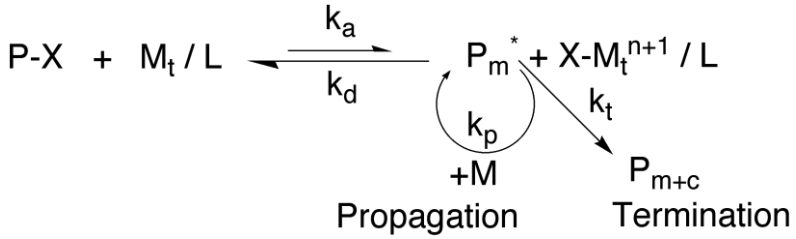


**Figure 4-14: Typical ATRP polymerization**

In order to obtain an end-capped polymer capable to be used as a macroinitiator for an ATRP polymerization, 2-bromo-propionyl bromide was used as an end capper. This molecule will react with a living anion at the end of a polymer chain, and expelling the bromide of the acyl bromide functional group. The other bromine atom is used for the ATRP-polymerization later. We used $^{13}C$ NMR to verify the attachment of the end capper. Theoretical calculations of the $^{13}C$ NMR chemical shift, predict the carbon of the keton to be visible at 207.1 ppm. The $^{13}C$ NMR of the end capped oligomer however, does not show such a signal, but does show a signal at 172 ppm. The explanation for

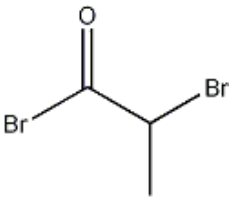


**Figure 4-15: 2-bromo-propionyl bromide**

this discrepancy can be found in a possible keto-enol equilibrium in the end capped polymer.

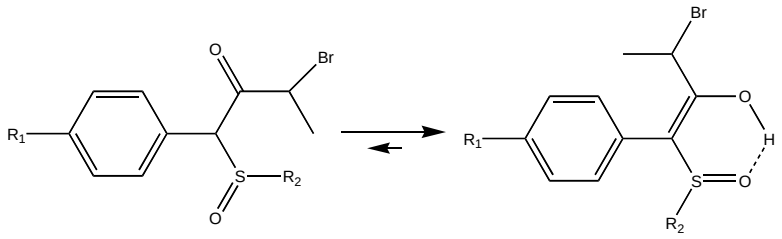


**Figure 4-16: keto-enol balance**

Probably the balance is mainly to the right, and therefore we only see a signal of an olefinic $sp^2$ carbon bearing an hydroxyl, which would appear around 170 ppm in a $^{13}C$ NMR. The integration value of this signal suggests complete end capping of the polymer, since it is of similar amount as the signal from the initiator.

### 4.6.3 Creation of block-co-polymers

Another way of creating block-co-polymers, is by addition of a second monomer after the first polymerization. The living anion at the end of the PPV-chain then can function as an initiator for the second monomer. We tested this possibility with two monomers, namely Methyl methacrylate (MMA) and Styrene. The polymerization reaction was started in presence of 0.1 equivalents of initiator (**14**) using 1.2 equivalents of base (LHMDS). After 10 minutes, one equivalent of the second monomer was added. 20 minutes after addition of the second monomer, the polymerization was stopped by addition of water and purified by precipitation and filtration.

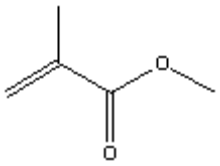


**Figure 4-17: Methyl methacrylate**

| *Type* | $M_n$ *(kD)* | *P.D.* |
|---|---|---|
| PPV homopolymer | 4.74 | 1.95 |
| PPV-PMMA copolymer | 7.87 | 2.03 |
| PPV-Polystyrene copolymer | 4.26 | 2.19 |

**Table 4-6: Results test block-co-polymerization**

As we can see in Table 4-6, only in the case of methyl methacrylate (MMA), a doubling of the numerical molecular weight was observed. Although this is only a single test, it does show a hopeful result that indeed block-co-polymerization is possible. Further testing is required to verify this possibility. Styrene does not seem to react with the PPV-anion because the formed anion after addition of one styrene unit is not as well stabilized as the anion on the PPV-chain. This means that there is no driving force for this reaction, and that therefore this initiation is not efficient. This is the reason that no higher molecular weight is found when styrene is added as second monomer.

## *4.7 Conclusions*

Chapter 3 concluded with the anionic polymerization of unsubstituted PPV. This chapter builds further on this polymerization procedure, and explores the possibility to use anionic initiators and end-cappers. Four slightly different initiators have been synthesized and tested on the anionic polymerization of PPVs. All have similar effect, lowering the molecular weight in an inverse proportional way compared to the amount of initiator used. This allows us to control the molecular weight of the polymer by adding more or less initiator to the polymerization reaction.

The use of multi-functional initiators has been explored. Initiators with two and four initiator sites were synthesized and used for the polymerization of unsubstituted PPV. The results are consistent with the expectations that multiple initiations take place at these compounds.

Also end capping of the PPV polymerization was investigated. The initial test using deuterated water, showed the possibility of end capping. Further test were performed using methoxy benzylchloride and 4-tert-butylbenzoyl chloride. In both cases, the attached end group could be found by $^{13}C$ NMR.

The number of experiments performed on the end capping of PPV made through an anionic pathway was quite limited. Notwithstanding, the experiments do give a strong indication that this polymer can indeed be end capped by a large variety of end cappers.

The use of both functional initiators and functional end cappers creates very exciting possibilities. Polymers with such functionalities could be used in the self-assembly of new polymer materials.

A simple test was performed to investigate the living character of the polymerization. It does not look promising to synthesize block-co-polymers by adding two different PPV premonomers, but this does not mean that block-co-polymerization is not possible with other premonomers. This was exemplified by the block-co-polymerization of PPV with MMA. Even though this was a single test, the results were promising, since a block-co-polymer was obtained.

## *4.8 Experimental part*

**Chemical and optical characterization.**

NMR spectra were recorded with a Varian Inova Spectrometer at 300 MHz for $^{1}H$ NMR and at 75 MHz for $^{13}C$ NMR using a 5 mm probe. Analytical Size Exclusion Chromatography (SEC) was performed using a Spectra series P100 (Spectra Physics) pump equipped with a pre-column (5 μm, 50 mm*7.5 mm, guard, Polymer Labs) and two mixed-B columns (10 μm, 2x300 mm*7.5 mm, Polymer Labs) and a SpectraSYSTEM RI-150 Refractive Index (RI) detector (Shodex) at 40 °C. HPLC grade tetrahydrofuran (THF) was used as the eluent at a flow rate of 1.0 mL/min. Toluene was used as flow rate marker. Molecular weight distributions are given relative to polystyrene standards with a narrow polydispersity.

**Chemicals**

Commercially available chemicals (Aldrich and Acros) were used without further purification unless stated otherwise. LHMDS was purchased as a 1 M solution in THF. THF was dried over sodium/benzophenone and distilled under nitrogen prior to use. All polymerization reactions were performed under a nitrogen atmosphere. All glassware used for the polymerization reaction was dried overnight in a drying oven at 110 °C prior to use.

**General procedure for the synthesis of the initiators (11-14)**

The starting product (**3-6**, 1 equivalent) was dissolved using a Teflon stirrer in ethanol in a three-necked flask together with NaI (1 mg). In a separate flask, n-octanethiol (2 equivalents) was diluted in ethanol to 2 molar. Na*t*BuO (2.1 equivalents) was added to the n-octanethiol solution while cooling the mixture. The deprotonated n-octane mixture was added slowly, over the course of 10 minutes, to the diluted starting product. After 1 hour the reaction was stopped by pouring into water, and the product was extracted with dichloromethane (3x 200 mL). After Extraction, the organic layer was washed with NaOH (2.5 N, 3x 200 mL) and water (3x 200 mL).

The organic layer was dried using $MgSO_4$, filtrated and the solvent was removed.

The intermediate product (**7-10**) (1 equivalent) was dissolved in methanol (5 M). $H_2O_2$ (35 %, 2 equivalents) was added dropwise after addition of Tellurium oxide (0.1 equivalents) and 1 mL of HCl (1N). The reaction was stopped when over-oxidation was visible (2h) on TLC by quenching with a saturated aqueous NaCl solution. The water phase was extracted three times with chloroform. The combined organic layers were dried on anhydrous $MgSO_4$, filtrated and concentrated in *vacuo*. Purification by flash chromatography (effluent: Hexane/ EtOAc 5/5).

**Synthesis of 1-chloro-(octylsulfinylmethyl)benzene 11**

The general procedure for the synthesis of the initiators was followed. 1-chloro-4-(chloromethylbenzene) **3** (10 g, 62 mmol) was dissolved in ethanol (74 mL). n-Octanethiol (18.141 g, 124 mmol) was deprotonated with Na*t*BuO (12.493 g, 130 mmol) and added to the starting product. A yellow-brown oil **7** was obtained (17.6 g). $^1$H NMR (400 MHz, $CDCl_3$, ppm): 0.9 (t, 3H, $CH_2C\underline{H}_3$), 1.3-1.5 (m, 10H, $C\underline{H}_2$), 1.8 (m, 2H, $SCH_2C\underline{H}_2$), 2.4 (t, 2H, $SC\underline{H}_2CH_2$), 4.0 (t, 2H, $C_2H_4C\underline{H}_2S$), 7.2 (d, 2H, $H_{arom}$), 7.4 (d, 2H, $H_{arom}$). The unpurified oil **7** was dissolved in methanol (325 mL) and oxidized using $H_2O_{2\ aqua}$ (12 mL) in presence of $TeO_2$ (1.01 g) and HCl (1 mL). Purification by flash chromatography (effluent: chloroform) and recrystallization in hexane. Melting point: 90-92 °C. $^1$H NMR ($CDCl_3$, 400 MHz, ppm): 0.9 (t, 3H, $CH_2C\underline{H}_3$), 1.3-1.5 (m, 10H, $C\underline{H}_2$), 1.8 (m, 2H, $S(O)CH_2C\underline{H}_2$), 2.8 (m, 2H, $S(O)C\underline{H}_2CH_2$), 4.0 (t, 2H, $C_2H_4C\underline{H}_2S$), 7.2 (d, 2H, $H_{arom}$), 7.4 (d, 2H, $H_{arom}$). IR (NaCl): $\nu$ 2958, 2919, 2849, 1493, 1468, 1415, 1096, 1025, 1018, 840, 814, 723, 677 $cm^{-1}$. MS: (EI; m/z; rel. int. (%)): 270 (7), 161(6), 155(11), 145(38), 143(4), 125(100).

**Synthesis of 1-*tert*-butyl-4-(octylsulfinylmethyl)benzene 12**

The general procedure for the synthesis of the initiators was followed. 1-*tert*-butyl-4-(chloromethyl)benzene **4** (12.57 g, 69 mmol) was dissolved in ethanol (55 mL). n-Octanethiol (20.18 g, 138 mmol) was deprotonated with Na*t*BuO (13.93 g, 145 mmol) and added to the starting product. A yellow-

brown oil **8** was obtained (26.75 g). $^1$H NMR (400 MHz, $CDCl_3$, ppm): 0.9 (t, 3H, $CH_2C\underline{H}_3$), 1.3-1.5 (m, 19H, $C\underline{H}_2$ and protons of *t*-Bu), 1.8 (m, 2H, $SCH_2C\underline{H}_2$), 2.4 (t, 2H, $SC\underline{H}_2CH_2$), 4.0 (t, 2H, $C_2H_4C\underline{H}_2S$), 7.2 (d, 2H, $H_{arom}$), 7.4 (d, 2H, $H_{arom}$). The unpurified oil **8** was dissolved in dioxane (368 mL) and oxidized using $H_2O_{2\ aqua}$ (16 mL) in presence of $TeO_2$ (1.46 g) and HCl (1 mL). Purification by flash chromatography (effluent: diethyl ether) and recrystallization in hexane. Melting point: 35-38 °C. $^1$H NMR (400 MHz, $CDCl_3$, ppm): 0.9 (t, 3H, $CH_2C\underline{H}_3$), 1.3-1.5 (m, 19H, $C\underline{H}_2$ and H on *t*-Bu), 1.8 (m, 2H, $S(O)CH_2C\underline{H}_2$), 2.6 (m, 2H, $S(O)C\underline{H}_2CH_2$), 4.0 (t, 2H, $C_2H_4C\underline{H}_2S$), 7.2 (d, 2H, $H_{arom}$), 7.4 (d, 2H, $H_{arom}$). IR (NaCl): $\nu$ 3425, 2958, 2856, 1517, 1466, 1414, 1364, 1269, 1202, 1108, 1042, 837, 723, 560 $cm^{-1}$. MS: (EI; m/z; rel. int. (%)): 292(18), 179(5), 161(6), 147(100), 132(13), 117(16), 105(8), 91(4), 77(1).

**Synthesis of 1-methoxy-(octylsulfinylmethyl)benzene 13**

The general procedure for the synthesis of the initiators was followed. 1-methoxy-4-(chloromethyl)benzene **5** (10.806 g, 69 mmol) was dissolved in ethanol (70 mL). n-Octanethiol (20.18 g, 138 mmol) was deprotonated with Na*t*BuO (13.93 g, 145 mmol) and added to the starting product. A yellow-brown oil **9** was obtained (26.38 g). $^1$H NMR (400 MHz, $CDCl_3$, ppm): 0.9 (t, 3H, $CH_2C\underline{H}_3$), 1.3-1.5 (m, 10H, $C\underline{H}_2$), 1.8 (m, 2H, $SCH_2C\underline{H}_2$), 2.4 (t, 2H, $SC\underline{H}_2CH_2$), 4.0 (t, 2H, $C_2H_4C\underline{H}_2S$), 7.1 (d, 2H, $H_{arom}$), 7.3 (d, 2H, $H_{arom}$), 3.8 (s, 3H, $C\underline{H}_3O$). The unpurified oil **9** was dissolved in methanol (470 mL) and oxidized using $H_2O_{2\ aqua}$ (16 mL) in presence of $TeO_2$ (1.5 g) and HCl (1 mL). Purification by flash chromatography (effluent: 50 v% chloroform/ 50 v% ethylacethate) and recrystallization in hexane. Melting point: 105-107 °C. $^1$H NMR (400 MHz, $CDCl_3$, ppm): 0.9 (t, 3H, $CH_2C\underline{H}_3$), 1.3-1.5 (m, 10H, $C\underline{H}_2$), 1.8 (m, 2H, $S(O)CH_2C\underline{H}_2$), 2.6 (m, 2H, $S(O)C\underline{H}_2CH_2$), 4.0 (t, 2H, $C_2H_4C\underline{H}_2S$), 6.9 (d, 2H, $H_{arom}$), 7.2 (d, 2H, $H_{arom}$), 3.8 (s, 3H, $C\underline{H}_3O$). $^{13}$C NMR (100 MHz, $CDCl_3$, ppm): 13.5 (s, $CH_2\underline{C}H_3$); 21.9 (s, $\underline{C}H_2CH_3$); 22.0 (s, $\underline{C}H_2CH_2CH_3$); 28.3 (s, $\underline{C}H_2(CH_2)_2CH_3$); 28.4 (s, $\underline{C}H_2(CH_2)_3CH_3$); 28.6 (s, $\underline{C}H_2(CH_2)_4CH_3$); 31.1 (s, $S(O)CH_2\underline{C}H_2$); 50.1 (s, $S(O)\underline{C}H_2CH_2$); 54.7 (s, $\underline{C}H_3O$) 56.9 (s, $Ar\underline{C}H_2S(O)$); 121.2 (s, $\underline{C}_{arom}$-$CH_2$); 130.6 + 113.8 (s $C_{arom}$); 159.1 (s,$\underline{C}_{arom}$-$OCH_3$). IR (NaCl): $\nu$ 3007, 2957, 2917, 2848, 2873, 2055, 1614, 1587, 1515, 1469, 1305, 1251, 1188, 1106, 1034, 839, 828, 817 $cm^{-1}$. MS:

(EI; m/z; rel. int. (%)): 266(14), 217(3), 181(8), 167(8), 137(5), 135(11), 121(100).

**Synthesis of 1-fluoro-(octylsulfinylmethyl)benzene 14**

The general procedure for the synthesis of the initiators was followed. 1-Fluoro-4-(chloromethyl)benzene **6** (10.806 g, 69 mmol) was dissolved in ethanol (70 mL). n-Octanethiol (20.18 g, 138 mmol) was deprotonated with Na*t*BuO (13.93 g, 145 mmol) and added to the starting product. A yellow-brown oil was **10** obtained (23.96 g). $^{1}$H NMR (400 MHz, $CDCl_3$, ppm): 0.9 (t, 3H, $CH_2C\underline{H}_3$), 1.3-1.5 (m, 10H, $C\underline{H}_2$), 1.8 (m, 2H, $SCH_2C\underline{H}_2$), 2.4 (t, 2H, $SC\underline{H}_2CH_2$), 4.0 (t, 2H, $C_2H_4C\underline{H}_2S$), 7.1 (d, 2H, $H_{arom}$), 7.2 (d, 2H, $H_{arom}$). The unpurified oil **10** was dissolved in methanol (424 mL) and oxidized using $H_2O_{2\ aqua}$ (15 mL) in presence of $TeO_2$ (1.36 g) and HCl (1 mL). Purification by flash chromatography (effluent: 98 v% diethyl ether / 2 v% methanol) and recrystallization in hexane. Melting point: 80-82 °C. $^{1}$H NMR (400 MHz, $CDCl_3$, ppm): 0.9 (t, 3H, $CH_2C\underline{H}_3$), 1.3-1.5 (m, 10H, $C\underline{H}_2$), 1.8 (m, 2H, $S(O)CH_2C\underline{H}_2$), 2.6 (m, 2H, $S(O)C\underline{H}_2CH_2$), 4.0 (t, 2H, $C_2H_4C\underline{H}_2S$), 6.9 (d, 2H, $H_{arom}$), 7.2 (d, 2H, $H_{arom}$). $^{13}$C NMR (100 MHz, $CDCl_3$, ppm): 14.0 (s, $CH_2\underline{C}H_3$); 22.5 (s, $\underline{C}H_2CH_3$); 22.5 (s, $\underline{C}H_2CH_2CH_3$); 28.8 (s, $\underline{C}H_2(CH_2)_2CH_3$); 28.9 (s, $\underline{C}H_2(CH_2)_3CH_3$); 29.1 (s, $\underline{C}H_2(CH_2)_4CH_3$); 31.7 (s, $S(O)CH_2\underline{C}H_2$); 50.9 (s, $S(O)\underline{C}H_2CH_2$); 57.0 (s, $Ar\underline{C}H_2S(O)$); 125.7 (d,J=0.049, $\underline{C}_{arom}$-$CH_2$; 131.7 (d,J=0.099, $C_{arom}$); 115.9 (d,J=0.280, $C_{arom}$); 162.7 (d,J=3.293, $\underline{C}_{arom}$-$OCH_3$). IR (NaCl): $\nu$ 2960, 2923, 2848, 1599, 1511, 1468, 1415, 1235, 1156, 1092, 1025, 842, 536 $cm^{-1}$. MS: (EI; m/z; rel. int. (%)): 281(1), 253(6), 155(9), 145(62), 139(24), 125(15), 109(100).

**Synthesis of 1,3-bis-(octane-1-sulfinylmethyl)-benzene 15**

1-octanethiol (20.7 g, 142.81 mmol) was dissolved in 140 mL ethanol and Na*t*BuO (13.7 g, 142.81 mmol) was added while stirring. In a second flask, 1,3-bis-chloromethyl-benzene (10 g, 57.12 mmol) and a small quantity of NaI were dissolved in 200 mL ethanol. After 1 hour of stirring, the deprotonated 1-octanethiol was added slowly to the second flask. After 2 hours the reaction mixtured was poured in an equal volume of water and extracted with dichoromethane (3x 100 mL). The combined organic layers were dried on anhydrous $MgSO_4$, filtrated, concentrated in vacuo and

analyzed by $^1$H NMR. $^1$H NMR (300 MHz, $CDCl_3$, ppm): 7.2-7.1 (m, 4H), 3.7 (s; 2H), 2.4 (t, 2H), 1.5 (m, 4H), 1.4-1.2 (m, 20H), 0.9 (t, 6H). The obtained 1,3-bis-octylsulfanylmethyl-benzene (~10 g, ~25.33 mmol) was dissolved in 160 mL methanol. After adding Tellurium oxide (0.403 g, 2.53 mmol) and 2 mL of HCl (1N), $H_2O_2$ (35 %, 9.83 g, 50.6 mmol) was added dropwise. The reaction was monitored using TLC (effluent $CHCl_3$ for final product, effluent 5/5 Hexane/$CHCl_3$ for starting product). The reaction was stopped when over-oxidation was visible (2h) by quenching by a saturated aqueous NaCl solution. The water phase was three times extracted with chloroform. The combined organic layers were dried on anhydrous $MgSO_4$, filtrated and concentrated in vacuo. The product was purified by recrystallization in a hexane/chloroform mixture. $^1$H NMR (300 MHz, $CDCl_3$, ppm): 7.4 (td, 1H, $J_{ortho}$=7.60), 7.3-7.2 (m, 3H), 3.9 (s, 4H), 2.5 (t, 4H), 1.8-1.6 (m, 4H), 1.5-1.1 (m, 20H), 0.9 (t, 6H, J=6.51)

**Synthesis of 1,2,4,5-tetrakis-octylsulfinylmethyl-benzene 16**

Synthesis is analogous to the synthesis of 1,3-bis-(octane-1-sulfinylmethyl)-benzene **15**. The deprotonated n-octanethiol was added to 1,2,4,5-tetrakis-bromomethyl-benzene to obtain 1,2,4,5-tetrakis-octylsulfanylmethyl-benzene. $^1$H NMR (300 MHz, $CDCl_3$, ppm): 7.3-7.2 (m, 2H), 4.3-3.9 (m, 8H), 2.7 (m, 8H), 1.8-1.7 (m, 8H), 1.5-1.2 (m, 40H), 0.9 (t, 12H, J=7.05). All chemicals except 1,2,4,5-tetrakis-bromomethyl-benzene were used in double quantity. $^1$H NMR (300 MHz, $CDCl_3$, ppm): 7.3-7.2 (m, 2H), 4.3-3.9 (m, 8H), 2.7 (m, 8H), 1.8-1.7 (m, 8H), 1.5-1.2 (m, 40H), 0.9 (t, 12H, J=7.05)

**Testing the stability of the fluorine initiator**

*Stability towards LHMDS:* 1-fluoro-4-(octylsulfinylmethyl)benzene **14** (0.27mg; 0.1mmol) was dissolved in 2 mL THF. LHMDS (2 mL, 1 M) was added and left to react with the fluorine initiator for one hour. The reaction was stopped by addition of water. After extraction by chloroform and drying over $MgSO_{4(anhydrous)}$, the solvent was removed and the product analyzed using $^1$H NMR. No difference was found compared to the starting product. $^1$H NMR (400 MHz, $CDCl_3$, ppm): 0.9 (t, 3H, $CH_2C\underline{H}_3$), 1.3-1.5 (m, 10H, $C\underline{H}_2$),

1.8 (m, 2H, S(O)$CH_2C\underline{H_2}$), 2.6 (m, 2H, S(O)$C\underline{H_2}CH_2$), 4.0 (t, 2H, $C_2H_4C\underline{H_2}S$), 6.9 (d, 2H, $H_{arom}$), 7.2 (d, 2H, $H_{arom}$).

*Stability towards air and water:* Three test tubes were dried in a drying oven at 110 °C. The fluorine initiator (80mg) was added and dissolved in a hexane / dichloromethane mixture (30 mL/10 mL). One tube was degassed by passing $N_2$-gas through the solution, to one tube water was added and one tube was not degassed. The three tubes were heated to 60 °C for 3 hours under continuous stirring by a Teflon stirrer. After 3 hours the solvent was evaporated and the resulting products analyzed by $^1$H NMR. Only in second tube, where water was added, significant loss of product was observed.

**Effect of the different initiators on the polymerization**

All glassware was dried overnight in a drying oven at 110 °C prior to use. A 100 mL three-necked flask with Teflon stirrer was dried by flaming it under vacuum. Dry THF was transferred to a flask and degassed for 20 minutes by passing of $N_2$ through the liquid for 30 minutes. The premonomer **1** was weighed (4x 200 mg, 4x 0.665 mmol) and transferred to the reaction flasks, all air was removed by applying sequentially vacuum and nitrogen to the flasks. A stock solution of the initiator was made (0.1197 mmol (**11-14**) in 18 mL dry THF). To obtain an initiator concentration of 0.1 equivalents, 10 mL of the 6.65 mM initiator solution was transferred to the reaction flask with the premonomer by use of a glass syringe and further diluted with 3.3 mL of dry THF to obtain a final premonomer concentration of 0.05 M. To obtain an initiator concentration of 0.5 equivalents, 5 mL of the stock solution was transferred and further diluted with 8.3 mL of dry THF. Solutions with 0.2 and 0.1 equivalents of initiator were made in analogous way. The flasks were brought to the appropriate reaction temperature and the base (LMHDS, 0.798 mL, 1.2 eq) was added by syringe in 1 shot to start the polymerization. The base was not cooled before addition to avoid precipitation of the base. After 1 hour the reactions were stopped by addition of water (50 mL) to the reaction mixture. Excess of base was neutralized by addition of 1.0 M aqueous hydrochloric acid, followed by extraction with dichloromethane (3x 10 mL). The combined organic layers were concentrated under reduced pressure. The polymer was redissolved in dichloromethane (5 mL), and precipitated in an ethylacethate/diethylether

mixture (20 mL/20 mL). The polymers were analyzed by SEC after filtration and drying under reduced pressure.

**Verification of anionic polymerization mechanism**

All glassware was dried overnight in a drying oven at 110 °C prior to use. A 100 mL three-neck flask with Teflon stirrer was dried by flaming it under vacuum. After weighing the premonomer (**1**, 200mg, 0.66 mmol), initiator (**14**, 0.066 mmol) and TEMPO (52 mg, 0.333 mmol) and adding it to the flask, all air was removed by applying sequentially vacuum and nitrogen to the flask. Dry THF (13.3 mL) was transferred to the reaction flask by use of a glass syringe. The flask was brought to 0 °C and adding the base (1.2 eq) by syringe started the polymerization. The reaction was stopped after 1 hour by adding water to the reaction mixture. Excess of base was neutralized by addition of 1.0 M aqueous hydrochloric acid, followed by extraction with dichloromethane. The combined organic layers were concentrated under reduced pressure. The polymers were analyzed by SEC without further purification.

**Effect of reversed addition**

All glassware was dried overnight in a drying oven at 110 °C prior to use. A 100 mL three-neck flask with Teflon stirrer was dried by flaming it under vacuum. The premonomer (**1**, 200mg, 0.66 mmol) was dissolved in THF (3 mL) and cooled to 0 °C. The initiator **14** (0.333 mmol or 0.066 mmol) was dissolved in THF (10.3 mL) in another flask and the base (LHMDS 0.80 mL), was added. This reaction flask was cooled to 0 °C. The dissolved premonomer was added slowly to the initiator/base solution over a period of 20 minutes. After complete addition of the premonomer, the polymerization mixture was allowed to react for an additional 20 minutes. Excess of base was neutralized by addition of 1.0 M aqueous hydrochloric acid, followed by extraction with dichloromethane. The combined organic layers were concentrated under reduced pressure. The polymers were analyzed by SEC without further purification.

**The use of multifunctional initiators 15 and 16**

All glassware was dried overnight in a drying oven at 110 °C prior to use. A 100 mL three-neck flask with Teflon stirrer was dried by flaming it under vacuum. After weighing the premonomer (200mg, 0.66 mmol) and the initiator (**15,** 14.18 mg, 0.033 mmol or **16,** 12.89 mg, 0.017 mmol) and adding them to the flask, all air was removed by applying sequentially vacuum and nitrogen to the flask. Dry THF (12.5 mL) was transferred to the reaction flask by use of a glass syringe. The flask was brought to 0 °C and adding the base (LHMDS, 1.3 eq) by syringe started the polymerization. The reaction was stopped after 1 hour by adding water (50 mL) to the reaction mixture. Excess of base was neutralized by addition of 1.0 M aqueous hydrochloric acid, followed by extraction with dichloromethane. The combined organic layers were concentrated under reduced pressure. The polymer was redissolved in dichloromethane (5 mL), and precipitated in an ethylacethate/diethylether mixture (20 mL/20 mL). The polymers were analyzed by SEC after filtration and drying under reduced pressure.

**The use of end cappers**

*End capping with 4-tert-butylbenzoyl chloride:*

The premonomer (400 mg, 1.33 mmol) and the initiator **14** (0.133 mmol, 35.95 mg) were dissolved in 53.16 mL dry THF and cooled to -64 °C. The base (LHMDS, 1.2 eq.) was added in one shot. After 1 hour, 4-tert-butylbenzoyl chloride (2eq., 196.7 mg) was added, and left to react at room temperature for 20 minutes. The reaction mixture was poured in water and extracted with dichloromethane (3x10 mL). Precipitation in an ethylacethate/diethylether mixture (20 mL/20 mL) failed; therefore the polymer was purified by dialysis. The polymer was dissolved in chloroform and put inside a porous membrane. The membrane was placed a large beaker with chloroform. The liquid outside the membrane was replaced 4 times. After 2 days, the dissolved polymer inside the membrane was concentrated under reduced pressure and analyzed by SEC.

*End capping with methoxy benzylchloride*

The general polymerization procedure was followed. The premonomer (200 mg, 0.665 mmol) and the initiator **14** (0.067 mmol, 17.98 mg) were dissolved in 25 mL THF and cooled to -64 °C. The base (LHMDS, 1.2 eq.) was added in one shot. After 1 hour, methoxy benzylchloride (2eq., 187 mg) was added, and left to react at room temperature for 20 minutes. The reaction mixture was poured in water and extracted with dichloromethane. The polymer was purified by membrane dialysis. After 2 days, the dissolved polymer inside the membrane was concentrated under reduced pressure and analyzed by SEC.

**Sequential addition**

The general polymerization procedure was followed. The premonomer (300 mg, 1.0 mmol) and initiator **14** (0.05 mmol, 13.52 mg) were dissolved in 11.4 mL THF and cooled to 0 °C using a water/ice bath. The base was added in one shot (1.1 mL LHMDS, 1.1 equivalents). After 20 minutes a sample was taken (2.5 mL) and a new portion of base (1.05 mmol) and premonomer (1 mmol) were added. After mixing of the second portion for 20 minutes, a second sample (2.5 mL) was taken and the reaction was terminated. The samples were mixed with water, extracted with dichloromethane, and after concentration under vacuum, analyzed by SEC.

**End capping to form an ATRP-macroinitiator**

The general polymerization procedure was followed. The premonomer (400 mg, 1.33 mmol) and the initiator **14** (0.133 mmol, 35.95 mg) were dissolved in 26.6 mL THF and cooled to 0 °C. The base (LHMDS, 1.2 eq.) was added in one shot. After 10 minutes, 2-bromo-propionyl bromide (70.45µl, 0.6645mmol) was added, and left to react at room temperature for 20 minutes. The reaction mixture was poured in water, extracted with dichloromethane, and after concentration under vacuum, analyzed by SEC.

**Creation of block-co-polymers**

The MMA and Styrene block-co-polymers were synthesized according to the previous polymerization: 'End capping to form an ATRP-macroinitiator'. Instead of adding the end capper, the second monomer was added (MMA: 0.133g, 1.33 mmol or styrene: 0.277g, 2.66 mmol). The reaction was stopped after 20 minutes, and after purification, analyzed by SEC.

## 4.9 References

[1] T. Schwalm; J. Wiesecke; S. Immel; M. Rehahn, *Macromolecules,* **40** (25), 8842–8854, (2007)

[2] B. R. Hsieh; Y. Yu; A. C. VanLaeken; H. Lee, *Macromolecules*, **30**, 8094, (1997)

[3] B. R. Hsieh; Y. Yu; E. W. Forsythe; G. M. Schaaf; W. A. Feld, *J. Am. Chem. Soc.*, **120**, 231, (1998)

[4] C. J. Neef; J. P. Ferraris, *Macromolecules*, **33** (7), 2311, (2000)

[5] C. J. Neef; J. P. Ferraris, *Macromolecules*, **37**, 2671, (2004)

[6] T. Schwalm; M. Rehahn, *Macromolecular Rapid Communications*, **29** (3), 207, (2008)

[7] C. M. Heller; H. I. Campbell; B. K. Laurich; D. L. Smith; D. D. C. Bradley; P. L. Burn; J. P. Ferraris; K. Müllen, *Phys Rev B*, **54**, 5516–5522, (1996)

[8] C. Zhang; S. Höger; K. Pakbaz; F. Wudl; A. J. J. Heeger, *Electron Mater*, **22**, 413–417, (1993)

[9] D. B. Romero; M. Schaer; L. Zuppiroli; B. Cesar; G. Widawski; B. François, *Opt Eng*, **34**, 1987–1992, (1995)

[10] B. François; G. Widawski; M. Rawiso; B. Cesar, *Synthetic Metals*, **69**, 463–466, (1995)

[11] B. François; G. Widawski; M. Rawiso, *Synthetic Metals*, **69**, 491–492, (1995)

# Chapter 5

# Comparison of the precursor routes by means of $^{13}$C-labeling

*As mentioned in chapter 1, different precursor routes exist, which all lead to the same conjugated polymer. However, depending on the chosen synthetic route, higher or lower quantities of defects could be present in the polymer backbone. These defects have a significant impact on the device performance.*

*In this chapter a comparison of Gilch, radical sulfinyl, anionic sulfinyl and dithiocarbamate route will be made by means of $^{13}$C-labeling of the monomer. The first two routes were already investigated in previous studies using $^{13}$C-labeling, and those results will be compared to the two new routes. The anionic polymerization via the sulfinyl route was already addressed in chapter 2, but a more detailed description of the results will be shown here.*

## 5.1 Introduction

Recently, a new polymerization route was developed in our research group, namely the dithiocarbamate route. This precursor route has been described already for PTV derivatives.[1] In a previous paper, PPV polymers with a bimodal molecular weight distribution were obtained by polymerizing the corresponding dithiocarbamate premonomer using LDA as the base.[2] A recent study showed that when LHMDS is used as the base, the bimodal distribution is absent or at least strongly suppressed. [3] The use of LHMDS leads to precursor polymers with high molecular weights and low polydispersities.

In this chapter a comparison will be made between the polymers obtained from the Gilch, the radical sulfinyl and the newly developed dithiocarbamate route. A further comparison is made with MDMO-PPV obtained from the anionic sulfinyl route.

There are several approaches toward the preparation of PPV and its derivatives, which can be classified as direct and precursor methods. The different precursor routes differ from each other in the nature of the functional group, which is used as polarizer and leaving group. Well-known precursor routes are the Wessling route, the Gilch route, the xanthate route, the dithiocarbamate route and the sulfinyl route, which were all described in chapter 1. The advantage of soluble precursor polymers is that they can be easily purified and processed into devices, which makes the use of precursor routes very attractive.

It is important to realize that the conjugated polymer backbone structure inherently includes defects and is not simply a planar monomer unit replicated to macroscopic dimensions. Some of these defects in PPV were already postulated by Schoo and Demandth.[4] In fact, the term "defects" is broad, since there are several kinds of defects, *e.g.* structural defects due to photo-oxidation, structural defects due to the synthesis itself or the presence of aggregates due to interchain interactions.

The presence of head-to-head and tail-to-tail linkages in MEH-PPV was shown to be detrimental to the lifetime of the prepared LEDs.[5,6] A way to improve the opto-electronic properties is to lower this concentration tail-to-tail linkages in the polymer chain, which interrupts the $\pi$-conjugation and head-to-head linkages, which cause chain stiffening (Figure 5-1). This might be possible if a polymerization method with a minimum of side reactions can be found or optimized.

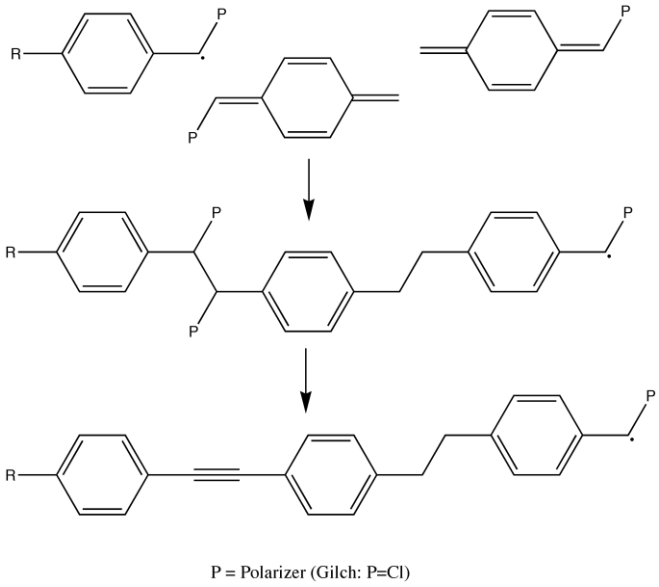


**Figure 5-1: Head-to-head (left) and tail-to-tail (right) linkage**

The presence of $sp^3$ defects due to incomplete elimination or tail-to-tail linkage, interrupting the $\pi$-conjugation, was also found to affect the physical properties (Figure 5-2). For conjugated/non-conjugated PPV based copolymers a strong increase of the quantum efficiency of both photo-luminescence (PL) and electroluminescence (EL) was found. [7-12] In addition, polyacetylene films with fewer $sp^3$ defects lead to a large improvement in conductivity.[13] The university of Delft devised a model to calculate the mobility of charges along molecular wires, such as poly-phenylenevinylene (PPV) chains. Experimental mobility data on di-alkoxy substituted PPV could be reproduced with this model, provided the effects of structural defects along the polymer chains were taken into account. According to the calculations, intra-chain hole and electron mobilities of the order of 100 $cm^2/Vs$ could be obtained for defect-free PPV chains.[14]

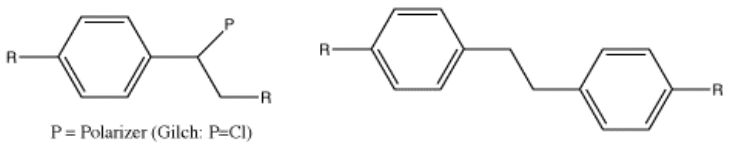


**Figure 5-2: $sp^3$ defects: incomplete elimination (left) and tail-to-tail linkage (right)**

Thermal oxidation or photo-oxidation results in the formation of carbonyl defects, which act as exciton dissociation sites leading to a quenching of the photoluminescence (Figure 5-3).[15] Photo-oxidation is likely to occur at the vinylene bond and is independent of the synthetic procedure used. [16] This results in chain scission with formation of aldehydes thus shortening the average conjugation length of the polymer chains.[17,18] Moreover, it was found that the chemical structure plays also a role in the photodegradation process. XPS measurements showed that extra oxygen can be built into the side chains of alkoxy substituted PPV giving rise to the formation of esters.[17] However, the presence of carbonyl defects does not only quench the PL but also increases the photoconductivity.[19]

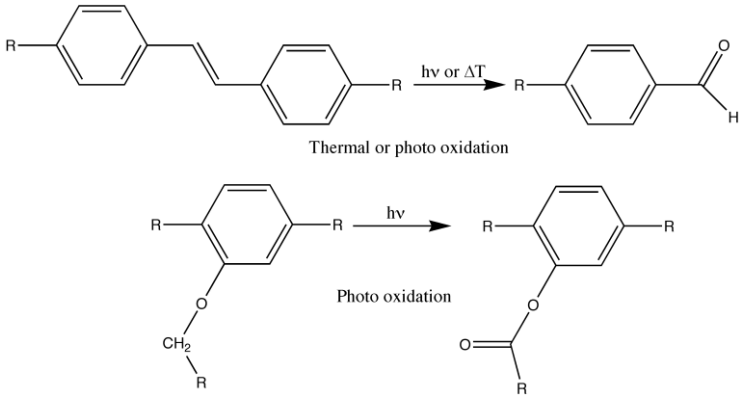


**Figure 5-3: Thermal or photo oxidation**

Furthermore, the conformational state of the polymer chain and thus the final morphology of the film is also determined by defects that alter the spatial direction of the polymer backbone.

Finally, the formation of interchain species (aggregates) was also found to influence the physical properties. As a result of such aggregates, the mobility of the charge carriers increases, while the EL luminescence decreases.[20-23]

These findings show that depending on the application for which the polymers will be used, some defects definitely have to be avoided, while others have to be deliberately built in in order to obtain high device performance.

### 5.1.1 The Gilch and the radical sulfinyl precursor route

Previous studies[24] already indicated that there was a difference in luminescence efficiency, gelation temperature and current-voltage characteristics between polymers obtained *via* the Gilch and sulfinyl routes. This despite the fact that the $^{13}C$ NMR spectra of unlabeled sulfinyl and Gilch polymers are the same at first glance. Moreover, a comparison[25] between state-of-the-art Gilch and sulfinyl synthesized MDMO-PPV/PCBM bulk hetero-junction solar cells pointed out that a power conversion efficiency $\eta_c$ of nearly 3% is reached for the sulfinyl based device compared with 2.5% for the Gilch one. This feature of sulfinyl MDMO-PPV/PCBM bulk hetero-junction solar cells is a consequence of a higher fill factor and a high short circuit current. This finding can be attributed to a different microstructure resulting from the higher chemical selectivity during polymerization. The microstructure is expected to be responsible for the different device characteristics as illustrated before. Becker *et al*.[26] elucidated the microstructure of Gilch-MDMO-PPV by introducing $^{13}C$ labels into the polymer chain. In that way, the defect signals, of which the concentration is expected to be very low, can be clearly detected, as their intensity will be increased by a factor 100. They found the presence of single (bisbenzyl moiety) and triple bonds (tolane moiety), the so-called tolane-bisbenzyl (TBB) moieties as main structural defects (Figure 5-4). After signal assignment by means of qualitative $^{13}C$ spectroscopy, they could roughly estimate the amount of the tolane-bisbenzyl moieties from the $^{1}H$ spectrum as being 1.5-2.2%. They further assumed a similar amount of single bonds and triple bonds, which means that in total 3-4.4% of the vinylene bonds were replaced by irregular bonds in the main chain. Later, a study by H. Roex[27] showed for Gilch-MDMO-PPV a much higher quantity of tolane-bisbenzyl defects (9.8%) and chlorovinyl bonds (*ca.* 1.4%) due to head-to-head and tail-to-tail addition next to the presence of non-eliminated locations (1.8%).

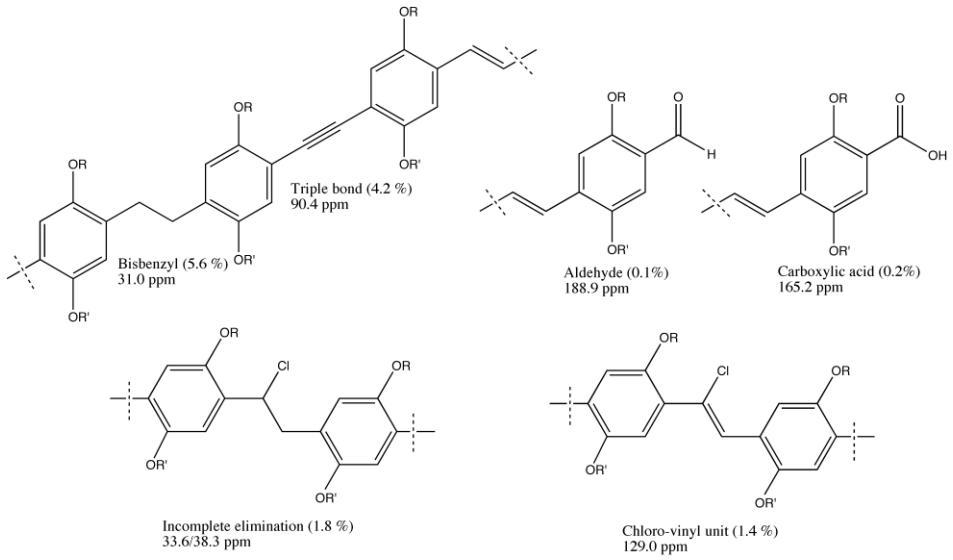


**Figure 5-4: Overview of the type and amount of structural defects present in the MDMO-PPV obtained *via* the Gilch route. Results taken from reference 27.**

In contrast, in the conjugated sulfinyl polymer synthesized radically using Na*t*BuO as the base and 2-butanol as solvent, the only defect found was the presence of non-eliminated groups (6.8%), which could be reduced by a two-step elimination procedure to less than 0.5%. The sulfinyl polymers, contained besides the non-eliminated groups no other defects, except for aldehyde end groups (0.3%) (Figure 5-5). In contrast to the Gilch route, the polymerization reaction *via* sulfinyl route is characterized by a very regular propagation step, due to the difference in polarizer and leaving group.

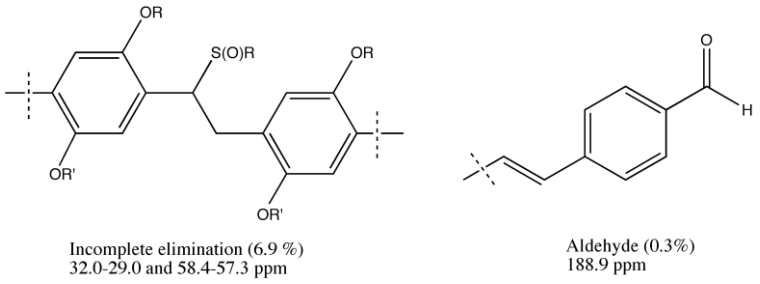


**Figure 5-5: Overview of the type and amount of structural defects present in the MDMO-PPV obtained *via* the sulfinyl route (Na*t*BuO/2-butanol). Results taken from reference 27.**

# 5.2 Synthesis of $^{13}C$ labeled premonomer for polymerization via anionic sulfinyl route and dithiocarbamate route

The $^{13}C$ labeled NMR of the Gilch route and the sulfinyl route were already described in literature, and now we want to add and compare the anionic sulfinyl and the dithiocarbamate route to these results. The $^{13}C$ NMR spectrum of the labeled polymer will be compared to the unlabeled NMR spectrum. In order to obtain a quantative NMR of the $^{13}C$-labeled polymer, the $^{13}C$-labeled premonomer needs to be synthesized and characterized by NMR.

## 5.2.1 Synthesis of $^{13}C$-labeled Gilch MDMO-PPV premonomer

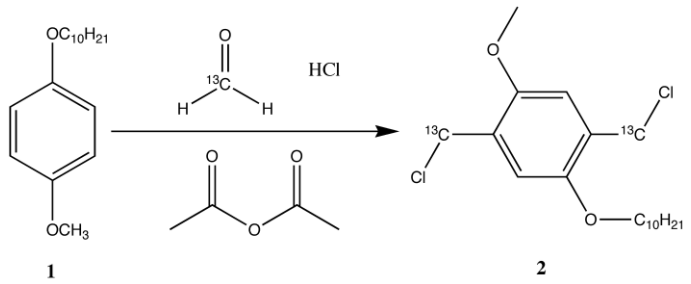


1 2

**Figure 5-6: Synthesis of $^{13}C$-labeled Gilch MDMO-PPV premonomer**

Both the sulfinyl and the dithiocarbanate premonomer have been synthesized starting from the Gilch premonomer (Figure 5-6).

Because of the high price of $^{13}C$-labeled para-formaldehyde, the preparation of 2,5-bis(chloromethyl)-1-(3,7-dimethyloctyloxy)-4-methoxy-benzene **(2)** was optimized prior to using the labeled compound (Figure 5-6). A set of four experiments was set up, changing the amount of *p*-formaldehyde, acidic anhydride and hydrochloric acid used. The temperature and reaction time were kept constant at 75 °C and 3.5 hours. The different amounts of reagents that were used are shown in Table 5-1.

| *Experiment* | *(**1**)* | *p-formaldehyde* | *Acetic Anhydride* | *HCl* |
|---|---|---|---|---|
| 1 | 1 eq<br>1.58 g | 2.75 eq<br>0.5 g | 10 eq<br>6.13 g | 5.5 eq<br>3.25 g |
| 2 | 1 eq<br>1.58 g | 2.2 eq<br>0.39 g | 10 eq<br>6.13 g | 5.5 eq<br>3.25 g |
| 3 | 1 eq<br>1.58 g | 2.75 eq<br>0.5 g | 30 eq<br>18.39 g | 5.5 eq<br>3.25 g |
| 4 | 1 eq<br>1.58 g | 2.75 eq<br>0.5 g | 30 eq<br>18.39 g | 16.5 eq<br>9.75 g |

**Table 5-1: Optimization of the chloromethylation reaction**

To avoid loss of material in the purification step, the workup of the reaction was kept to a minimum. The product (**2**) was filtered and redissolved in dichloromethane before analysis by NMR and GC/MS. The results of the experiments can be found in Table 5-2. The highest yield could be found for experiment 4, with a calculated yield of 71%. $^{1}$H NMR analysis showed a large amount of monochlorinated product for experiment 1 and 2 and not for experiment 4. The fourth experiment however did have an amount of starting product left. Reaction setup 4 was tried on a larger amount of unlabeled product and a similar yield (69 %) was obtained.

| *Experiment* | *Total obtained mass (g)* | *Amount product according to $^{1}$H NMR (%)* | *Amount product according to GC/MS (%)* | *Calc. total yield (%)** |
|---|---|---|---|---|
| 1 | 1.66 | 70 | 66 | 54 |
| 2 | 1.42 | 71 | 65 | 47 |
| 3 | 0.97 | 22 | 7 | 10 |
| 4 | 1.99 | 78 | 74 | 71 |

*** based on total mass obtained and amount of pure product according to 1H-NMR**

**Table 5-2: Optimization of the chloromethylation reaction: Results of GC/MS and $^{1}$H NMR**

The conditions used in experiment 4 were taken to synthesize the $^{13}$C labeled Gilch MDMO-PPV premonomer (**2**). After drying over anhydrous $MgSO_4$, the premonomer was purified by recrystallization in hexane. In the

$^{13}$C NMR spectrum, the signal of the $^{13}$C labeled chloromethyl group appears at 41.2 ppm (Figure 5-7).

An unknown impurity was found in the spectrum at a chemical shift of 36.6 ppm. This impurity is not visible in $^{13}$C NMR spectra of the unlabeled premonomer, and based on its intensity, can be assigned to a $^{13}$C labeled carbon. Integration of the spectrum makes it possible to estimate the amount of the impurity to be 1.1% in case that there is only one labeled $^{13}$C in the composition of the impurity.

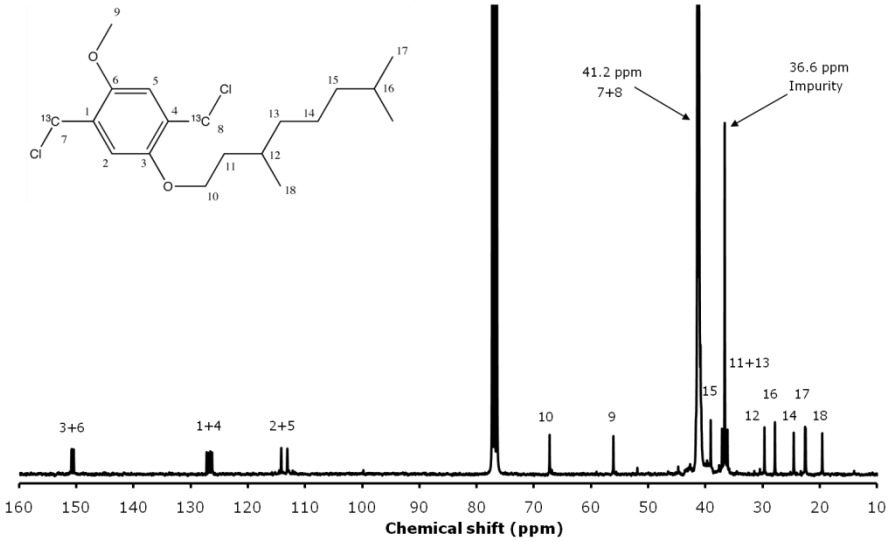


**Figure 5-7: $^{13}$C Spectrum of labeled Gilch MDMO-PPV premonomer**

### 5.2.2 Synthesis of $^{13}$C-labeled Sulfinyl MDMO-PPV premonomer

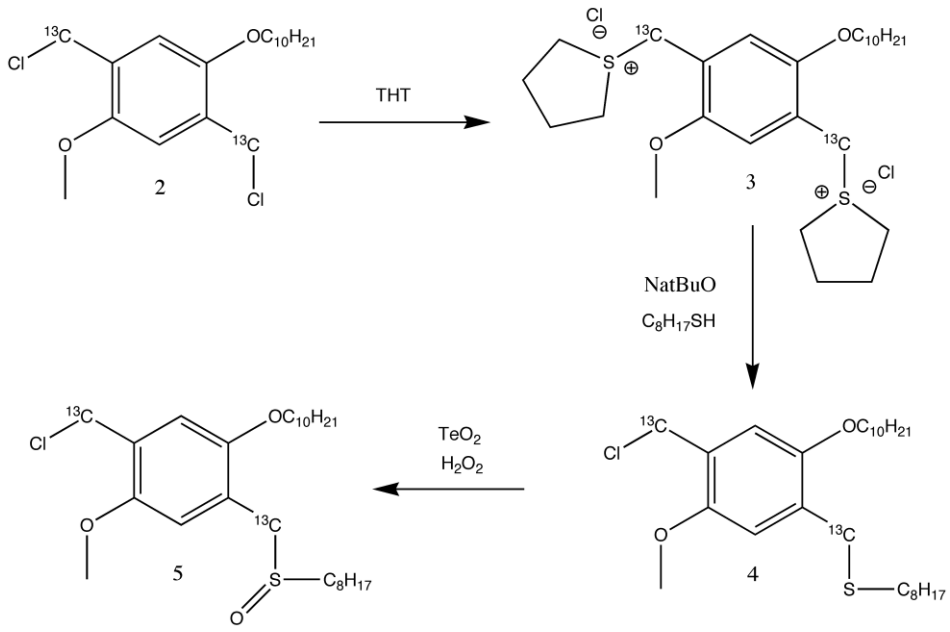


**Figure 5-8: Synthesis of the labeled MDMO-PPV sulfinyl premonomer**

The synthesis of the $^{13}$C labeled sulfinyl MDMO-PPV premonomer is identical to the synthesis of the unlabeled MDMO-PPV premonomer, with the only difference that a labeled Gilch MDMO-PPV premonomer was used as starting compound (Figure 5-8). In this reaction 3.70 g of the labeled Gilch MDMO-PPV premonomer (**2**) was converted into the bissulfonium salt (**3**) and through an elimination and addition reaction the labeled sulfanyl premonomer (**4**) was obtained. After oxidation with hydrogen peroxide and tellurium oxide as catalyst, the $^{13}$C labeled sulfinyl MDMO-PPV premonomer (**5**) was obtained. The final overal yield was 49%, calculated starting from the Gilch MDMO-PPV premonomer. Both the sulfanyl and the sulfinyl premonomer were analyzed by $^{13}$C NMR. The labeled carbon next to the sulfanyl group gives a signal at 30.0 ppm, the carbon next to the sulfinyl group at 52.6 ppm (Figure 5-9). A strong signal was found at 68.7 ppm that could not be assigned to any carbon of the premonomer. The signal was found in both the spectrum of the sulfanyl and the sulfinyl premonomer, but not in the spectrum of the Gilch MDMO-PPV premonomer. Since this signal is

much stronger than observed for the unlabeled carbons of the premonomer, and the impurity cannot be found in the $^{1}$H NMR spectrum, the signal in the $^{13}$C NMR must be of a labeled carbon. The exact identity of the impurity could not be established. Also the $^{13}$C labeled Gilch premonomer had a labeled impurity. As in the synthesis of both the bissulfonium salt (**3**) and the sulfanyl premonomer (**4**), methanol is used and the signal of the impurity is in the range of the alkyl benzyl ethers; it is plausible that the impurity in question is caused by a replacement of a chloride with a methoxy group. The impurity could not be removed by fast column chromatography. Since the Gilch premonomer is not stable during the chromatography, better purification without significant loss of premonomer was not possible. In the future, the formation of the impurity must be prevented rather than removed by purification steps. This might be possible by using another solvent instead of methanol during the synthesis of the premonomer. Or by more rigorous purification of the Gilch premonomer.

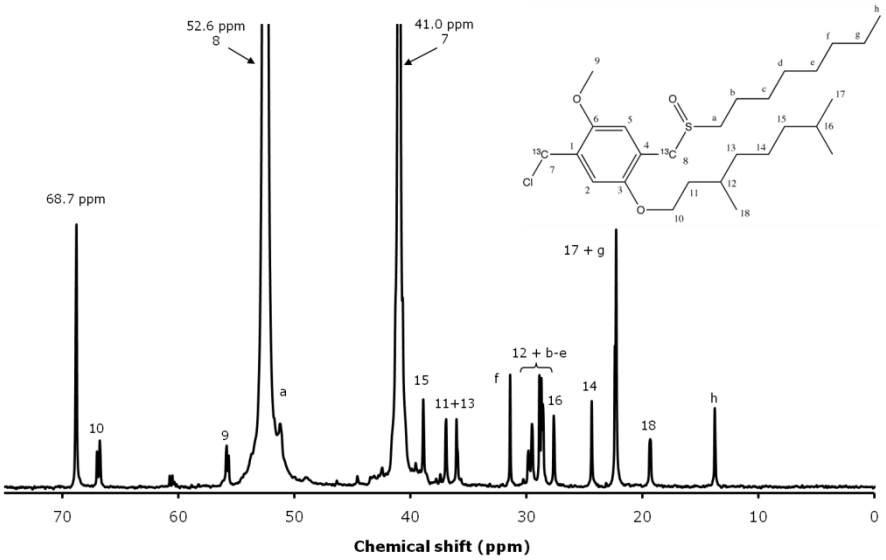


**Figure 5-9: $^{13}$C Spectrum of labeled sulfinyl MDMO-PPV premonomer (detail)**

### 5.2.3 Synthesis of $^{13}C$ labeled bisdithiocarbamate MDMO-PPV premonomer

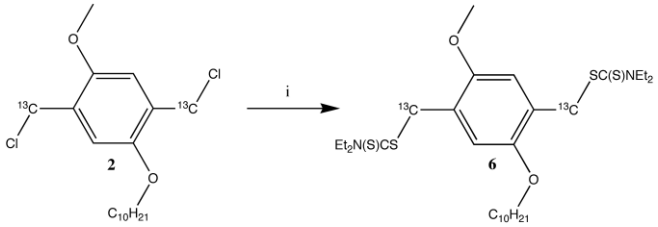


**Figure 5-10: Synthesis of bisdithiocarbamate premonomer. (i) $NaSC(S)NEt_2 \cdot 3H_2O$**

The bisdithiocarbamate MDMO-PPV premonomer **6** is synthesized in one step from the corresponding Gilch MDMO-PPV premonomer **2** (Figure 5-10)[28]. The dichloride is dissolved in ethanol and solid sodium diethyldithiocarbamate trihydrate is added to the mixture to obtain the bisdithiocarbamate premonomer. The yield was almost quantitative. This one step synthesis is more straightforward than the synthesis of sulfinyl premonomers, which takes three steps starting from the Gilch premonomers.

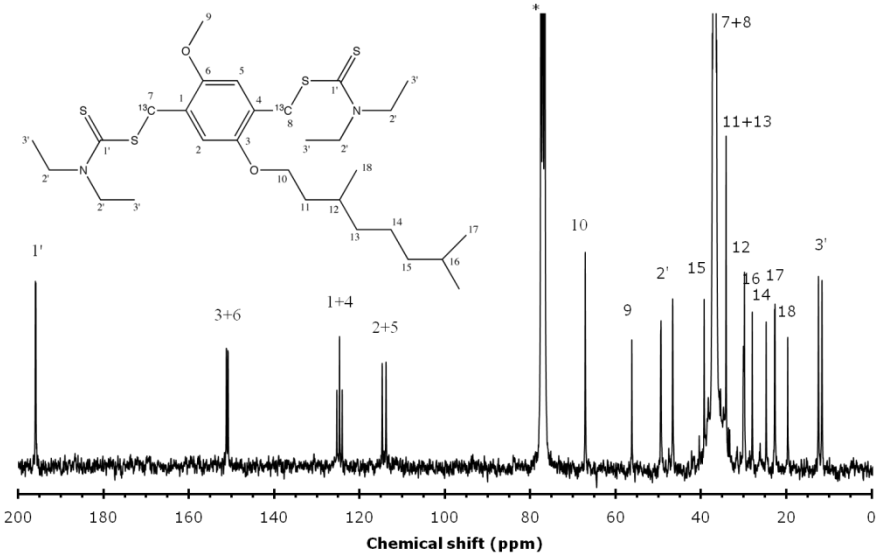


**Figure 5-11: $^{13}C$ Spectrum of labeled bisdithiocarbamate MDMO-PPV premonomer**

The labeled carbon between the dithiocarbamate group and the aromatic ring has a chemical shift of 36.8 ppm.

## 5.3 Method of recording a fully quantitative $^{13}C$ spectrum

To obtain the nature and amount of structural defects from a $^{13}C$ NMR spectrum, fully quantitative NMR spectra were necessary. To acquire quantitative $^{13}C$ spectra, a preparation delay of five times the longest $T_1$ relaxation decay time had to be respected between consecutive pulses in order to let the magnetization return to equilibrium. Dr. Hilde Roex already determined the $T_1$ decay times of all carbon resonances by means of the inversion recovery technique during the investigation of defects in polymers made using the radical sulfinyl route (Table 5-3). The influence of the paramagnetic relaxation agent chromium(III) acetylacetonate on the $T_1$ relaxation decay times was also already investigated.

| *T1 (s)* | | | |
|---|---|---|---|
| *carbon atom* | *δ (ppm)* | *native* | *25 mM Cr(III)* |
| 3+6 | 151.4 | 2.40 | 0.76 |
| 4+1 | 127.0 | 1.89 | 0.53 |
| 7+8 | 123.3 | 0.38 | 0.16 |
| 2+5 | 110.5 | 0.12 | 0.23 |
| 10 | 67.9 | / | 0.29 |
| 9 | 56.4 | 0.93 | 0.30 |
| 15 | 39.2 | 1.10 | 0.67 |
| 13 | 37.4 | 0.44 | 0.37 |
| 11 | 36.6 | 0.35 | 0.30 |
| 12 | 30.2 | 0.75 | 0.44 |
| 16 | 27.9 | 2.68 | 1.02 |
| 14 | 24.6 | 0.75 | 0.52 |
| 17 | 22.6 | 1.67 | 0.79 |
| 18 | 19.8 | 0.82 | 0.49 |

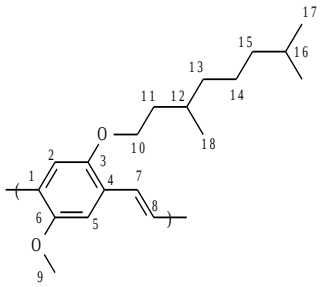


**Table 5-3: Chemical shift assignments of the carbon atoms of MDMO-PPV in $CDCl_3$ and $T_{1C}$ relaxation decay times with and without chromium(III) acetylacetonate as relaxation agent. Taken from reference 29**

The longest $T_1$ relaxation decay in the presence of 25 mM of chromium(III) acetylacetonate was determined to be 1.02 s, allowing acquisitional quantitative data with a preparation delay of 5.1 s (5x 1.02s ). Moreover,

NOE build-up, which already does not take place in the inverse gated decoupling technique is further suppressed by chromium(III) acetylacetonate. Paramagnetic relaxation agents mainly provide an additional relaxation mechanism that dominates the C-H dipole-dipole relaxation responsible for the NOE enhancement.[30] An increase of the filter bandwidth equal to the spectral width was also applied to improve quantification of the peaks at the edges of the spectrum.

## *5.4 Polymerization of the $^{13}C$ labeled premonomers*

As the Gilch and the radical sulfinyl polymerization were already well described in literature, those routes were not repeated; only MDMO-PPVs through the anionic and the dithiocarbamate route were synthesized to be able to make a comparison.

### 5.4.1 Polymerization *via* the anionic sulfinyl route

The sulfinyl MDMO-PPV premonomer was polymerized through the anionic sulfinyl route using LHMDS as the base at 0 °C in dry THF under a nitrogen atmosphere. After polymerization, the reaction mixture was poured in ice water, neutralized by hydrochloric acid and extracted with $CHCl_3$. The precursor polymer was obtained by removing the solvent under reduced pressure. After analysis by $^{13}C$ NMR, the precursor polymer was redissolved in toluene. By heating under reflux, the sulfinyl groups of precursor polymer were eliminated and the conjugated MDMO-PPV polymer was obtained. The polymer was precipitated in methanol and the elimination was performed a second time to ensure complete removal of the sulfinyl groups. The obtained polymer was analyzed using $^{13}C$ NMR after precipitation in methanol, filtration and drying under reduced pressure to remove the last remains of the solvent.

### 5.4.2 Polymerization *via* the dithiocarbamate route

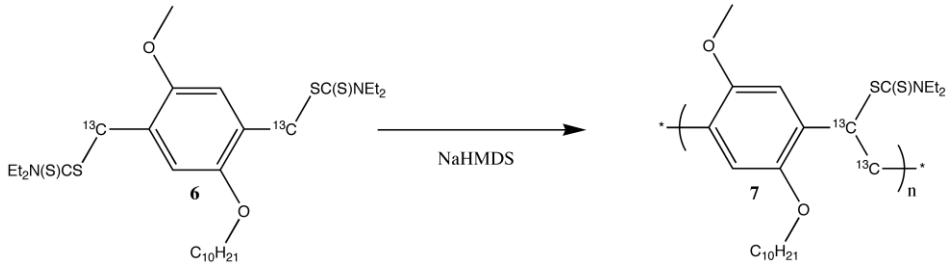


**Figure 5-12: Synthesis of dithiocarbamate precursor polymers**

The polymerization was performed in a three-necked flask under nitrogen atmosphere and in dry THF. NaHMDS (1 M, 1.5 equivalents) was used as the base. After polymerization, the reaction mixture was poured in ice water, neutralized by hydrochloric acid and extracted with $CHCl_3$. The precursor polymer was obtained by precipitation in cold methanol. Molecular weights ($M_w$) were determined by GPC relative to polystyrene (PS) standards with THF as the eluent.

## *5.5 $^{13}C$ NMR analysis of the $^{13}C$ labeled MDMO-PPV polymers*

### 5.5.1 $^{13}C$ NMR analysis of the MDMO-PPV polymer obtained from the anionic sulfinyl route

In this paragraph the results of the $^{13}C$ labeling already presented in chapter 2 (page 58-62) will be repeated and explained in greater detail.

## Analysis of the precursor polymer

Analysis of the precursor polymer synthesized *via* the anionic sulfinyl route by $^{13}C$ NMR showed the signals of the labeled positions on the polymer backbone around 54.8 and 32.2 ppm (Figure 5-13). A small signal was found at 188.9 ppm (marked with °, 0.35%), which can be attributed to an aldehyde end group. An impurity was found at 69 ppm (marked with Δ). This impurity was already present in the $^{13}C$ labeled premonomer. Due to overcrowding, no further information could be obtained from this spectrum. Molecular weight according to GPC was determined to be $M_n$: 10.4 kD, $M_w$: 26.8 kD.

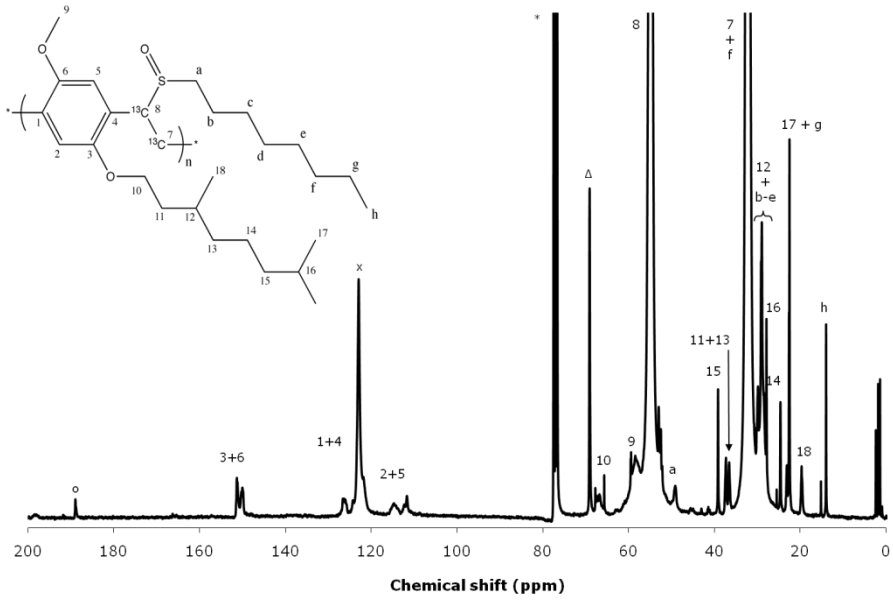


**Figure 5-13: $^{13}C$ spectrum of sulfinyl precursor labeled MDMO-PPV polymer. The resonance marked with a ° results from an aldehyde functionalization, the resonance marked with * from $CDCl_3$, the resonance marked with Δ from a build-in impurity and the resonance marked with x from base induced elimination.**

## Analysis of the conjugated polymer

After conversion to the conjugated form, the molecular weight was determined to be $M_n$: 17.7 kD, $M_w$: 57.6 kD according to GPC. This is higher than the GPC result of the premonomer, due to the increase of the hydrodynamic volume of the polymer chain after elimination. As already mentioned in chapter 2, the signal of the double bond at 123 ppm is the most prominent signal in the spectrum. After the first elimination, the only signals that do not conform to the polymer are found at 41.7, 53.1, 69.4 and 189.1 ppm. Analysis of the labeled premonomers taught us that the labeled carbon next to the sulfinyl group of the sulfinyl premonomer appears at 52.6 ppm. The labeled carbon of the chloromethyl produces a signal at 41.3 ppm. An incomplete elimination would be visible by signals at 54.8 and 32.2 ppm. The aldehyde function can be found at 188.9 ppm. The impurity in the premonomer, which is most likely a methylether function or a methylol group, was found at 68.7 ppm. This enables us to assign the found non-conforming signals to a sulfinyl end group, a chloromethyl end group, an aldehyde and the premonomer impurity.

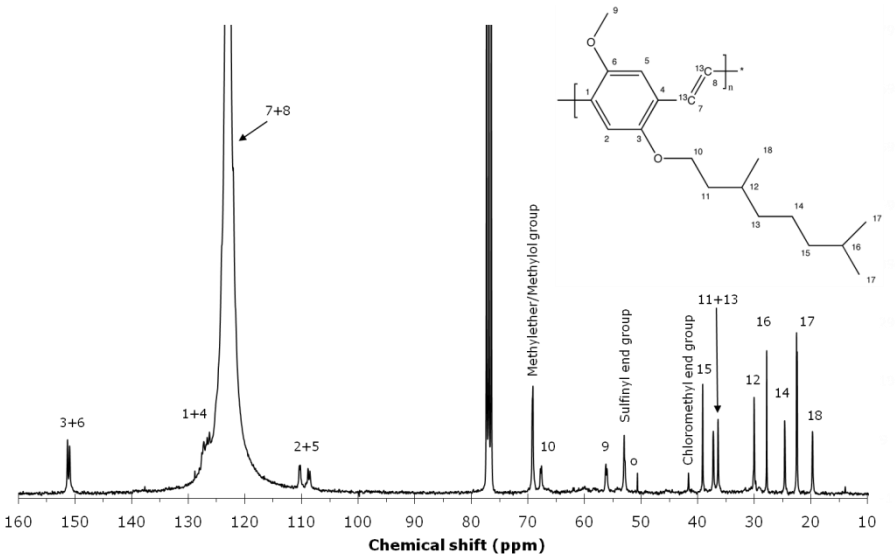


**Figure 5-14: $^{13}C$ Spectrum of converted labeled MDMO-PPV polymer**

The polymer was subjected to a second elimination step by heating in refluxing toluene, to ensure complete elimination of the sulfinyl groups. The

results of the second elimination can be found in Table 5-4. The signal of the sulfinyl groups assigned as 'sulfinyl end groups' does not decrease after the second elimination reaction, confirming that these sulfinyl groups are indeed end groups. No proof of head-to-head defects were found.

| | *First elimination* | *Second elimination* |
|---|---|---|
| Incomplete elimination | 0% | 0% |
| Aldehyde | 0.96% | 1% |
| Sulfinyl end group (53.1 ppm) | 1.4% | 1.3% |
| Chloromethyl end group (41.7 ppm) | 0.2% | 0.3% |
| Impurity (69.4 ppm) | 2.8% | 2.9% |

**Table 5-4: Defects found in MDMO-polymer synthesized *via* anionic sulfinyl route**

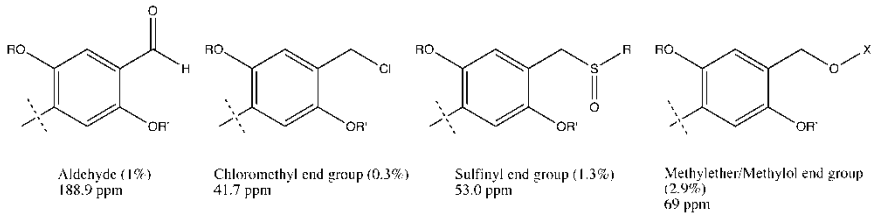


**Figure 5-15: Overview of the type and amount of structural defects present in the MDMO-PPV obtained *via* the anionic sulfinyl route.**

The ideal anionic polymerization would have only sulfinyl end groups and the groups of the initiator, which would be chloromethyl groups in case the polymerization is initiated by the deprotonated premonomer. It is also expected that part of the sulfinyl groups oxidize to aldehyde groups during workup. Oxygen is excluded systematically during the polymerization reaction, and this should prevent the creation of the aldehyde end group during polymerization. According to this expectation only 0.3% of the functional groups of the initiator and 2.3% of the end function are found.

Research was done in the past on the effect of impurities on the radical sulfinyl polymerization route and it was found that impurities were not build into the polymer chain. In chapter 2, a direct link between premonomer purity and molecular weight was found that was confirmed in chapter 4. It seems that the impurities can act as initiators for the anionic polymerization, explaining the low molecular weight obtained. As the ether or methylol end

group is originating from an impurity, it stands to reason that this functional group is part of the actual initiator.

Compared to the other routes, the anionic polymerization route can have some extra benefits, as it will be possible to end cap the polymers, reducing the amount of aldehyde end groups. Carbonyl defects can act as exciton dissociation sites leading to a quenching of the photoluminescence.[15]

### 5.5.2 $^{13}$C NMR analysis of the MDMO-PPV polymer obtained from the dithiocarbamate route

Analysis of the precursor polymer

Analysis of the precursor polymer by $^{13}$C NMR showed the signals of the labeled positions on the polymer backbone between 52.0 and 50.5 ppm and between 35.0 and 33.5 ppm (Figure 5-16). The shifts are consistent with two different labeled carbons with $^{13}$C-$^{13}$C J coupling. A small signal was found at 188.9 ppm (0.35%), which can be attributed to an aldehyde functionality. Due to overcrowding, no further data could be obtained from this spectrum. We could however say that the spectrum was as expected for the precursor polymer.

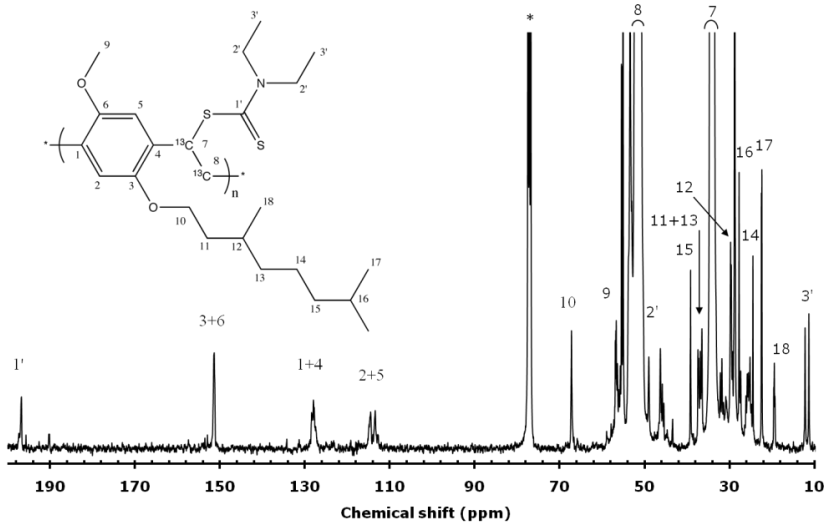


**Figure 5-16: $^{13}$C NMR spectrum of labeled DTC precursor MDMO-PPV at 40 °C. The resonances marked with an asterisk results from $CDCl_3$.**

## Thermal Conversion

The precursor polymer was converted into its conjugated equivalent *via* thermal elimination. Upon heating, the dithiocarbamate groups of precursor polymer **7** were eliminated to form the corresponding conjugated polymer **8**. The polymers were isolated *via* precipitation in cold methanol. Molecular weight according to GPC was determined to be $M_n$: 394 kD, $M_w$: 1113 kD.

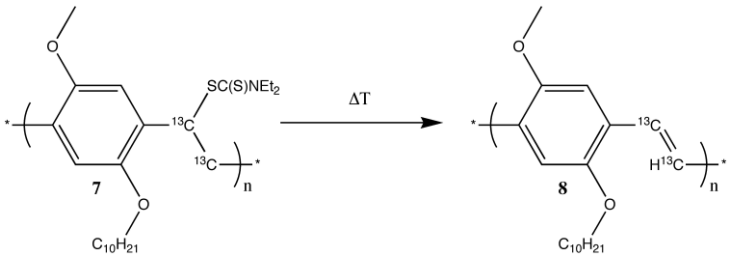


**Figure 5-17: Thermal conversion of precursor polymer 7 to conjugated polymer 8**

## Analysis of the conjugated polymer

By comparing the $^{13}C$ NMR spectra of the unlabeled (Figure 5-18) and labeled converted conjugated polymer (Figure 5-19) obtained *via* the dithiocarbamate route, some additional resonances could be detected upon labeling. These resonances were situated at 189.1 ppm, 36.8 ppm and a shoulder at 31 ppm. The signal at 189.1 ppm can be attributed to an aldehyde functionality (0.6%); this defect was also found in the Gilch route (0.1%), the radical sulfinyl route (0.3%) and the anionic sulfinyl route (1.0%). Since MDMO-PPV is stable up to about 175 °C [31], this functionality can be assigned to the end groups of the polymer.

The $^{13}C$ NMR of the labeled DTC premonomer provides us with an estimate for the NMR shift of the labeled carbon next to the dithiocarbamate group at the end of a polymer (36.8 ppm). The labeled precursor polymer elucidates the position of the signals of the carbons next to the dithiocarbamate group on the polymer chain (52.0-50.5 and 35.0-33.5 ppm). This enables us to assign the small peak found at 36.8 ppm to a dithiocarbamate functionality at the end of the polymer chain (< 0.1%). No non-eliminated groups could be found at the NMR detection level (<0.1%). The only other defect visible can be found as a shoulder at 31 ppm, which can be attributed to a bisbenzyl

unit (0.6%) originating from a head-to-head addition or the initiating diradical (Figure 2-1, page 36). The triple bond (90.4 ppm) and carboxylic acid (165.2 ppm) defects that could be found in the Gilch route by H. Roex were not found in the dithiocarbamate polymer. No change was noted after the second elimination. This further verifies that the origin of the aldehyde end groups lies not at the elimination step at relative high temperature, but rather at the polymerization step of the polymer.

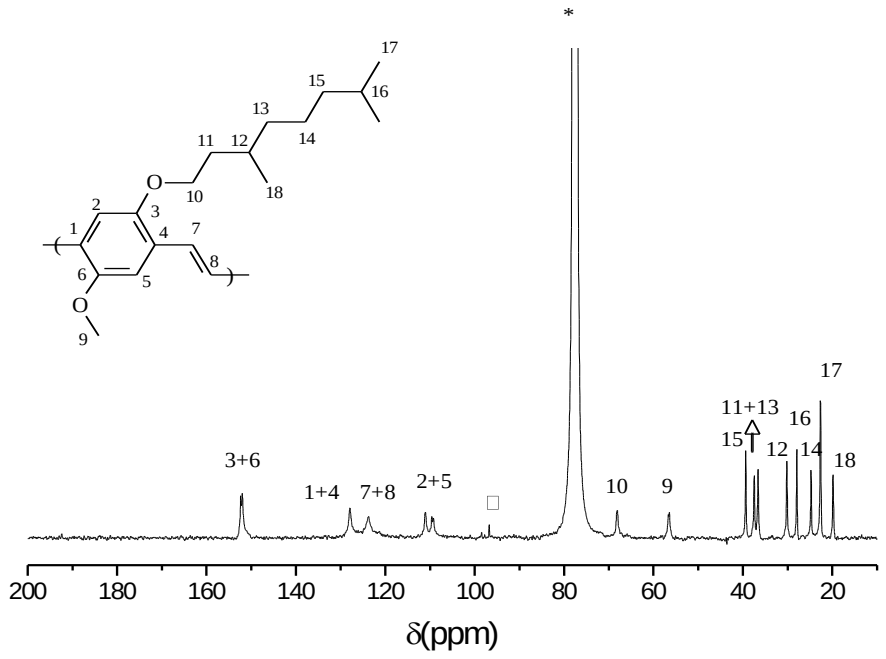


**Figure 5-18: $^{13}$C NMR spectrum of unlabeled conjugated MDMO-PPV at 40 °C. The resonances marked with an asterisk and an open square result from $CDCl_3$ and the transmitter offset, respectively.**

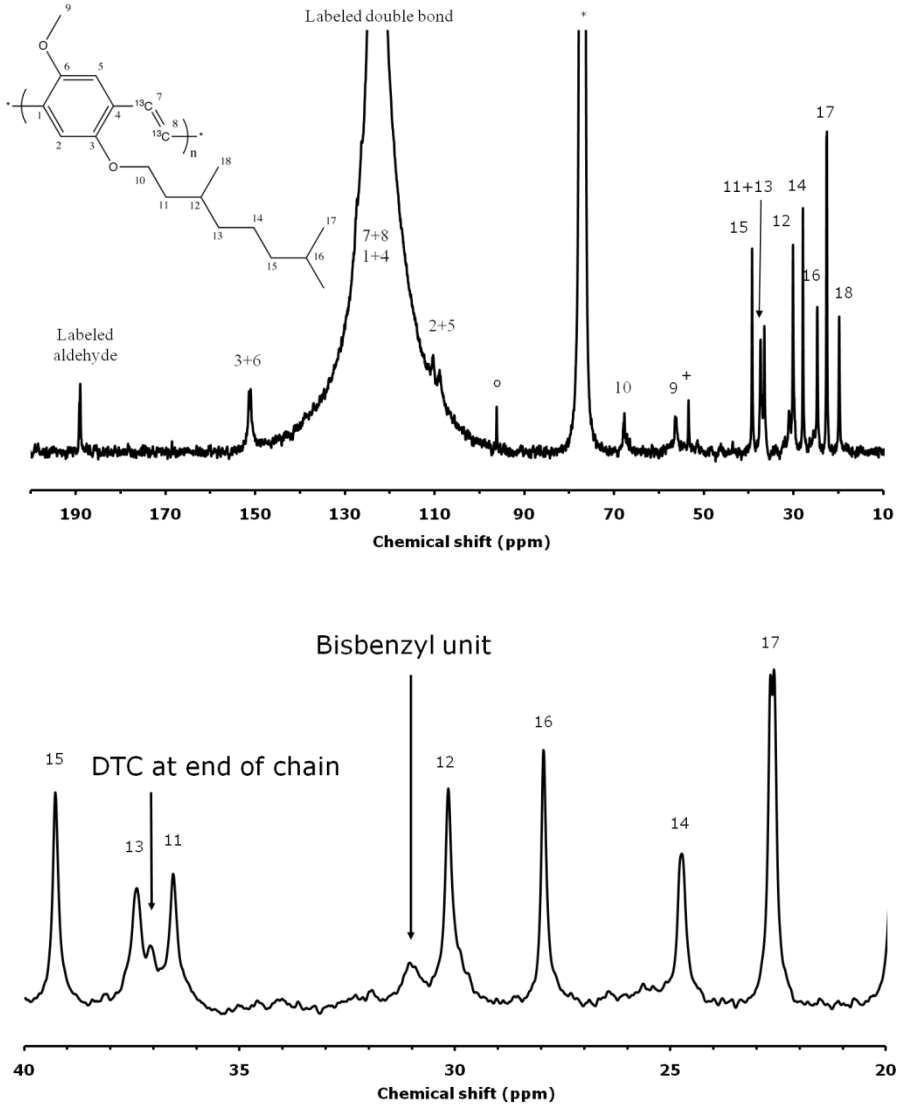


**Figure 5-19: top: $^{13}C$ NMR spectrum of labeled dithiocarbamate MDMO-PPV after second elimination. Bottom: Zoom-in of the spectrum between 20 and 40 ppm. The resonances marked with an asterisk and an open circle result from $CDCl_3$ and the transmitter offset, respectively. The resonance mark with '+' is the result of remaining solvent.**

| *Defect* | *First elimination* | *2nd elimination* |
|---|---|---|
| *Aldehyde* | 0.6 % | 0.6 % |
| *bisbenzyl-unit* | 0.6 % | 0.6 % |
| *dithiocarbamate end group* | <0.1 % (detection limit) | < 0.1 % (detection limit) |
| *non eliminated groups* | <0.1 % (detection limit) | < 0.1 % (detection limit) |

**Table 5-5: Amounts of different types of structural defects in DTC MDMO-PPV after first and second elimination**

If we compare these results (Table 5-5) with the results obtained for the Gilch and the radical sulfinyl route, we can conclude that, besides the sulfinyl route, also the dithiocarbamate route leads to polymers with very few defects and therefore a highly regular microstructure.

## 5.6 Conclusions

In this chapter a comparison was made between the polymers obtained from the Gilch, the radical sulfinyl route, the anionic sulfinyl route and the newly developed dithiocarbamate route. The conjugated polymer backbone structure inherently includes defects and as the defects are an integral part of the polymer structure, they are linked to the precursor route employed. The defects present in the MDMO-PPVs polymers from the different routes were investigated, compared and presented in Table 5-6.

| ***Route*** / *Defect* | ***Gilch*** | ***Radical sulfinyl*** * | ***Anionic sulfinyl*** | ***Dithiocarbamate*** |
|---|---|---|---|---|
| *Aldehyde end group* | 0.1 % | 0.3 % | 1.0 % | 0.6 % |
| *Carboxylic acid end group* | 0.2 % | < 0.1 % | < 0.1 % | < 0.1 % |
| *bisbenzyl-unit* | 5.6 % | < 0.1 % | < 0.1 % | 0.6 % |
| *Triple bond* | 4.2 % | < 0.1 % | < 0.1 % | < 0.1 % |
| *Chlorovinyl* | 1.4 % | < 0.1 % | < 0.1 % | < 0.1 % |
| *Chloromethyl end group* | < 0.1 % | < 0.1 % | 0.3 % | / |
| *Sulfinyl end group* | / | < 0.1 % | 1.3 % | / |
| *dithiocarbamate end group* | / | / | / | < 0.1 % |
| *Other end group* | / | / | 2.9 % | / |
| *non eliminated groups* | 1.8 % | 0.5 % | < 0.1 % | < 0.1 % |

**Table 5-6: Overview of the defects found in labeled MDMO-PPV synthesized *via* different precursor routes. * After two elimination steps**

When we compare the results of the Gilch polymerization with the sulfinyl polymerization, then we can note that the sulfinyl route, whether anionic or radical, shows almost no head-to-head or tail-to-tail couplings. This is a clear advantage over the Gilch route. Skeptics might say that the small increase in polymer purity does not outweigh the downside of the more complex

premonomer synthesis. However, research has shown that mobility increases drastically as the polymer purity increases and as fewer defects also leads to higher solar cell efficiencies.

The synthesis of high quality MDMO-PPV with the dithiocarbamate route has been established. The use of NaHMDS as a base results in polymers with high molecular weight and low PD. In addition, the dithiocarbamate premonomer is easily synthesized, compared to the synthesis of the sulfinyl premonomer. Unlikely to the Gilch route, $^{13}C$ NMR studies have shown that polymerization of bisdithiocarbamate premonomers mainly proceeds *via* head-to-tail additions and only very small amounts of defects are present in the resulting microstructure. These results prove that the dithiocarbamate route is an optimal balance between the straightforwardness of the Gilch route and the excellent material qualities of the sulfinyl route.

# *5.7 Experimental part*

**Chemical and optical characterization.**

Analytical Size Exclusion Chromatography (SEC) was performed using a Spectra series P100 (Spectra Physics) pump equipped with a pre-column (5 μm, 50 mm*7.5 mm, guard, Polymer Labs) and two mixed-B columns (10 μm, 2x300 mm*7.5 mm, Polymer Labs) and a SpectraSYSTEM RI-150 Refractive Index (RI) detector (Shodex) at 40 °C. HPLC grade tetrahydrofuran (THF) was used as the eluent at a flow rate of 1.0 mL/min. Toluene was used as flow rate marker. Molecular weight distributions are given relative to polystyrene standards with a narrow polydispersity. NMR spectra were recorded with a Varian Inova Spectrometer at 300 MHz for $^{1}H$ NMR and at 75 MHz for $^{13}C$ NMR using a 5 mm probe.

**Chemicals**

Commercially available chemicals (Aldrich and Acros) were used without further purification unless stated otherwise. LHMDS and NaHMDS were purchased as a 1 M solution in THF and used as such. THF was dried over sodium/benzophenone and distilled under nitrogen prior to use. All polymerization reactions were performed under a nitrogen atmosphere. All glassware used for the polymerization reaction was dried overnight in a drying oven at 110 °C prior to use.

**Synthesis of premonomers**

Synthesis of 2,5-bis(chloro-methyl)-1-(3,7-dimethyloctyloxy)-4-methoxy-benzene is described in chapter 2, page 69.

**Preparation of 2,5-bis(chloro-$^{13}$C-methyl)-1-(3,7-dimethyloctyloxy)-4-methoxy-benzene (2)**

A 3.16 g (12 mmol) of **2** and 1.0 g (33.3 mmol) of paraformaldehyde-$^{13}C$ (isotopic purity of 99%, Cambridge Isotope Laboratory, Inc., Andover) were placed in a 100 mL three-neck round bottom flask in an ice bath. After dropwise addition of 19.5 g of 37 % HCl (198 mmol) under $N_2$ a white suspension was formed. 36.78 g (360 mmol) of acetic anhydride was added

dropwise at such a rate that the internal temperature did not exceed 70 °C. After stirring for 3.5 h at 75 °C, the mixture was cooled and poured in 60 mL of water. The resulting white precipitate is collected by filtration. The product was dissolved in hexane and dried over anhydrous $MgSO_4$. After recrystallization in hexane, pure product was obtained. $^1H$ NMR (300 MHz, $CDCl_3$, ppm): 6.94 (dd, 1H, $H_{arom}$); 6.91 (dd, 1H, $H_{arom}$); 4.64 (dd, 4H, $CH_2Cl$,$^1J$=153 Hz, J=2.2 Hz); 4.02 (m, 2H, $OCH_2$); 3.87 (s, 3H, $OCH_3$); 1.9-1.45 (4H); 1.4-1.1 (6H); 0.96 (d, 3H, J=6.51); 0.85 (d, 6H, 2x$CH_3$, J=6.5Hz). $^{13}C$ NMR (300 MHz, $CDCl_3$, ppm): 19.7 (1C, CHC$\underline{H}_3$); 22.6 (1C); 22.7 (1C); 24.7 (1C); 28.0 (1C); 29.8 (1C); 36.3 (1C); 37.2 (1C); 39.2 (1C); 41.2 (1C, Cl$^{13}\underline{C}H_2$); 56.2 (1C, $OCH_3$); 67.4 (1C, $OCH_2$); 113.2 (1C); 114.3 (1C); 126.4-127.4 (2C); 150.7 (2C). MS(CI, m/z): 362 ($M^+$), 222 ($M^+$-$C_{10}H_{20}$), 186.

**Preparation of bis-tetrahydrothiophenium salt of 2,5-bis(chloro-$^{13}$C-methyl)-1-(3,7-dimethyl-octyloxy)-4-methoxybenzene (3)**

A solution of 3.70 g (10.27 mmol) of 2,5-bis(chloro-$^{13}$C-methyl)-1-(3,7-dimethyloctyloxy)-4-methoxybenzene **2** and 4.623 g (51.35 mmol) of tetrahydrothiophene in MeOH (7.4 mL) was stirred for 3 days at ambient temperature under $N_2$ atmosphere. After precipitation in cold acetone (100 mL, 0 °C), the precipitate was filtered off on a glass filter and washed with cold hexane. The product was dried under reduced pressure at room temperature. (3.49 g, 61.2 %).

**Preparation of 2-(octylsulfanyl)-$^{13}$C-methyl)-5-(chloro-$^{13}$C-methyl)-1-(3,7-di-methyloctyloxy)-4-methoxybenzene (4)**

A mixture of NaO*t*Bu (0.604 g, 6.29 mmol) and n-octanethiol (0.902 g, 6.17 mmol) in MeOH (12.8 mL) was stirred for 60 min at room temperature. The clear solution was added in one portion to a stirred solution of **3** (3.49 g, 6.29 mmol) in MeOH (19.3 mL). After three hours the reaction mixture was neutralized with aqueous HCl, if necessary, and concentrated in vacuo. The obtained oil was diluted with octane (25 mL) and concentrated again to remove the tetrahydrothiophene by azeotropic distillation.[32] This sequence was repeated three times to afford light yellow viscous oil. The crude product was diluted with $CH_2Cl_2$ (25 mL) and washed with brine. The water layer was

extracted with $CH_2Cl_2$. The organic layers were combined, dried with $MgSO_4$, filtered and concentrated under reduced pressure. 2.80 g (5.93 mmol, 94.3% yield) of crude product was formed. $^1$H NMR (300 MHz, $CDCl_3$, ppm): 6.9/6.8 (2H, $H_{ar}$); 4.6 (dd, 4H, $CH_2Cl$,$^1$J=153 Hz, J=2.2 Hz); 4.0 (m, 2H, $OCH_2$); 3.9 (s, 3H, $OCH_3$); 3.5 (s, 2H, $CH_2S(R)$); 2.5 (m, 2H, $SC\underline{H}_2R$); 1.9-1.2 (14H); 1.0 (d, 3H, $CH_3$, J=6.43); 0.9 (d, 9H, 3x$CH_3$, J=6.51). $^{13}$C NMR (300 MHz, $CDCl_3$, ppm): 14.1 (1C, $CH_2C\underline{H}_3$); 19.7 (1C, $CHC\underline{H}_3$); 22.6 (3C); 24.7 (1C); 27.9 (1C); 29.0 (1C); 29.8 (1C); 30.2 (s, 1C, $RS^{13}\underline{C}H_2$); 31.8 (1C); 36.7 (1C); 37.2 (1C); 39.2 (1C); 41.1 (1C); 41.3+41.6 (1C, $Cl^{13}\underline{C}H_2$); 56.1 (d, 1C, $OCH_3$); 67.3 (d, 1C, $OCH_2$); 69.2 (impurity); 113.2 (1C); 114.3 (1C); 124.8 (1C); 128.8 (1C); 150.7 (2C).

**Preparation of 2-(octylsulfinyl)-$^{13}$C-methyl)-5-(chloro-$^{13}$C-methyl)-1-(3,7-dime-thyloctyloxy)-4-methoxybenzene (5)**

An aqueous (35 wt%) solution of $H_2O_2$ (0.98 g, 8.64 mmol) was added dropwise to a solution of crude thioether **4** (2.70 g, 5.73 mmol), $TeO_2$ (0.12 g, 0.75 mmol) and one drop of diluted HCl (1N) in 1,4-dioxane (22 mL). The reaction was followed on TLC and as soon as the overoxidation took place, it was quenched by a saturated aqueous NaCl solution (10 mL). After extraction with $CH_2Cl_2$ (3 x 10 mL), the organic layers were dried over $MgSO_4$ and concentrated in *vacuo*. (2.37 g, 4.87 mmol) The reaction mixture was purified by fast column chromatography ($SiO_2$, eluent hexane/ethylacetate 60/40) to give pure **7.** $^1$H NMR (300 MHz, $CDCl_3$, ppm): 6.9 (d, 1H, $H_{ar}$); 6.8 (d, 1H, $H_{ar}$); 4.5 (d, 2H, $^1$J=154Hz, J=2.7 Hz, $CH_2Cl$); 4.2+3.7 (dd, 2H, $CH_2S(O)R$); 3.9 (m, 2H, $OCH_2$); 3.7 (d,3H, OCH3); 2.5 (m, 2H); 1.6–1.9 (m, 2H), 1.4– 1.6 (m, 2H), 1.1–1.3 (m, 6H), 0.9 (dd, 3H, $CH_3$); 0.8 (m, 6H; 2 x $CH_3$). $^{13}$C NMR (100 MHz, $CDCl_3$, ppm): 13.8 (1C); 19.4 (1C); 22.3 (2C); 22.4 (1C); 24.4 (1C); 27.7 (1C); 28.6 (1C); 28.8 (1C); 28.9 (1C); 29.6 (1C); 29.9 (1C); 31.5 (1C); 36.0 (1C); 37.0 (1C); 39.0 (1C); 41.1 (1C $^{13}CH_2Cl$); 51.5 (1C); 52.4+52.7 (1C $^{13}CH_2S(O)R$); 55.9 (d, 1C); 66.8 (d, 1C); 68.9 (Impurity); 113.5 (1C); 114.4 (1C); 119.7 (1C); 126.1 (1C); 150.6 (2C).

**2,5-Bis(N,N-diethyl dithiocarbamate-$^{13}$C-methyl)-1-(3,7-dimethyloctyloxy)-4-methoxy-benzene (6)**

To 50 mL of an ethanol solution of 2,5-bis(chloro-$^{13}$C-methyl)-1-(3,7-dimethyloctyloxy)-4-methoxy-benzene **2** (1 g, 2.75 mmol), sodium diethyldithiocarbamate trihydrate (1.43 g, 6.33 mmol) was added as a solid. The mixture was stirred for 3 hours at ambient temperature under a nitrogen atmosphere. Subsequently, water (100 mL) was added and the mixture was filtered over a Buchner to obtain white crystals, which were washed with ethanol and water and used without further purification. Yield: 100% $^{1}$H NMR (300 MHz, $CDCl_3$, ppm): 7.1 (s, 2H), 4.6 (dd, 4H, $CH_2Cl$,$^{1}$J=145.5 Hz, J=10.5 Hz), 4.0 (m, 4H+2H), 3.8 (s, 3H), 3.7 (m, 4H), 1.7–1.9 (m, 2H), 1.5– 1.6 (m, 2H), 1.3 (t, 12H), 1.1–1.4 (m, 6H), 0.9 (d, 3H, J=6.5 Hz), 0.9 (d, 6H, J=6.7 Hz); $^{13}$C NMR (100 MHz, $CDCl_3$, ppm): 196.0 (1C), 195.9 (1C), 151.2 (1C), 150.9 (1C), 125.3-124.1 (2C), 114.7 (1C), 113.8 (1C), 67.1 (1C), 56.1 (1C), 49.4 + 46.6 (4C), 39.2 (1C), 36.8 (*), 34.0 (2C), 29.7 (1C), 27.9 (1C), 24.7 (1C), 22.7 (1C), 22.6 (1C), 19.6 (1C), 12.4 + 11.5 (4C). (*) $^{13}$C labeled carbon

**Polymerization of 2-(octylsulfinyl)-$^{13}$C-methyl)-5-(chloro-$^{13}$C-methyl)-1-(3,7-dimethyloctyloxy)-4-methoxybenzene *via* anionic sulfinyl precursor route**

All glassware was dried overnight in a drying oven at 110 °C and heated with a Bunsen burner under vacuum prior to use. The premonomer **5** (243 mg, 0.5 mmol) was placed in a 50 mL three-necked flask equipped with a Teflon stirrer and the flask was degassed by 3 consecutive vacuum/nitrogen cyclings. Dry, degassed THF (8.75 mL) was transferred to the premonomer flask by use of a glass syringe. The dissolved premonomer was cooled to 0 °C and the reaction started by the addition of LHMDS (1.25 mL, 1.25 mmol). The reaction was stopped after 60 minutes. The excess of base was neutralized by addition of a 1.0 M aqueous hydrochloric acid solution, followed by extraction with dichloromethane. The precursor polymer was obtained by concentrating the combined organic layers under reduced pressure.

**Thermal elimination of labeled sulfinyl precursor polymer to labeled conjugated polymer**

A solution of precursor polymer (0.5 mmol) in toluene (2.5 mL) was degassed for 30 minutes by passing through a continuous stream of nitrogen. The solution was heated to 110 °C and stirred for 3 h. After cooling to room temperature, the solution was added dropwise to cold methanol (25 mL) resulting in the precipitation of the polymer. The polymer was filtered off on a Teflon filter, washed with cold methanol and dried at room temperature under reduced pressure. The procedure was repeated a second time to ensure complete elimination of the sulfinyl groups. The labeled conjugated MDMO-PPV was obtained as a red polymer (118.6 mg, 0.43 mmol).

$^{13}$C NMR (100 MHz, $CDCl_3$, ppm): 189.06 (*); 151.3 (2C); 127.0 (2C), 123.1 (2C, $^{13}C=^{13}C$); 110.3 (1C); 108.8 (1C); 69.4 (*); 67.6 (1C); 56.2 (1C); 50.8 (*); 41.7 (*), 39.3 (1C); 37.4 (1C); 36.5 (1C); 30.1 (1C); 27.9 (1C); 24.8 (1C); 22.5 (2C); 19.8 (1C); (*) Detected defects in the polymer chain

**Polymerization of 2,5-Bis(N,N-diethyl dithiocarbamate-methyl)-1-(3,7-dimethyloctyloxy)-4-methoxy-benzene *via* the dithiocarbamate precursor route (7)**

294.5 mg (0.5 mmol) of premonomer **6** was dissolved in dry THF (2.5 mL). The mixture was stirred at 30 °C under a continuous flow of nitrogen. 1.5 equivalents (0.75 mmol) of a NaHMDS solution (1 M in THF) were added in one go to the stirred premonomer solution. The reaction proceeded for 1.5 hours at 30 °C under a nitrogen atmosphere, and the mixture was subsequently quenched in 50 mL ice water. The excess of base was neutralized by addition of a 1.0 M aqueous hydrochloric acid solution, followed by extraction with dichloromethane. The precursor polymer was obtained by concentrating the combined organic layers under reduced pressure.

$^{1}$H NMR (300 MHz, $CDCl_3$, ppm): 6.5–7.0 (br m, 2H), 5.5–5.9 (br s, 1H), 3.1–4.2 (br m, 11H), 1.0–2.0 (br m, 16H), 0.7–1.0 (m, 9H); $^{13}$C NMR (100 MHz, $CDCl_3$, ppm): 195.8, 150.9 (2C), 127.7 (2C), 114.1, 113.1, 67.1, 56.4,

52.0, 49.1, 46.4, 39.3, 37.5, 36.6, 34.5; 29.9, 27.9, 24.7, 22.7, 22.6, 19.7, 12.5, 11.6

**Thermal elimination of labeled dithiocarbamate precursor polymer to labeled conjugated polymer (8)**

A solution of **7** (160.5 mg) in dichlorobenzene (80 mL) was degassed for 1h by passing through a continuous stream of nitrogen. The solution was heated to 180 °C and stirred for 3 h. After cooling to room temperature, the solvent was removed under reduced pressure. The polymer was redisolved in a small quantity of chloroform and precipitated dropwise in cold methanol in a ration chloroform/methanol 1/10. The polymer was filtered off, washed with cold methanol and dried at room temperature under reduced pressure. A 63.3 mg (0.22 mmol, 43%) of conjugated polymer **8** was obtained as a red polymer. The elimination procedure was performed a second time (32 mL dichlorobenzene) to ensure complete elimination.

$^{1}H$ NMR (300 MHz, $C_2D_2Cl_4$, ppm): 7.5 (br, 2H) 7.2 (br, 2H) 4.6-3.2 (br m, 5H) 2.1-0.6 (br m; 19H); $^{13}C$ NMR (100 MHz, $CDCl_3$, ppm): 188.9 (*); 151.3 (2C); 127.0 (2C, $^{13}C=^{13}C$), 123.3 (2C); 110.4 (1C); 108.8 (1C); 67.6 (1C); 56.1 (1C); 39.1 (1C); 37.2 (1C); 36.8 (*); 36.4 (1C); 31.0 (*); 30.0 (1C); 27.8 (1C); 24.6 (1C); 22.5 (2C); 19.8 (1C); (*) Detected defects in the polymer chain

**Unlabeled dithiocarbamate conjugated polymer**

The unlabeled polymer was obtained by the same procedure as the labeled polymer, except that unlabeled 2,5-Bis(N,N-diethyl dithiocarbamate-methyl)-1-(3,7-dimethyloctyloxy)-4-methoxy-benzene was used. This polymer was synthesized and analyzed by Joke Vandenberg.

$^{13}C$ NMR (100 MHz, $CDCl_3$, ppm): 151.4 (2C); 127.0 (2C), 123.3 (2C); 110.5 (1C); 108.8 (1C); 67.9 (1C); 56.4 (1C); 39.2 (1C); 37.4 (1C); 36.6 (1C); 30.2 (1C); 27.9 (1C); 24.6 (1C); 22.6 (2C); 19.8 (1C).

## 5.8 References

[1] A. Henckens; K. Colladet; S. Fourier; T.J. Cleij; L. Lutsen; J. Gelan, *Macromolecules*, **38(1)**,19, (2005)

[2] A. Henckens; I. Duyssens; L. Lutsen; D. Vanderzande; T.J. Cleij, *Polymer*, **47**, 123-131, (2006)

[3] F. Banishoeib; S. Fourier; T.J. Cleij; L. Lutsen; D. Vanderzande, *Eur. Phys. J. Appl. Phys.*, (2007)

[4] H. F. M. Schoo; R. J. C. E. Demandt, *Philips J. Res.*, **51**, 527, (1998)

[5] H. Becker; O. Gelsen; E. Kluge; W. Kreuder, H. Schenk; H. Spreitzer, *Synthetic Metals,* **111**, 145, (2000)

[6] H. Becker; H. Spreitzer; W. Kreuder; E. Kluge; H. Vestweber; H. Schenk, *Synthetic Metals,* **122**, 105, (2001)

[7] P. L. Burn; A. B. Holmes; A. Kraft; D. D. C. Bradley; A. R. Brown; R. H. Friend; R. W. Gymer, *Nature*, **356**, 47, (1992)

[8] E. G. J. Staring; R. C. Demandt; D. Braun; G. L. J. Rikken; Y. A. Kessener; A. H. J. Venhuizen; H. Wynberg; W. ten Hoeve; K. J. Spoelstra, *Adv. Mat.*, **6**, 934, (1994)

[9] D. Braun; E. G. J. Staring; R. C. Demandt; G. L. J. Rikken; Y. A. Kessener; A. H. J. Venhuizen, *Synthetic Metals*, **66**, 75, (1994)

[10] P. L. Burn; A. Kraft; D. R. Baignent; D. D. C. Bradley; A. R. Brown; R. H. Friend; R. Guymer; A. B. Holmes; R. W. Jackson, *J. Am. Chem. Soc.*, **115**, 10117, (1993)

[11] G. G. Malliaras; J. K. Herrema; J. Wildeman; R. H. Wieringa; R. E. Gill; S. S. Lampoura; G. Hadziioannou, *Adv. Mat.*, **5**, 721, (1993)

[12] C. Zhang; D. Braun; A. J. Heeger, *J. Appl. Phys.*, **73**, 5177, (1993)

[13] N. Basescu; Z. X. Liu; D. Moses; A. J. Heeger; H. Naarmann; N. Theophilou, *Nature*, **327**, 403 (1987)

[14] P. Prins; F.C. Grozema; L. D. A. Siebbeles, *Molecular Simulation*, **32**(**9)**, 695-705, (2006)

[15] L. J. Rothberg; M. Yan; F. Papadimitrakopoulos; M. E. Galvin; E. W. Kwock; T. M. Miller, *Synthetic Metals*, **80**, 41, (1996)

[16] G. D. Hale; S. J. Oldenburg; N. J. Halas, *Appl. Phys. Lett.*, **71(11)**, 1483, (1997)

[17] B. H. Cumpston; K. F. Jensen, *Synthetic Metals*, **73**, 167, (1995)
[18] B. H. Cumpston; I. D. Parker; K. F. *J.* Jensen, *Appl. Phys.*, **81(8)**, 3716, (1997)
[19] H. Antoniadis; L. J. Rothberg; F. Papadimitrakopoulos; M. Yan; M. E. Galvin; M. A. Abkowitz, *Phys. Rev.*, **50**, 14911, (1994)
[20] I. D. W. Samuel; G. Rumbles; C. J. Collison; S. C. Moratti; A. B. Holmes, *Chemical Physics*, **227**, 75, (1998)
[21] T. Nguygen; V. Doan; B. J. Schwarz, *J. Chem. Phys.*, **110(8)**, 4068, (1999)
[22] Y. Shi; J. Liu; Y. Yang, *Macromol. Symp.,* **154**, 187, (2000)
[23] T. Nguygen; I. B. Martini; J. Liu; B. J. Schwarz, *J. Phys. Chem.*, **104**, 237, (2000)
[24] L. Lutsen; P. Adriaensens; H. Becker; A. J. Van Breemen; D. Vanderzande; J. Gelan, *Macromolecules*, **32**, 6517-6525, (1999)
[25] T. Munters; T. Martens; L. Goris; V. Vrindts; J. Manca; L. Lutsen; W. De Ceuninck; D. Vanderzande; L. De Schepper; J. Gelan; N. S. Sariciftci; C. J. Brabec, *Thin Solid Films*, **403-404**, 247-251, (2002)
[26] H. Becker; H. Spreitzer; K. Ibrom; W. Kreuder, *Macromolecules*, **32**, 4925-4932, (1999)
[27] H. Roex; P. Adriaensens; D. Vanderzande; J. Gelan, *Macromolecules*, **36**, 5613, (2003)
[28] A. Henckens; L. Lutsen; D. Vanderzande; M. Knipper; J. Manca; T. Aernouts; J. Poortmans, *SPIE Proc.*, **26-30** April, Strasbourg, France, (2004)
[29] H. Roex, *PhD dissertation*, UHasselt, (2003)
[30] J. K. M. Sanders; B. K. Hunter, *Modern NMR spectroscopy*, Oxford University press, **181**, (1987)
[31] H. N. Cho; D. Y. Kim; Y. C. Kim; J. Y. Lee; C. Y. Kim, *Adv. Mat.*, **9**, 326, (1997)
[32] CRC Press, *Handbook of chemistry and physics*, **64$^{th}$ edition**, page D-17, (1983-1984)

# Samenvatting

Geleidende polymeren maken hun opmars in de elektronica markt. Tot op heden bevindt de meest opvallende toepassing van geleidende polymeren zich in light-emitting diodes (LEDs), waar het silicium vervangt. Polymere LEDs worden teruggevonden in klokradio's, televisies, GSMs, enz. Geleidende polymeren hebben ook hun nut in de ontwikkeling van allerhande sensoren, zoals onder andere biosensoren.

Tegenwoordig worden vooral poly(phenylenevinylene) (PPV) en derivaten hiervan als actieve laag in deze opto-elektronische toepassingen gebruikt. De laatste 40 jaar zijn er verscheidene precursor routes ontwikkeld voor de synthese van PPV en derivaten. Bij al deze routes is het *p*-quinodimethaan systeem het eigenlijke monomeer. Aangezien er in dit werk gebruik gemaakt wordt van 3 verschillende precursorroutes wordt er in **hoofdstuk 1** een overzicht gegeven van deze verschillende precursor routes. Er wordt vooral aandacht gegeven aan de polymerisatiemechanismen van deze routes. In het verleden zijn er verschillende studies uitgevoerd om het polymerisatiemechanisme op te helderen. Enkele groepen beweren dat de Gilch precursor polymerisatie *via* een radicalair mechanisme verloopt, andere beweren een anionische route. De onderzoeksgroep Organische en (bio)-Polymere Chemie van de Universiteit Hasselt heeft in 1999 een competitie tussen het radicalaire en anionische mechanisme in de sulfinyl precursor route kunnen aantonen. De onderzoeksgroep heeft kunnen aantonen dat het hoog moleculair gewicht polymeer in de sulfinyl route afkomstig is van een zelf-geïnitieerde radicalaire polymerisatie en dit voor alle solventen waarin de polymerisatie uitgevoerd wordt. Anderzijds, wanneer laag moleculair gewicht polymeer teruggevonden wordt, is het afkomstig van een anionisch polymerisatiemechanisme. De reactieomstandigheden bepalen de competitie tussen deze twee mechanismen zodat ook een bimodale verdelingen (hoog en laag moleculair gewicht) kunnen voorkomen.

De invloed van allerhande polymerisatieparameters zoals concentratie, solvent en temperatuur worden aangehaald in **hoofdstuk 1**.

Dankzij de gezondheidszorg groeit het domein van biosensoren steeds sneller. In de afgelopen jaren is er een toename van het aantal gepubliceerde artikels over het gebruik van elektrisch geleidende polymeren in de transducer laag van biosensoren. Er is grote vooruitgang geboekt met impedimetrische immunosensoren gebaseerd op een spin-coated film van poly [2 - (3,7-dimethyloctyloxy)-5-methoxy-1 ,4-fenyleen vinyleen]. De commerciële naam voor dit PPV derivaat is $OC_1C_{10}$-PPV of MDMO-PPV. De oplosbaarheid in de geconjugeerde staat is een belangrijke rede voor de interesse in dit specifieke PPV derivaat. De binding tussen het polymeer (MDMO-PPV) en de biomolecule (antistof) is gebaseerd op zwakke intermoleculaire interacties in plaats van covalente bindingen. Deze interacties hebben de neiging om de antistoffen te denatureren en hebben een negatieve invloed hebben op de levensduur en de stabiliteit van de biosensor. Bovendien kunnen niet-specifieke interacties op het MDMO-PPV polymeren oppervlak leiden tot vervuiling van de sensor.

De PPV polymeren worden fysiek aangehecht op het substraat door middel van spin-coating. Ook al is de polymeerlaag is zeer dun (~100nm), is het nog steeds aanzienlijk dikker dan nodig. Een ideale biosensor zou bestaan uit een enkele laag PPV-polymeer, waaraan de antilichamen covalent gebonden zijn om zo de stabiliteit van de sensor te verhogen. Aan de andere kant, moet het PPV-materiaal ook stevig hechten aan een substraat. We moeten dus een goede controle hebben over de initiatie, de terminatie en de ketenlengte. Indien we de anionische polymerisatie van PPV's beheersen, dan wordt de gecontrolleerde synthese van zulke geleidende polymeren mogelijk. Hoewel dit kan ook worden bereikt door middel van gecontroleerde radicaal-polymerisatie, zal dit werk zich alleen richten op het beheersen van de anionische polymerisatie.

In **hoofdstuk 2** wordt de synthese van poly[2-(3,7-dimethyloctyloxy)-5-methoxy-1,4-phenyleen vinyleen] besproken. Dit PPV derivaat is commercieel bekend als $OC_1C_{10}$-PPV of MDMO-PPV en is industrieel aantrekkelijk omdat het oplosbaar is in zijn geconjugeerde toestand. Startend van de resultaten van voorgaand onderzoek, werd er geopteerd om een set van polymerisaties uit te voeren van het sulfinyl MDMO-premonomeer met tetrahydrofuraan (THF) als solvent en Lithium diisopropylamine (LDA) als base. Reactiecondities zoals de polymerisatie

temperatuur, toevoegsnelheid en volgorde van toevoegen (base-monomeer) werden onderzocht, maar steeds werden enkel oligomeren met zeer laag moleculair gewicht ($M_n$ ~1.5 kDa) teruggevonden. Dit wijst op een heel efficiënte spontane initiatie die geen controle toelaat van de initiatie stap en de ketenlengte. Het gebruik van een meer sterisch gehinderde base zoals Lithium bis(trimethylsilyl)amide (LHMDS) leidde tot een hoger moleculair gewicht ($M_n$ ~4.0 kDa), opbrengst en maximale golflengte van UV-licht absorptie. Om het anionisch karakter van de polymerisatie aan te tonen, werd het effect van een radicaal inhibitor zoals TEMPO onderzocht. In schril contrast met de klassieke Gilch polymerisatie, waarbij de polymerisatie helemaal geblokkeerd kan worden door toevoeging van 1 equivalent TEMPO, heeft toevoeging van TEMPO hier geen invloed op de polymerisatie. Om de aard van de eindgroepen op het polymeer te achterhalen werd een hoeveelheid polymeer gescheiden op moleculair gewicht door gebruik te maken van Biobeads® (microporeuse korrels). Hoewel het mogelijk was het polymeer te scheiden in fracties met verschillend moleculair gewicht, was het toch niet mogelijk om duidelijke conclusies te trekken over de aard van de eindgroepen. Een gevoeligere techniek was vereist. Vandaar dat in een volgende poging om de eindgroepen te detecteren, de monomeer methyleen koolstoffen naast de polarisator en leaving groep $^{13}C$ gemerkt werden. Hierdoor worden signalen van mogelijke defecten en eindgroepen in een $^{13}C$ NMR spectrum versterkt met ruwweg een factor 100. De $^{13}C$ NMR analyse van het geconjugeerde polymeer gesynthetiseerd *via* de anionische sulfinyl route, toonde aan dat het bekomen polymeer geen head-to-head defecten en resterende sulfinyl groepen had. Verder werden volgende eindgroepen gevonden: 0.96% aldehyde, 1.3% sulfinyl, 0.3% chloromethyl en 2.9% eindgroepen ten gevolge van een onzuiverheid overblijvend na de monomeer synthese.

Voor de anionische polymerisatie is de zuiverheid van het monomeer essentieel tot het bekomen van een hoogmoleculair polymeer. Dit in tegenstelling tot de radicalaire polymerisatie, waar met hetzelfde monomeer een hoog moleculair gewicht wordt bekomen. Hoofdstuk 2 eindigt met de conclusie dat het inderdaad mogelijk is om PPV polymeer te bekomen *via* een anionisch polymerisatiemechanisme, maar om dit met diepgang te

bestuderen moet er een monomeer gekozen worden dat gezuiverd kan worden tot een hoger niveau.

In **hoofdstuk 3** werd 1-(Chloromethyl)-4-[(n-octylsulfinyl)methyl]benzeen of 'PPV monomeer' onderzocht als nieuw monomeer voor het verdere onderzoek naar de anionische polymerisatie van PPV's. Na een dubbele herkristallisatie van het monomeer werden polymerisaties uitgevoerd met LHMDS als base in THF, maar ook het gebruik van LDA als base werd bekeken. Door gebruik te maken van LHMDS als base was het mogelijk een polymeer te bekomen met een relatief hoog moleculair gewicht ($M_n$ ~20 kDa), terwijl met LDA wederom laag moleculair polymeer ($M_n$ ~1.9 kDa) bekomen werd. De anionische aard van de polymerisatie kon bevestigd worden door te polymeriseren in aanwezigheid van een radicaal inhibitor (TEMPO). Verscheidene polymerisatie parameters werden onderzocht zoals: concentratie van het monomeer, polymerisatie temperatuur en hoeveelheid base. Er is echter een beduidende spreiding op het bekomen moleculair gewicht indien de polymerisatie herhaald wordt. De oorzaak van deze spreiding kon niet achterhaald worden, maar is waarschijnlijk te wijten aan kleine hoeveelheden aan onzuiverheden.

De mechanistische studie uitgevoerd op de sulfinyl route in hoofdstuk 2 en 3 leidde tot de conclusie dat een uitsluitend anionische polymerisatie van PPV's mogelijk is. In het geval van poly(fenyleen vinyleen) werden polymeren bekomen met een redelijk moleculair gewicht. In **hoofdstuk 4** werden vier gelijkaardige initiators gesynthetiseerd en de invloed van hun concentratie op de anionische polymerisatie werd getest. De resultaten tonen aan dat de initiators inderdaad werken zoals verwacht, dit wil zeggen, hogere concentraties aan initiator resulteren in lagere moleculair gewichten. Bovendien toont NMR dat ze gebonden zijn aan het polymeer. Deze bevinding creëert vele nieuwe mogelijkheden, waaronder het synthetizeren van PPVs met functionele eindgroepen. Hierdoor wordt het mogelijk om op deze wijze blok-co-polymeren te synthetiseren, namelijk door koppeling van de eindgroep aan een ander (multi)gefunctionaliseerd polymeer. Ook kan een slim gefunctionaliseerd PPV polymeer gemodificeerd worden zodat het gebruikt kan worden als macro-initiator voor een volgende polymerisatie. Indien de polymeren levend zijn, dan kunnen blok-co-polymeren bekomen worden door toevoegen van een tweede monomeer. Het is duidelijk dat het

gebruik van functionele initiators vele nieuwe mogelijkheden biedt voor het bekomen van specifieke polymeer architecturen.

Zoals reeds vermeld, leiden verschillende precursor routes allemaal tot hetzelfde geconjugeerde polymeer. Echter, afhankelijk van de gekozen route kunnen er meer of minder defecten aanwezig zijn in het polymeer. In **hoofdstuk 5** wordt er een vergelijking gemaakt tussen polymeren bekomen *via* de Gilch radicalaire route, de radicalaire en anionische sulfinyl route en de dithiocarbamaat route die enkele jaren geleden ontwikkeld werd in de onderzoeksgroep. De defecten aanwezig in deze polymeren werden onderzocht door middel van $^{13}C$ NMR. Hiertoe werden $^{13}C$ gemerkte premonomeren aangemaakt en gepolymeriseerd. De eerste twee routes, de Gilch en radicalaire sulfinyl, waren reeds op deze manier onderzocht in voorgaande studies. Deze resultaten werden vergeleken met deze van de twee nieuwe ontwikkelde routes.

De gemerkte premonomeren voor de sulfinyl en dithiocarbamaat route werden gemaakt vertrekkend van het gemerkte Gilch MDMO-PPV premonomeer. Deze gemerkte premonomeren werden geanalyseerd met $^{13}C$-NMR zodat de chemische verschuiving van de chloromethyl, sulfinylmethyl en dithiocarbamaat-methyl groep gekend zijn. Vervolgens werd het MDMO-PPV gesynthetiseerd *via* de anionische sulfinyl route en de dithiocarbamaat route. Zowel het precursor polymeer als het geconjugeerde polymeer werden onderzocht door middel van $^{13}C$-NMR spectroscopie. De resultaten worden weergegeven in volgende tabel.

| ***Route*** / *Defect* | ***Gilch*** | ***Radicale sulfinyl*** * | ***Anionische sulfinyl*** | ***Dithio-carbamaat*** |
|---|---|---|---|---|
| *Aldehyde eindgroep* | 0.1 % | 0.3 % | 1.0 % | 0.6 % |
| *Carbonzuur eindgroep* | 0.2 % | < 0.1 % | < 0.1 % | < 0.1 % |
| *Bisbenzyl eenheid* | 5.6 % | < 0.1 % | < 0.1 % | 0.6 % |
| *Drievoudige binding* | 4.2 % | < 0.1 % | < 0.1 % | < 0.1 % |
| *Chlorovinyl* | 1.4 % | < 0.1 % | < 0.1 % | < 0.1 % |
| *Chloromethyl eindgroep* | < 0.1 % | < 0.1 % | 0.3% | / |
| *Sulfinyl eindgroep* | / | < 0.1 % | 1.3 % | / |
| *dithiocarbamaat eindgroep* | / | / | / | < 0.1 % |
| *Andere eindgroep* | / | / | 2.9 % | / |
| *Niet geëlimineerde groepen* | 1.8 % | 0.5 % | < 0.1 % | < 0.1 % |

**Overzicht van defecten gevonden door middel van $^{13}C$ merking in MDMO-PPV bekomen *via* verschillende precursorroutes. * na dubbele eliminatie van de sulfinyl leaving groepen.**

We kunnen concluderen dat geen structurele defecten ten gevolge van kop-kop of staart-staart koppelingen voorkomen in de anionische sulfinyl route, de radicalaire sulfinyl route en de dithiocarbamaat route (tenzij het initiërend deeltje voor de radicalaire polymerisatie). Dit is een duidelijk voordeel ten opzichte van de Gilch route. Betreffende de voornaamste eindgroepen bij de dithiocarbamaat route kunnen we stellen dat enkel de aldehyde functie in een significante hoeveelheid teruggevonden kon worden. Bovendien kan het dithiocarbamaat monomeer makkelijk en met een hoog rendement bekomen worden, vertrekkend van het Gilch monomeer. De dithiocarbamaat route combineert de hoge kwaliteit van de sulfinyl route met het gemak van de Gilch route. De 'Andere eindgroep' teruggevonden bij de anionische sulfinyl route is afkomstig van een onzuiverheid die waarschijnlijk de polymerisatie initieert aangezien er een directe link kon gelegd worden tussen de zuiverheid van het monomeer en het moleculair gewicht van het bekomen polymeer. Alle andere defecten van de anionische sulfinyl route zijn ook eindgroepen. Ondanks het lager moleculair gewicht heeft de anionische sulfinyl route het voordeel dat controle over de eindgroepen en nieuwe polymeerarchitecturen die PPVs bevatten via deze route mogelijk zijn.

# Summary

Conducting polymers are on the rise in the electronics market. Until now, the most noticeable application for the use of conduction polymers is in light emitting diodes (LEDs), where it replaces silicium based electronics. Such polymer LEDs can be found in devices such as clock-radios, televisions and mobile phones. Conducting polymers also have their role in the development of different kinds of sensors, such as biosensors.

Nowadays, especially poly(phenylenevinylene) (PPV) and derivates hereof are used as active layer in these optoelectronic devices. Over the last 40 years different precursor routes have been developed to synthesize PPV derivatives. All these routes use the polymerization behavior of the *p*-quinodimethane system. Because three different precursor routes will be addressed in this thesis, an overview of the different precursor routes is presented in **Chapter 1**. Special attention is given to the polymerization mechanisms that have been suggested over time. In the past, many studies have been done on elucidating the polymerization mechanism. Some groups claim that the Gilch precursor polymerization is radical in nature, other envision an anionic mechanism. In 1999, the research group of organic and (bio)polymer chemistry of University Hasselt has clearly shown that for the sulfinyl route a competition exists between the radical polymerization and the anionic polymerization. The research group has clearly shown that for the sulfinyl route the high molecular weight material originates from a self-initiating radical polymerization, and this for any solvent in which the polymerization is performed. Low molecular weight polymer, when observed, originates from an anionic polymerization mechanism. The polymerization conditions determine the competition between these two mechanisms, whereby also a bimodal molecular weight distribution can be found (high and low molecular weight).

The effects of polymerization parameters such as concentration, solvent and temperature on the obtained molecular weight are also presented in Chapter 1.

Summary

Biosensors represent a rapidly expanding field, the major drive coming from the health-care industry. In recent years, an increased number of papers are published dealing with biosensors utilizing electrically conducting polymers in the transducer layer. Major progress was made with impedimetric immunosensors based on thin spin coated films of poly[2-(3,7-dimethyloctyloxy)-5-methoxy-1,4-phenylene vinylene]. This PPV derivate is commercially known as $OC_1C_{10}$-PPV or MDMO-PPV. A reason for the interest in this specific PPV derivative lies in its solubility in the conjugated state. The bond between the polymer (MDMO-PPV) and the biomolecule (antibody) is based on weak intermolecular interactions instead of covalent bonds. These interactions have a tendency to denature antibodies and have a negative impact on the biosensor lifetime and stability. Moreover, non-specific interactions on the MDMO-PPV polymers film may result in fouling of the sensor surface.

Previously mentioned PPV polymers were physically attached to the substrate by spin-coating. Even though that the layer of polymer is very thin (~100nm), it is still considerably thicker than needed. We would envision an ideal biosensor as a single layer of PPV-polymer, to which the antibodies are covalently attached to increase the stability of the sensor. On the other hand, the PPV-material also needs to attach firmly to a substrate. We would need to have good control over the initiation reaction, the termination and chain length. If we would understand the anionic polymerization of PPVs, then the controlled synthesis of conductive polymers becomes possible. Although this could also be achieved through controlled radical polymerization, this work will only focus on controlling the anionic polymerization.

In **chapter 2,** the synthesis of MDMO-PPV in an aprotic polar solvent such as tetrahydrofurane (THF) was investigated. Based on the results of foregoing research, a set of polymerizations were performed using Lithium diisopropylamine (LDA) as the base and sulfinyl MDMO-premonomer. Reaction conditions such as the polymerization temperature, speed of addition and order of addition (base-premonomer) was investigated, but each time oligomers with very low molecular weight ($M_n$ ~1.5 kDa) was found. It seems that the initiation is spontaneous and very efficient. This makes control over the chain length impossible. The use of a more sterically

hindered base such as Lithium bis(trimethylsilyl)amide (LHMDS) led to a higher molecular weight ($M_n$ ~4.0 kDa), yield and maximum UV-absorption wavelength. To highlight the anionic character of the polymerization, the effect of adding a radical inhibitor such as TEMPO to the polymerization was investigated. The result of the test showed that TEMPO has no effect on the polymerization outcome. This is in sharp contrast to the classical Gilch polymerization, where the polymerization is completely suppressed by addition of 1 equivalent of TEMPO. To elucidate the nature of the end groups on the polymers, a certain quantity of the polymer obtained *via* anionic polymerization was separated by size by means of Biobeads ® (porous beads). Even though that is was possible to separate the polymer in fractions with different molecular weight, it was not possible to make any clear conclusions on the nature of the end groups. A more sensitive technique was needed; therefore the methylene carbons next to the leaving group (chloride) and the polarizer (sulfinyl) of the premonomer were labeled with $^{13}C$. Signals of possible defects and end groups are hereby magnified by a factor of about 100 in a $^{13}C$ NMR spectrum. The $^{13}C$ NMR analysis of the conjugated polymer made by the anionic sulfinyl route showed that the polymer does not contain any head-to-head defects or remaining sulfinyl groups on the polymer backbone. Following end groups were found: 0.96% aldehyde groups, 1.3% sulfinyl, 0.3% chloromethyl and 2.9% end groups which result of an impurity that remained present after the premonomer synthesis.

For the anionic polymerization the premonomer purity is the most important factor in achieving high molecular weight polymers. This is in contrast to the radical polymerization, where the same monomer yields very high molecular weight material. Chapter 2 ends with the conclusion that we indeed have a good method to synthesize PPVs *via* an anionic polymerization mechanism, but if we want to further investigate the possibilities of this polymerization mechanism, a different premonomer has to be found, which can be purified to a higher level of purity.

In **Chapter 3** 1-(Chloromethyl)-4-[(n-octylsulfinyl)methyl]benzene or 'unsubstituted PPV premonomer' was investigated as new premonomer fur the further study of the anionic polymerization of PPVs. After a double recrystallization of the premonomer, polymerizations were performed with

LHMDS as the base in THF, but also the use of LDA as the base was addressed. It was possible to obtain polymer with relatively high molecular weight ($M_n$ ~20 kDa) when LHMDS was used as the base, while with LDA as base, again low molecular weight ($M_n$ ~1.9 kDa) polymer was obtained. The anionic nature was verified by polymerizing in presents of a radical inhibitor (TEMPO). Various polymerization conditions were explored such as premonomer concentration, polymerization temperature and amount of base. Repetition of the polymerization yields in a significant spread of the obtained molecular weight. The root cause of the spread could not be uncovered, but is probably due to a small amount of impurities.

The mechanistic study on the sulfinyl route in chapters 2 and 3 led to the conclusion that an exclusively anionic polymerization of PPV is possible. In case of unsubstituted PPV, a relatively high molecular weight is obtained. In **chapter 4**, four similar initiators were synthesized and tested in different concentrations on the polymerization. The results indicate that indeed the initiators work as expected, this means that higher concentration of initiator resulted in lower molecular weight. NMR analysis showed that the initiator was incorporated in the polymer chain. This opens up many new possibilities to synthesize conjugated polymers bearing functional end groups. In this way, block-co-polymers could be obtained by coupling of the end group to another (multi)functional polymer. It might also be possible to modify a cleverly functionalized PPV to be used as a macro–initiator for a next polymerization. In case the polymers are living, then block-co-polymers can be obtained by addition of a second monomer. Clearly the use of functional initiators opens up many new possibilities for specific polymer architectures.

As already mentioned, different precursor routes exist which all lead to the same conjugated polymer. However, depending on the chosen synthetic route, higher or lower quantities of defects could be present in the polymer backbone. In **chapter 5** a comparison is made between the polymers obtained from the Gilch radical route, the radical and anionic sulfinyl route and the dithiocarbamate route which was developed recently by the research group. The defects present in those polymers from the different routes were investigated by means of $^{13}$C-NMR. For this investigation, $^{13}$C labeled premonomers were synthesized and polymerized. The first two routes, the Gilch and the radical sulfinyl route, were already investigated in previous

studies using $^{13}C$-labeling. Those results were compared to the two newly developed routes.

The labeled premonomers for the sulfinyl and dithiocarbamate route were synthesized starting from the labeled Gilch MDMO-PPV premonomer. The positions of the $^{13}C$ NMR signals of the chloromethyl, sulfinylmethyl and dithiocarbamate-methyl group were noted by analyzing the labeled premonomers. Subsequently the MDMO-PPV was synthesized *via* the anionic sulfinyl route and the dithiocarbamate route. The precursor and the conjugated polymer were investigated by means of $^{13}C$-NMR spectroscopy. The results are presented in the table below.

| ***Route*** / *Defect* | ***Gilch*** | ***Radical sulfinyl*** | ***Anionic sulfinyl*** | ***Dithiocarbamate*** |
|---|---|---|---|---|
| *Aldehyde end groups* | 0.1 % | 0.3 % | 1.0 % | 0.6 % |
| *Carboxylic acid end groups* | 0.2 % | < 0.1 % | < 0.1 % | < 0.1 % |
| *bisbenzyl-unit* | 5.6 % | < 0.1 % | < 0.1 % | 0.6 % |
| *Triple bond* | 4.2 % | < 0.1 % | < 0.1 % | < 0.1 % |
| *Chlorovinyl* | 1.4 % | < 0.1 % | < 0.1 % | < 0.1 % |
| *Chloromethyl end group* | < 0.1 % | < 0.1 % | 0.3 % | / |
| *Sulfinyl end group* | / | < 0.1 % | 1.3 % | / |
| *dithiocarbamate end group* | / | / | / | < 0.1% |
| *Other end group* | / | / | 2.9 % | / |
| *non eliminated groups* | 1.8 % | 0.5 % | < 0.1 % | < 0.1 % |

**Overview of the defects found *via* $^{13}C$ labeling in MDMO-PPV synthesized *via* different precursor routes**

We can conclude that no structural defects caused by head-to-head or tail-to-tail coupling could be found when using the anionic sulfinyl route, the radical sulfinyl route or the dithiocarbamate route (except for the initiating unit for the radical routes). This is a clear advantage compared to the Gilch route. Concerning the main end groups of the polymer obtained by the

dithiocarbamate route, we can state that only the aldehyde group could be found in a significant amount. Furthermore, the dithiocarbamate premonomer can be synthesized easily and with high yield starting from the Gilch premonomer. The dithiocarbamate route combines the excellent material qualities of the sulfinyl route and the straightforwardness of the Gilch route. The "other end group" found when using the anionic sulfinyl route is originating from an impurity that probably initiates the polymerization, as a direct link between premonomer purity and attained molecular weight could be made. All other defects of the anionic sulfinyl route are also end groups. The anionic sulfinyl route has despite the lower molecular weight the advantage that control over the end groups and new polymer architectures that contain PPVs are possible.

# Dankwoord

Aan het einde van dit proefschrift heb ik de mogelijkheid om die personen te bedanken welke in belangrijke mate hebben bijgedragen aan de totstandkoming ervan.

Het begint natuurlijk bij mijn promotor Prof. Dr. Dirk Vanderzande en copromoter Prof. Dr. Thomas Cleij. Door jullie manier van coachen, motiveren, en vrijheid in de voorbije jaren heb ik mijn doctoraat kunnen afronden. Hartelijk dank hiervoor en voor de waardevolle input tijdens de doctoraatstudie.

Ik kan natuurlijk mijn andere copromoter ook niet vergeten, Prof. Dr. Peter Adriaensens. Bedankt voor je onvermoeibare gedrevenheid om me te laten kennismaken met de wondere wereld van NMR. Geen inspanning was je teveel om steeds weer op zoek te gaan naar een oplossing wanneer er een nieuw probleem de kop opstak en je kritische geest heeft zeker een positieve inbreng gehad in mijn doctoraatswerk.

Jan Czech ben ik als echte expert op het gebied van massa spectormetie gaan beschouwen. Ik dank hem voor zijn enthousiaste hulp bij het analyseren van massa spectra.

Iris Duyssens en Veerle Vrindts bedank ik voor het opnemen van de vele GPC staaltjes en het bespreken van de resultaten ervan.

Verder moeten ook nog al mijn collega's zeker vermeld worden, niet alleen voor hun technisch wetenschppelijke bijdrage aan dit werk, maar ook, en zeker zo belangrijk, voor de "babels" en onmiskenbare vriendschappelijke sfeer op het kantoor en in het labo. Zonder hen was het doctoreren aan de Universiteit Hasselt, vast minder amusant geweest. Ik zal de goede werksfeer en collegialiteit missen en hoop met heel mijn hart dat de opgebouwde vriendschappen blijven duren.

Dankwoord

Mijn ouders, die me de kans gegeven hebben om verder te studeren, voor hun annhoudende steun en belangstelling. Mama en papa nogmaals bedankt, in al die jaren was niets jullie te veel!

Een special woordje van dank richt ik vervolgens aan Dr. Eva Pokorna. Tussen de polymerisaties in, was er tijd om jou te leren kennen. Ondertussen zijn we al enkele jaren samen en heb ik al veel van je kunnen leren. Dank zij jouw geduld, begrip en continue steun is dit werk nu toch ten einde kunnen komen.